UNIVERSITA' DEGLI STUDI DI UDINE

Corso di dottorato di ricerca congiunto in

Biologia Molecolare

Ciclo XXX

in convenzione con:

Università degli Studi di Trieste

International Center for Genetic Engineering and Biotechnology

Scuola Internazionale Superiore di Studi Avanzati

THE MITOCHONDRIAL NATURE OF THE DNA REPAIR PROTEIN APE1

Dottorando:

Arianna BARCHIESI

Relatore:

Dott. Carlo Vascotto

ANNO 2018

TABLE OF CONTENT

TABLE OF CONTENT **1**

INTRODUCTION **7**

1. The mitochondrion **7**

1.1 Sorting pathways of mitochondria 8

2. The Disulfide Relay System **10**

2.1 Cellular factors influencing the DRS 13

3. Mia40 ..... **16**

3.1 Yeast and human Mia40 structure 16

3.1.1 Yeast Mia40 ..... *16*

3.1.2 Human Mia40 ..... *17*

3.2 Canonical and non-canonical substrates of the DRS 18

3.2.1 Canonical substrates *19*

3.2.2 Complex substrates *19*

3.2.3 Novel substrates *19*

3.3 The DRS and diseases 20

3.3.1 Genetic disorders *20*

3.3.2 Neurodegenerative disorders *21*

3.3.3 Cancer *21*

4. APE1/Ref-1 ..... **22**

4.1 APE1 gene and transcriptional regulation 23

4.1.1 APE1 gene *23*

4.1.2 Transcriptional regulation *24*

4.2 APE1 structure 25

4.3 APE1 functions 26

4.3.1 The unstructured N-terminal domain *26*

4.3.2 The N-terminal domain: transcriptional factors activation *27*

4.3.3 The C-terminal domain: DNA repair activity *27*

4.3.4 APE1 endonuclease activity on abasic RNA *29*

4.4 Post-translational modifications 30

4.5 APE1 intracellular trafficking and localization 31

4.6 APE1 in cancer 32

5. The nucleoid **33**

5.1 Mitochondrial genome 33

5.2 mtDNA organization in nucleoids 33

5.3 Nucleoids protein composition 34

5.4 mtDNA damage and repair 36

6. The mitochondrial RNA granules (MRGs): regulation and coordination of mitochondrial gene expression **38**

6.1 Mitochondrial RNA granules protein composition 38

7. mtRNA processing and metabolism **41**

7.1 mtRNA transcription and regulation 41

7.2 Transcript processing 41

7.3 mt-tRNA processing and modification 43

7.4 mt-rRNA modification 45

7.4.1 Maturation of the 12S mt-rRNA *45*

7.4.2 Maturation of the 16S mt-rRNA *45*

7.5 mt-mRNA processing and metabolism 46

7.5.1 mt-mRNA polyadenilation *46*

7.5.2 mt-mRNA stability and decay *47*
8. Translation process in mitochondria **49**
8.1 Mitoribosome biogenesis and structure 49
8.2 The mitochondrial translation process 50
8.3 Regulation of mitochondrial translation 51
9. mt-RNA processing, mt-translation and diseases **53**

LIST OF PUBLICATIONS **54**
1. Mitochondrial translocation of APE1 relies on the MIA pathway 54
2. Isolation of mitochondria is necessary for precise quantification of mitochondrial DNA damage in human carcinoma samples 54
3. DNA Repair Protein APE1 Degrades Dysfunctional Abasic mRNA in Mitochondria 55

AIMS **56**

MATERIAL AND METHODS **57**
1. Cell culture and treatments 57
2. Transient transfection experiments 57
3. Preparation of total cell extracts and anti-Flag affinity purification 57
4. Anti-Flag affinity purification from isolated mitochondria 58
5. Preparation of subcellular fractions 58
6. Mitochondria isolation 58
7. Western blot analysis 58
8. DNA extraction and mtDNA damage measurement by quantitative PCR 59
9. RNA extraction and Real time-PCR 59
10. Expression and purification of recombinant proteins 60
11. GST pull-down assay 60
12. Endonuclease assay 61
13. Proximity ligation assay (PLA) 61
14. Mitochondrial translation evaluation 61
15. BN-PAGE analysis 62
16. mRNA accumulation and half-life calculation 62
17. Northern blot analysis 62
18. Analysis of mitochondrial mRNA half-life 62
19. OXPHOS efficiency evaluation 62
20. Mass spectrometric analysis of APE1-FLAG complexes. 62
21. Immunofluorescence 63
22. AP-sites quantification 63
23. Statistical analyses 64

RESULTS **65**
1. Role of MIA pathway in the mitochondrial internalization of APE1 ..... **65**
1.1 APE1 and Mia40 interact through disulfide bonds 65
1.2 Mia40 is required for mitochondrial translocation of APE1 74
2. Uncanonical role of APE1 on mitochondrial messanger RNA **80**
2.1 APE1 interacts with ribosomal and RNA processing proteins in mitochondria 80
2.2 APE1 binds and processes abasic mitochondrial RNA 84
2.3 Mitochondrial mRNA half-life is dependent on APE1 87
2.4 APE1 mutant E96A is not able to exert enzymatic activity on mitochondrial mRNA species 91
2.5 Loss of mitochondrial APE1 negatively affects mitochondrial translation and respiration 95

DISCUSSION AND CONCLUSIONS **101**

BIBLIOGRAPHY 107

INTRODUCTION

1. The mitochondrion

Mitochondria arose around two billion years ago from the engulfment of an α-proteobacterium by a precursor of the modern eukaryotic cell [1]. Nowadays they are the principal source of energy production and metabolism that are fundamental processes for the survival and wellbeing of the cell.
Mitochondria are organelles with a double membrane, the outer (OM) and the inner membrane (IM), and together they delimit two aqueous compartments: the matrix, in the inner side, and the intermembrane space (IMS) (Figure 1).

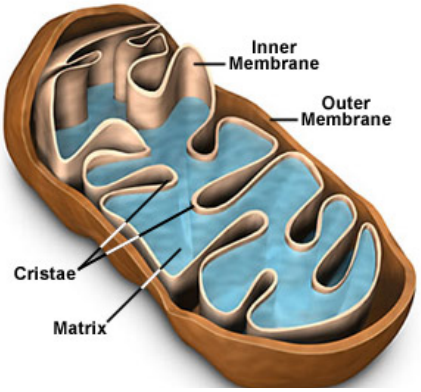

Figure 1: Mitochondrial structure. Mitochondria possess a double membrane: the outer membrane (OM) and the inner membrane (IM). Between the two membranes there is the intermembrane space (IMS), while inside, delimited by the IM there is the matrix (https://micro.magnet.fsu.edu/cells/mitochondria/mitochondria.html).

The main function of mitochondria is exerted in the IM through the electron transport chain (ETC) that produce energy in the form of ATP via oxidative phosphorylation (OXPHOS). In the matrix, tricarboxylic acid cycle (TCA) enzymes generate electron carriers (NADH and $FADH_2$), which donate electrons to the ETC.
The ETC consists of four protein machines (I–IV), which through sequential redox reactions undergo conformational changes to pump protons from the matrix into the IMS. The proton gradient generated by complexes I, III, and IV is released through the rotary turbine-like ATP synthase machine or complex V, which drives phosphorylation of ADP to ATP [2,3]. Complexes I and III also could lose some electrons that can react with O_2 generating reactive oxygen species (ROS), including oxygen radicals and hydrogen peroxide, which may damage key components of cells, including lipids, nucleic acids, and proteins [4,5].
Beyond ATP production, the inner-membrane electrochemical potential generated by OXPHOS is a vital feature of the organelle [6]. Membrane potential is harnessed for other essential mitochondrial functions, such as mitochondrial protein import [7] and is used to trigger changes on the molecular level that alter mitochondrial behaviors in response to mitochondrial dysfunction.
Besides the role in energy production and in other metabolic pathways involving carbohydrates (Krebs cycle) lipids, amino acids and iron, mitochondria play a central role in the programmed cell death process (apoptosis) that is important for the correct development of organisms, for tissue homeostasis and as a response to cellular stress or pathogens.
Although mitochondria have maintained the double membrane character of their ancestors and the core of ATP production, their overall form and composition have been drastically altered, and they

have acquired myriad additional functions within the cell. As part of the process of acquiring new functions during evolution, most of the genomic material of the α-proteobacterium progenitor was rapidly lost or transferred to the nuclear genome [8] . What remains in human cells is a small, approximately 16 kilobase, circular genome, which is present in cells in a vast excess of copies relative to nuclear chromosomes. Mitochondrial DNA (mtDNA) contains 37 genes: 13 codify for proteins, 22 are tRNA, and 2 are for the ribosomal RNA subunits. We know from a combination of proteomics, genomics and bioinformatics analysis that modern day mitochondria are comprised of well over 1,000 proteins. The majority of the proteins present in this organelle are nuclear encoded and the composition changes with and between species in response to cellular and tissue-specific organismal needs [9–11].

The nucleus-encoded proteins that make up most of the mitochondrial proteome are translated on cytosolic ribosomes and actively imported and sorted into mitochondrial subcompartments by outer and inner membrane translocase machines [7,12].

1.1 Sorting pathways of mitochondria

Translocation of proteins across organelle membranes is critical process for the cell survival. The targeting sequences carried by the proteins provide the specificity for the destination organelle, while the machineries that are designed to translocate the proteins into the various compartments provide the import.

Different mechanisms are used by mitochondria for the import of such proteins, depending on their destination [13]. The "mitochondrial portal" for all the proteins is TOM (translocator of the outer membrane) that permits the substrates to pass the OM. If the protein is a transmembrane protein and is carrying a non-cleavable signal, it becomes substrate of the SAM machinery (Sorting and assembly machinery of the outer mitochondrial membrane) that assists the β-barrel assembly and the α-helical folding of thus proteins in the outer membrane. TIM23 (Translocase of the inner mitochondrial membrane 23) and TIM22 (Translocase of the inner mitochondrial membrane 22) are the machineries assigned to the import of the proteins in the matrix and into the inner membrane, respectively. Proteins with a presequence containing a sorting signal or a bipartite presequence are substrates of these machineries. The OXA (Insertase/export machinery of the inner membrane) complex is responsible for the translocation of mitochondrial encoded proteins from the matrix into the inner membrane [13] (Figure 2).

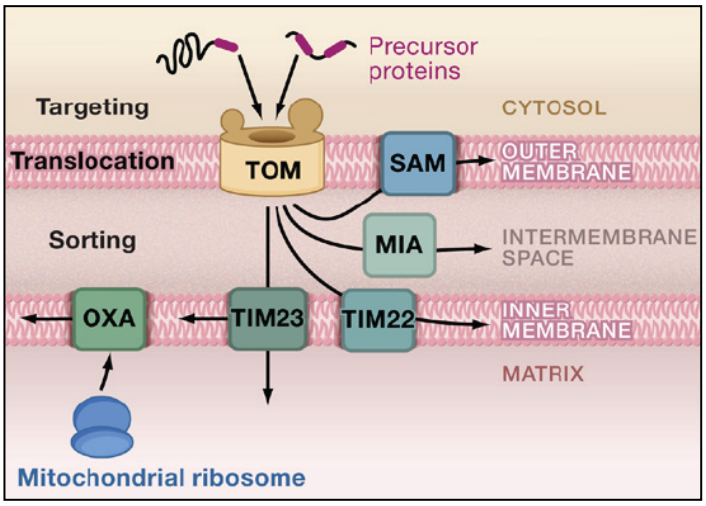

Figure 2: Sorting pathways of mitochondria. The translocase of the outer membrane (TOM complex) is the main entry gate into mitochondria. Subsequently, the precursor proteins follow different sorting pathways. SAM, sorting and assembly machinery; TIM22 complex, carrier translocase of the inner membrane; TIM23 complex, presequence translocase of the inner membrane; OXA, insertase/export machinery of the inner membrane; MIA, mitochondrial intermembrane space assembly (Adapted image from Chacinska et al., 2009).

Instead of the other compartments, none of the proteins present in the IMS is encoded by mitochondria so, if the protein is a soluble cytein-rich IMS protein this could be a substrate for the disulfide relay system (DRS), an import machinery that uses a redox system for cysteine enriched proteins, to drive them in this compartment [13,14]. The DRS is composed by two main proteins: Mia40 is the oxidoreductase that catalyzes the formation of the disulfde bonds in the substrate, while Erv1/ALR reoxidizes Mia40 after the import [14,15].

2. The Disulfide Relay System

The IMS proteins Mia40 and Erv1/ALR represent the central components of the DRS.

As said before, all IMS proteins are nuclear encoded and only a few of them contain MTS or internal targeting sequence. Most of them are cysteine-enriched proteins with conserved cysteine patterns that are recognised by Mia40. To be able to interact with Mia40 these proteins have to be kept in an unfolded state into the cytosol and this is achieved by cytosolic glutharedoxin in human cells and by the thioredoxin system in yeast [16,17]. In this way proteins are able to pass the TOM pore and enter mitochondria.

After the passage throughout the outer membrane via TOM pore, substrate proteins are recognised by Mia40 thanks to the MISS/ITS sequence via hydrophobic interactions [18,19] (Figure 3. (2)).

Mia40 is an IMS protein composed by a highly conserved C-term domain that contains the catalytic CPC (cysteine-proline-cysteine) motif and a hydrophobic cleft. After the recognition of the substrate the thiolate anion of a cysteine in the substrate performs a nucleophilic attack on the oxidezed CPC motif of Mia40 (Figure 3. (3)). This finally results in an intermolecular disulfide bond that is subsequently resolved by another nucleophilic attack of the other thiolate anion (Figure 3. (4)) [20,21]. At the same time, Mia40 is also able to induce a conformational change in the substrate, in particular in that hydrophobic region that is interacting with Mia40 (MISS/ITS sequence). This region in the substrate passes from a completely unfolded state to a-helix conformation as shown in Figure 3 [22]. Finally, the result of this reaction is an oxidized and folded substrate in the IMS and a reduced Mia40 molecule (Figure 3 (4)).

Once Mia40 has oxidized its substrate, the CPC motif remains in a completely reduced form and has to be re-oxidized for another cycle of import [21,23]. Erv1 (Essential for respiration and vegetative growth 1) in yeast and ALR (augmenter of liver regeneration) in human mitochondria are responsible for this process (Figure 3(5)).

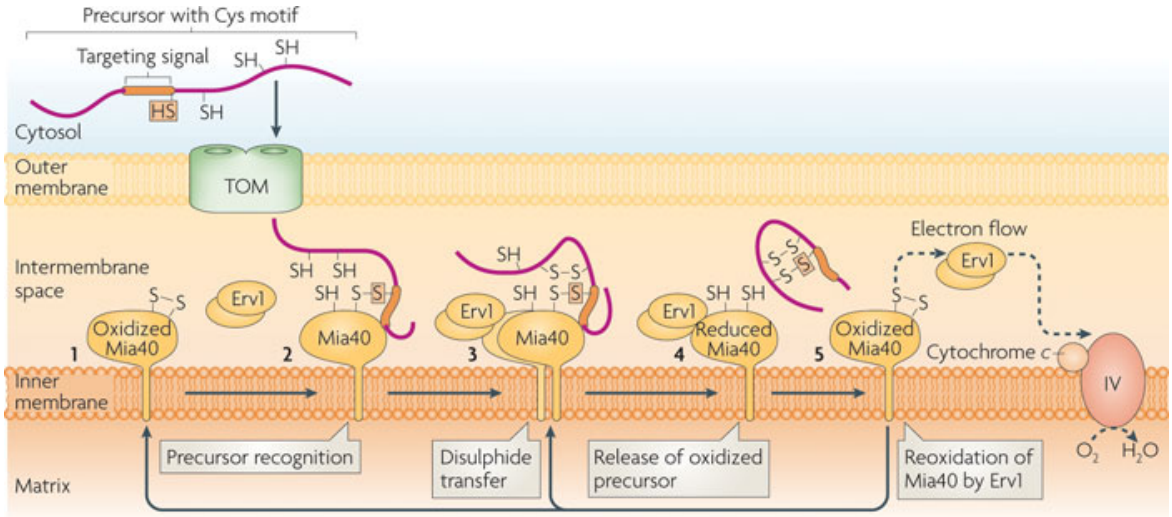

Figure 3: Oxidation of the substrate by Mia40. (1) Mia40 is present in an oxidized state in the IMS; **(2)** Precursors are recognized by Mia40 thanks to the MISS/ITS sequence and the intramolecular bond is formed; **(3)** The intermolecular disulfide bond is resolved and a folded substrate is released; **(4)** Mia40 has to be reoxidized by Erv1/ALR; **(5)** Once Mia40 is reoxidized Erv1/ALR can pass the electrons to the Cyt. C, and then to the O_2 (Adapted image from Meisinger et al. 2010).

Human ALR is present as two alternatively-spliced forms: a long form (23 kDa), that is extensively present in the IMS and a short one (15 kDa) that lacks an 80 amino acids N-terminal extension and acts as an extracellular cytokine [24–26]. In yeast Erv1 is present in one unique form that corresponds to the long human form of ALR and is present exclusively in the mitochondrial intermembrane space [27].
Erv1 and ALR are sulfhydryl oxidase coupled with one molecule of FAD and acting as homodimer in solution. Both proteins present a CXXC motif that is engaged in the binding with the FAD molecule and a pair of conserved cysteines in their N-terminal domain, also called N-term shuffle domain or CRAC motif in ALR, that is responsible for the interaction with Mia40 (Figure 4) [21,28–30]. Erv1 and ALR present 40% of homology for the C-terminal domain that contains the CXXC motif for the binding of the FAD molecule, while the N-terminal domain is not conserved.

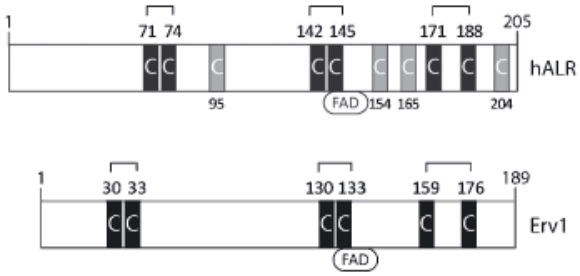

Figure 4: Schematic representation of Erv1 and ALR proteins. Cysteines highlighted in black are conserved residues while cysteines highlighted in grey are more recently acquired residues. The first two conserved cysteines form the N-Term shuffle domain responsible for the electron transfer from Mia40 to the FAD molecule. Cysteines 142-145 in ALR and 130-133 in Erv1 form the CXXC domain that binds the FAD molecule (Adapted image from Sztolsztener et al. 2013).

It has been demonstrated that ALR is able to regenerate Mia40 for a new import cycle when Mia40 is reduced [28,31]. Indeed, ALR interacts with Mia40 through its N-terminal domain thanks to hydrophobic interactions with the hydrophobic cleft of Mia40 that is the same segment used by the protein to recognise and fold its substrate proteins. So using a "substrate mimicry" strategy this domain is able to mediate the electron transfer from Mia40 to Erv1/ALR [29,30]. This interaction does not affect ALR N-terminal domain but permits the electron transfer between the two proteins. The CPC motif of Mia40 interacts with the CRAC motif of ALR and is able to pass its electrons to the two conserved cysteines (Figure 5).
Once the electrons are passed, Mia40 is ready to start a new import cycle. The N-terminal shuffle domain of ALR, in turn, has to be reoxidized to become able to regenerate another Mia40 protein, so the electrons are passed from the CRAC motif of the N-terminal domain to the CXXC motif of the FAD binding domain, and then to the Cyt *c* that transfers the electrons to the respiratory chain [29].
It has been proposed that the reaction of import and oxidation of Mia40 in yeast take place in a ternary complex with the substrate, Mia40 and Erv1. Bottinger *et al.* demonstrate that Erv1 is necessary for the conformational change required for the oxidation of the substrate. Erv1 is able to bind an alternative region of Mia40 upon binding of the substrate to ensure that semi-oxidized substrates are not released in the IMS [32].

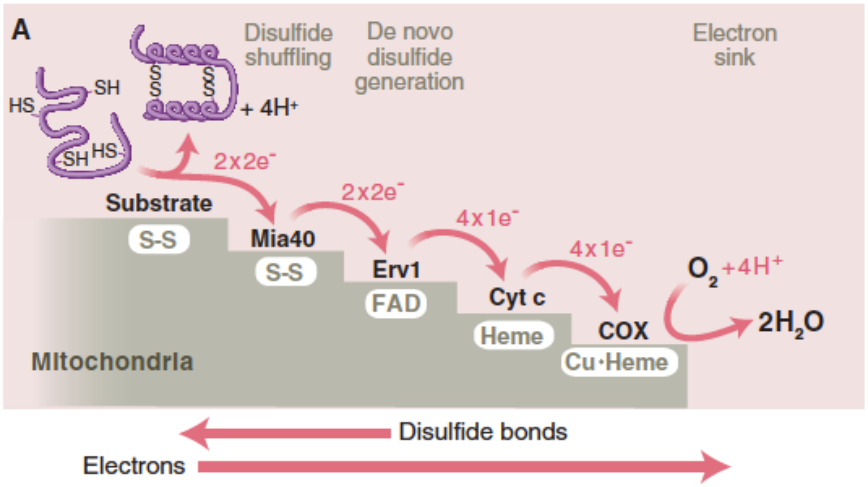

Figure 5: Electron flow in a cycle of import. Oxidized Mia40 interacts with substrates and facilitates their stable folding by the introduction of disulfide bonds. A cascade of redox-active proteins transfers electrons from Mia40 to Cyt *c* oxidase, which converts oxygen to water. The flavoprotein Erv1 mediates the switch from two-electron to one-electron transfer (Adapted image from Herrmann et al. 2009).

After passage of the electrons from Mia40 to Erv1/ALR, these electrons have to be passed to another component of the DRS, the Cyt *c*, in order to reoxidize Erv1/ALR that, in this way, is ready for another cycle of import (Figure 6) [21,33,34].

Bihlmaier *et al.* demonstrate that Erv1 and the Cyt *c* can interact, and Erv1 directly passes the electrons to the Cyt *c*, connecting the DRS to the respiratory chain and preventing the generation of hydrogen peroxide. The same was also proved to occur in human cells for ALR [31]. It was also shown that the redox state of Mia40 depends on the activity of the respiratory chain complexes. Indeed, in the absence of oxidized Cyt *c* or Cyt *c* oxidase, Mia40 is present in the mitochondria in a reduced state, whereas an increase of oxidized Cyt *c* lead to an increase of the oxidized form of Mia40. Mutation of other components of the respiratory chain (e.g. F_1 F_0 ATPase), however, did not change the redox state of Mia40 indicating a specific function of Cyt *c* in this process. Moreover, import in the absence of Cyt *c* or Cyt *c* oxidase is decreased and is hypersensitive to the treatment with reducing agents as DTT [34].

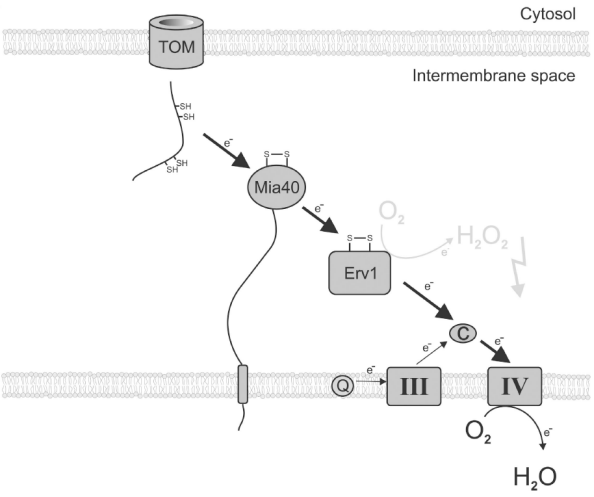

Figure 6: Model for the interaction of the DRS and the mitochondrial respiratory chain. The electron flow from the imported proteins to the final electron acceptor oxygen is indicated. The cytochrome c–independent side reaction of Erv1 with oxygen is shown in light gray. Cyt *c* reductase and oxidase complexes are indicated as complexes III and IV, respectively. Q indicates the ubiquinone pool (Adapted from Bihlmaier et al. 2007).

2.1 Cellular factors influencing the DRS

Two of the most influencing factors of this redox import pathway are the IMS GSH pool and the percentage of molecular oxygen (pO_2).

The GSH pool of the IMS is interconnected to the one in the cytosol by the porins inserted in the OM of mitochondria (Figure 7) [35]. Under normal physiological conditions 70% of Mia40 is oxidized thanks to Erv1 that efficiently avoid the accumulation of the reduced form of Mia40. Kojer *et al.* demonstrate that in yeast strains lacking Erv1, Mia40 can be reduced by GSH *in vivo*. In cells lacking Glr1 (Glutathione disulfide reductase 1) the recovery of Mia40 is impaired, so local GSH pool can provide the reducing equivalents to Mia40 [35].

According to these previous findings Bien *et al.* proposed an essential role of the GSH pool for the proper functioning of DRS. At physiological concentrations GSH is able to counteract the generation of incorrect intermediates and long-lived unproductive disulfide arrangements. In this way the mitochondrial import is more efficient and futile cycles of oxidation and reduction are prevented [20,21].

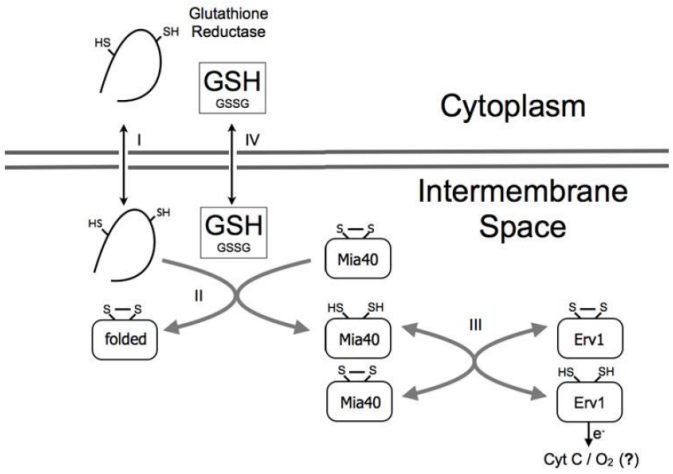

Figure 7: Mia40 pathway is influenced by cytoplasmatic GSH. (I) Reduced and unfolded substrates cross the outer mitochondrial membrane **(II)** and are recognized by oxidized Mia40. **(III)** Following the formation of an intermolecular disulfide bond, the substrate is released, oxidized and folded while Mia40 CPC motif is reduced. Mia40 is then reoxidized by Erv1 that can transfer electrons to cytochrome C or directly to oxygen forming H_2O_2. GSH has been shown *in vitro* to influence the oxidative folding of several substrates by promoting disulfide reshuffling. **(IV)** Free diffusion of GSH:GSSG from the cytoplasm to the IMS thanks to the presence of porins. The GSH pool in the cytoplasm also influences the redox state of Mia40 but the molecular mechanisms involved remain unclear (Adapted image from Ventura *et al.* 2013).

Also pO_2 is able to influence DRS pathway. It has been demonstrated that the electrons can be passed from Mia40 to Erv1 and then to either via Cyt *c* to oxygen or to oxygen in a direct way *in vitro* and *in organello* [33,34]. Kojer *et al.* studied the influence of oxygen in yeast strains were complex III and IV of the respiratory chain were absent. In the presence of 20% O_2 no difference was observed in comparison with the WT, instead in 1% O_2 conditions Mia40 was more reduced when the complex IV was absent. So Erv1 is able to pass electrons to molecular oxygen via Complex IV *in vivo*, and at oxygen concentrations of 20% the re-oxidation of Mia40 can be efficiently driven by the direct interaction of Erv1 and oxygen *in vivo* [35].

Hot13 protein was also proposed to have an influence in the redox state of Mia40. Hot13 (Helper of Tim 13) is a zinc-binding protein and is a chaperone for the assembly of the small Tim proteins in the IMS [36,37]. Yeast strains lacking Hot13 present unchanged levels of Mia40 but a more abundant reduced form of the protein. Moreover in the presence of low concentration of GSH, the absence of Hot13 lead to a more reduced form of Mia40 [36]. Mesecke *et al.* demonstrate that Mia40 can physically interact with Hot13, but without the participation of disulfide bonds.

Because it was demonstrated that the zinc binding stabilize the reduced form of Mia40 due to the fact that Erv1 cannot efficiently bind this form, it has been proposed that Hot13 is able to convert the zinc-bind form of Mia40 in the zinc-free form, enabling Erv1 to oxidize it (Figure 8) [37].

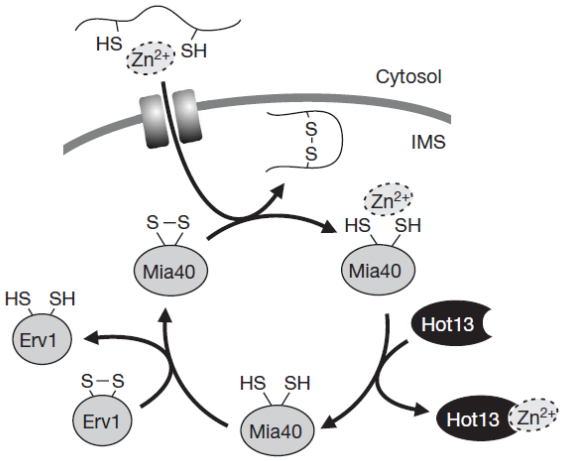

Figure 8: Model for the influence of metal ions on protein import into the IMS. Imported proteins can be associated with zinc ions. These are passed through Mia40 to Hot13 and further to an unknown acceptor. Hot13-mediated demetalation of Mia40 presumably improves the reoxidation of the import receptor by Erv1 (Adapted image from Meseke et al. 2008).

3. Mia40

Mia40 (Mitochondrial Intermembrane Space Import and Assembly Protein) is a protein that localize in the mitochondrial intermembrane space. Mia40 is a fundamental part of DRS and its main function is to translocate its protein substrates from the cytoplasm to the IMS of mitochondria and to assist their folding inside this space. The substrates of Mia40 are nuclear encoded proteins that fulfil their function in the IMS or in the matrix, through an import process that implicates the formation of disulfide bonds between Mia40 and the precursor protein [38].

3.1 Yeast and human Mia40 structure

3.1.1 Yeast Mia40

Mia40 was firstly described in yeast by Chacinska *et al.* in 2004 as a component of the DRS. Yeast Mia40, also known as Tim40, is a nuclear encoded protein by the ORF JKL195w, it contains a cleavable presequence and is imported into mitochondria via TIM23 complex [38,39].

Yeast Mia40 is composed by 403 amino acids and can be divided into two principal domains: the C-term of the protein that contains the catalytic motif and the N-term that contains the transmembrane domain and the cleavable N-term presequence (Figure 9). Once this presequence is cleaved, Mia40 is anchored to the inner membrane thanks to the hydrophobic transmembrane segment while the large C-term domain is exposed to the IMS. The C-term domain contains six cysteines and the replacement of one of these is lethal. In particular, the first two cysteines, Cys 296 and Cys 298, form a CPC motif able to bind to the target cysteine of the substrate, while the other four cysteines, Cys 307, 317, 330, and 340, form twins CX_9C motifs that have probably only a structural function. The disulfide bonds between these residues are present in the fully oxidized form of the protein [38,39].

Likewise other IMS proteins, this protein is principally constituted by two 13-residue α-helices that from an antiparallel hairpin, which are virtually connected by two disulfide bonds formed by Cys307-Cys340 and Cys317-Cys330. The other two functional cysteines are exposed to the IMS lumen and they are able to attack the cysteine residues of the substrates.

This structure confers to Mia40 a fruit-dish-like shape in which the hydrophobic residues of the helices are exposed to the outer space in a concave surface mainly formed by phenylalanine residues [40,41]. This concave surface has a very important role for the coupling with the substrates. Indeed, it has been demonstrated that the hydrophobic region is positioned in close proximity to the redox-active cysteines of the CPC motif, and serves as a binding region for the substrates and for the recognition by the so-called MISS or ITS (Mitochondrial IMS-sorting signal, or ITS for IMS-targeting signal) sequence present in the client proteins [18,19].

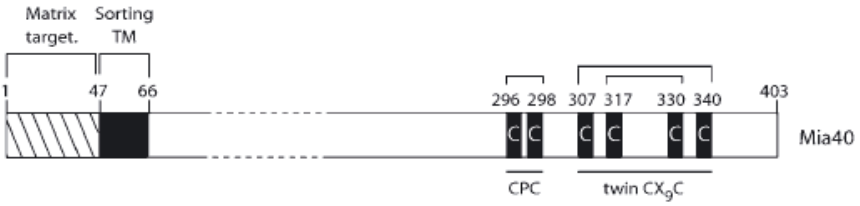

Figure 9: Schematic representation of yeast Mia40. In the structure are present seven cystines residues, six of which are conserved. These residues form the CPC catalytic motif and the twin CX_9C structural motif. The Matrix targeting signal and the transmembrane segment are located at the N-term (Adapted image from Sztolsztener et al. 2013).

3.1.2 Human Mia40

Human Mia40 is a soluble IMS protein and belongs to the protein family whose members share six highly conserved cysteine residues constituting a -CXC-CX_9C-CX_9C- motif [42]. Protein sequence alignment of the region comprises between amino acids 47 and 102 reveals a 75% similarity to *S. cerevisiae* Mia40 and 98% to *D. Melanogaster* (Figure 10). Outside this cysteine domain the similarity is low because, as said before, *S. cerevisiae* like *S. pombe* and other yeast species carry the large N-terminal extension that is not present in the human Mia40.

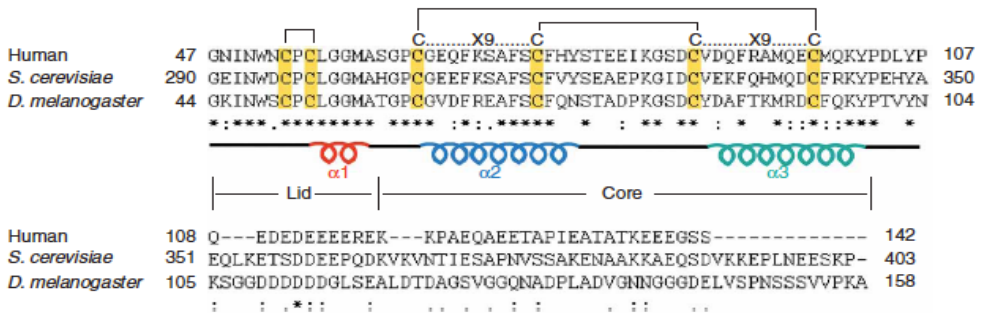

Figure 10: Mia40 sequence alignment. Alignment of the conserved CXC-CX_9C- CX_9C domain of Mia40 hortologs (Adapted image from Yang et al. 2012).

Human Mia40, also known as CHCHD4.1, is encoded by *CHCHD4* gene and exist in two isoforms, CHCHD4.1 and CHCHD4.2, which are produced by alternative splicing sites as shown in Figure 11 [42,43]. Little is known about the human Mia40 because the majority of the studies in literature are focused on the yeast Mia40.

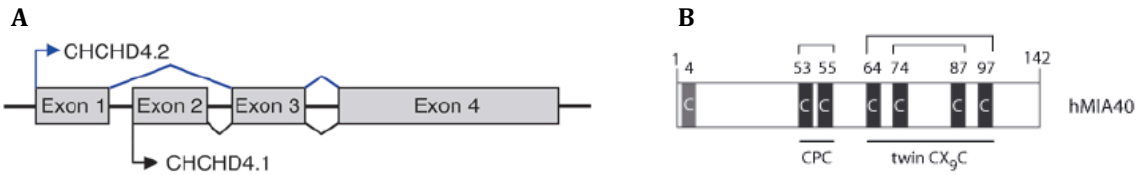

Figure 11: Scheme of MIA40 human gene and protein. (A) Mia40 gene is formed by 4 exons. The isoform 1 (CHCHD4.1), is composed by exons 2, 3 and 4, the second form (CHCHD4.2) is lacking exon 2 but encodes exon 1(Adapted image from Yang et al. 2012). **(B)** Schematic representation of isoform 1protein (CHCHD4.1): the protein presents seven cystines residues, six of which are conserved (highlighted in black) (Adapted image from Sztolsztener et al. 2013).

The shorter form (CHCHD4.1), which is nearly identical to yeast Mia40, presents seven cysteines residues: six of them are filogenetically conserved and is demonstrated to have the same function as in the yeast homologue [44]. Cys4 at the N-terminal domain is not conserved. The longer form (CHCHD4.2) lacks exon 2 so it do not contain the Cys4, however different functionality or substrate specificity are still unknown (Figure 11 A).

The CHCHD4.1 isoform (from here on referred to as Mia40) has an ubiquitous expression in human tissues and the highest levels of Mia40 were found in liver, brain and kidney at transcript and protein levels [42,43]. The main function of the human protein, as the yeast one, is to introduce nuclear encoded

proteins into the IMS. It has been demonstrated that if the human Mia40 is expressed in yeast strains that lacks the endogenous Mia40, this form is capable to fulfil the function of the yeast [44]. Several features of Mia40 have been recapitulated in yeast models for the human DRS, including the import of IMS precursors and formation of disulfide-bonded Mia40 intermediate complexes followed by oxidation of IMS client proteins [44].

In human Mia40 the CPC motif is formed by Cys53 and Cys55 (Figure 11 B). The cysteine responsible for the intermolecular disulfide bond is the Cys55. The mutation of this cysteine results in a loss of function of Mia40 that is no more able to interact with the substrate. On the contrary, mutation of Cys53 has not this dramatic effect: Mia40 is still able to interact with the substrates but in a less efficient manner [40,45–47].

3.2 Canonical and non-canonical substrates of the DRS

It is believed that Mia40 could recognise its substrates by the presence of the MISS sequence on these proteins. The MISS sequence is composed by anphipathic residues of the substrate with a specific succession of amino acids. This succession is specific for the class of protein considered: for example in the case of CX_9C proteins the consensus is *aromatic-XX-hydrophobic-hydrophobic-XXC* [18,19], instead in the case of small Tim proteins it is *LXXXCF*.

The sequence is not located at a precise point of the substrate protein but it can be everywhere in proximity to the cysteines bound by Mia40. For example, Cox17 protein presents the MISS sequence at its C-terminal domain, while Tim proteins present the sequence at the N-terminal domain [19]. This sequence is docked onto the binding cleft of Mia40 and in both cases the signatures are in direct proximity to the critical cysteine residues, which attacks the redox-sensitive CPC sequence of Mia40.

The MISS sequence serves as docking site to position the sequences in the binding cleft of Mia40 in an orientation that allows the interaction of the redox-active CPC motif of Mia40 with the cysteine residues in the client protein (Figure 12) [40]. Because only unfolded proteins are able to traverse TOM pore, Mia40 is capable of redox-fold the proteins as a chaperone and release them in a stably conformation in the IMS. Mutants substrates in which individual cysteins are mutated are still folded as long as the MISS sequence is not destroyed [21,40].

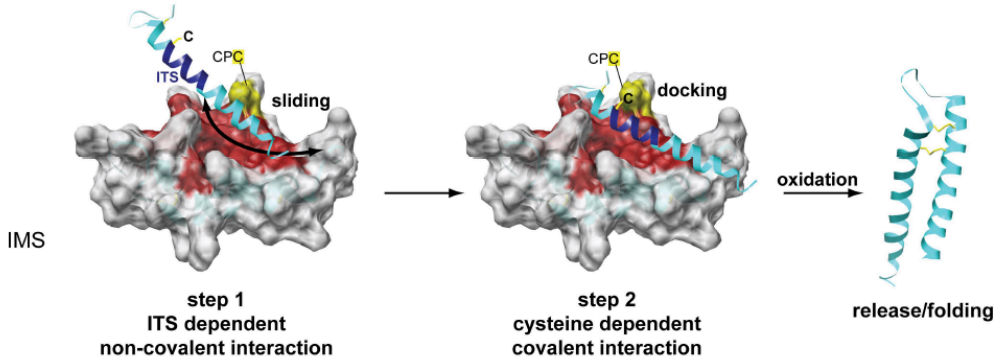

Figure 12: Sliding–docking model for the interaction of substrates with Mia40. (**step 1, sliding**) The substrate slides onto Mia40, where it is oriented by the MISS/ITS through noncovalent, mainly hydrophobic interactions in the cleft of Mia40. The correct Cys of the substrate is thus primed to make the disulfide with Mia40; (**step 2, docking**) The substrate now docks onto Mia40 via the covalent mixed disulfide bond between the substrate-docking Cys and the juxtaposed active site Cys of Mia40. Finally, complete oxidation releases the substrate in a folded state (Adapted image from Banci et al. 2010).

3.2.1 Canonical substrates

Typical substrates of the DRS are small proteins, around 10 kDa, which destination is the IMS or the matrix. These proteins are cysteine enriched, they belong to the families of the twin CX_3C and CX_9C proteins and fulfil different functions in the mitochondria. CX_3C and CX_9C proteins have the same structure: they share a common core formed by two a-helices in an antiparallel orientation. These two helices are held together and stabilized by the disulfide bonds between the cysteins of the twin motifs, giving an helix-loop-helix conformation to the core [48].

The family of the CX_3C proteins is composed by five proteins in yeast, fungi and animals: Tim8, Tim9, Tim10, Tim12 and Tim13, and their orthologs. These proteins form hexameric or heteromultimeric complexes in the IMS and they act as chaperones for the hydrophobic proteins helping them to cross the lumen of the IMS [49].

On the contrary, the family of the twin CX_9C proteins, has a more wide and heterogeneous composition. There are 14 proteins belonging to this family in yeast and most of them are conserved in higher eukaryotes and also in humans. Notably some bioinformatic analyses suggest that the number of the proteins belonging to this family could be at least twice in humans than in yeast [50,51]. Typical members of this family are Cox17 or Cox19 and their function is to assist the assembly and give stability to some of the proteins of the respiratory chain (i.e.: cytochrome *b*) [50,52]. Some other proteins belonging to this family are Mdm35, a critical factor for the mitochondrial lipid homeostasis [53], and for importing Ups proteins, Yme1 and Som1 that are peptidases of the IMS. Interestingly, proteins of these families differ considerably in the primary sequence, except for the four cysteines of the CX_9C motif and it has been demonstrated that no other residue is maintained invariant. However, the amino acids in key positions for the interaction with the hydrophobic cleft of Mia40 are hydrophobic residues in all of the proteins of this family [50].

3.2.2 Complex substrates

As well as the twin CX_3C and CX_9C proteins, other more complex proteins are imported in the IMS via Mia40. These proteins include Cox11 and Cox12, Sod1, and its copper chaperone Ccs1, ALR, the complex III subunits Qcr6 and Rip1, the two thioredoxin like proteins Sco1 and Sco2.

Cox11 and Cox12 proteins contain two domains CX_9C-$CX_{10}C$ that are really close to the twin motif proteins. Cox12 is part of the Cyt *c* oxidase and Cox11, like the other proteins discussed above, is an assembling factor for the Cyt *c* oxidase [54]. Sod1 and Ccs1 are part of the anti-oxidative system that turns the superoxide ions into hydrogen peroxide. Sod1 is a dimeric protein and contains one disulfide bond per unit which is introduced by Ccs1 (Copper chaperone for Sod1) and facilitates the translocation of Sod1 into the organelle [55]. Like Sod1 also Ccs1 has one structural disulfide bond that is introduced by Mia40 during import in mitochondria [56–58]. ALR is itself one of the principal proteins of the DRS, and it has been proved to be itself a substrate for Mia40 [59]. The disulfide bond in Rip1 is introduced by Mia40 and is critical for its enzymatic activity [60,61].

3.2.3 Novel substrates

Recently, other novel substrates for Mia40 have been described in yeast and humans. Tim22 is a subunit of TIM22 chaperone complex in the IMS. This complex binds a specific class of proteins, the membrane-multispanning carrier family and TIM22 pathway helps these proteins during the integration in the IM [62]. Tim22 possesses only two cysteine residues that are supposed to form a disulfide bond. It has been demonstrated that Mia40 is able to bind Tim22 and form this disulfide bond. Moreover, the interaction is stabilized by hydrophobic interactions with the hydrophobic cleft of Mia40. Defects in the cleft of Mia40 result in a defective biogenesis of Tim22. Interestingly, Mia40 is able to bind Tim22 without any involvement of disulfide bonds, but with a reduced efficiency [62].

Another protein present within the IMS is Atp23, a protease required for the processing of the subunit 6 of the mitochondrial ATPases (Atp6). Atp23 is mitochondrial encoded and is synthetized as a precursor protein. Mia40 is able to bind Atp23 and to introduce five disulfide bonds in this protein. Also in this case, Mia40 binds Atp23 only via hydrophobic interactions [63].
Mrp10 (also known as CHCHD1) is a highly conserved subunit of the mitochondrial ribosome and is located in the matrix. It has been demonstrated that Mrp10 possesses an unconventional MTS sequence enriched in proline residues and is not processed by the matrix processing peptidase. As far as we know, this protein has four conserved cysteine residues that are oxidized by Mia40 during import. The semifolded protein with one disulfide bond is able to pass the inner membrane to localize in the matrix. Here, the protein could be found in a complete oxidized form in the presence of Mia40. Conversely, if Mia40 is silenced the protein in the matrix is only partially folded and degraded because is not able to be assembled in the ribosomes [64].
Also the tumor suppressor protein p53 was found to localize in mitochondria through to the DRS and its import is respiration-dependent and activated by oxidative stress. Mitochondrial p53 is able to maintain the integrity of mtDNA, which is more susceptible to the oxidative damage owing to its structure and proximity to electron transfer reactions [65].
Recently, the Apurinic/apyrimidinic endonuclease 1 (APE1) was also described as a possible substrate of Mia40. APE1 protein, the main human endonuclease, is a fundamental component of the Base Excision Repair (BER), a pathway involved in the DNA repair activity of damaged bases. It was already demonstrated that APE1 is localized for a small portion in mitochondria having a role in the mtDNA maintanence [66,67]. In addition, Vascotto *et al.* demonstrated that APE1 localize in the IMS and, through a PLA (proximity ligation assay) analysis, they demonstrate the interaction between APE1 and Mia40 [67]. Data reported in this thesis depict the molecular mechanisms involved in the interaction between APE1 and Mia40 and the contribution of DRS in the maintenance and repair of mtDNA.

3.3 The DRS and diseases

3.3.1 Genetic disorders

Because mitochondria are essential for energy production in eukaryotes, errors in their metabolism are normally associated with pathological states.
Regarding the DRS pathway there are two known and well characterized genetic diseases associated with the mutation of DRS substrates. The first one is an X-chromosome-linked neurodegenerative disorder that implicates a mutation in TIMM8, one of the most studied substrates of Mia40 [68]. The disease associated with this mutation is the Human deafness dystonia syndrome, which leads to hearing loss, mental retardation and blindness. The mutation is located in the CX_3C motif of TIMM8 that means that the protein cannot be transported and properly folded in mitochondria via Mia40 [69,70]. Because of the improper folding the mutated protein cannot be assembled into the TIMM13 complex that is responsible for the import of TIM23, with deleterious effects for health.
The second disorder associated with the DRS pathway involves ALR [71]. The Autosomal recessive myopathy (ARM) is a recessive disorder in which the homozygous mutation R194H in the ALR gene is present. This condition is characterized by cataract, muscle hypotonia, hearing loss and developmental delay. This mutation affects the stability of ALR and enhances its degradation. ALR acts in the IMS as a homodimer and arginine 194 is usually located at the interface. R194H has a minimal effect on the enzymatic activity but affects the stability of the protein increasing the rate of dissociation of the FAD ribose and increasing its susceptibility to proteolysis [72]. As a consequence, the biogenesis of Mia40 substrates is impaired [44].

3.3.2 Neurodegenerative disorders

Over one third of genetic mutations associated with the inherited predisposition to neurodegeneration are functionally linked to mitochondria.

Huntington disease (HD) is a genetically inherited disorder caused by the expansion of polyglutamine repeats in the huntingtin protein. This disease is additionally associated to mitochondrial dysfunctions, and abnormalities found in patient and mouse models are numerous and complex. It has been recently demonstrated that in mice affected by HD the levels of ALR were decreased with unchanged or slightly reduced Mia40 levels. Consequently the substrates of the DRS were altered, with reduced activity of the respiratory chain [73].

A role in the Amyotrophic lateral sclerosis (ALS) was also proposed for Mia40. ALS affects motor neurons and is frequently associated with mutations in Sod1. In yeast Sod1 is imported in mitochondria with the help of Mia40. In human cells a mechanism was proposed trough which Mia40 and Mitofillin, a component of the mitochondrial contact site and cristae organizing system (MICOS), have a role in the biogenesis of the pathogenic variants of Sod1 [74].

3.3.3 Cancer

We know that cancer cells rely on the Wartburg effect to produce energy so they utilize glycolysis more than oxidative phosphorylation, but counter-intuitively mitochondrial biogenesis is linked with tumor progression [75].

As said before p53 could be found in mitochondria to preserve the mitochondrial genome. p53 is mutated in many types of cancer as a strategy of the cancer cells to avoid apoptosis. The mutated form of p53 has several functional abnormalities and some of them are mitochondrial correlated. Normally p53 promotes aerobic respiration whereas the mutated form sustains the non-aerobic respiration enhancing the Wartburg effect and the escape from apoptosis [75,76].

An increased expression of Mia40 has been found in many types of tumors as breast carcinoma, pancreatic ductal carcinoma and glioma and this increase has been associated with poor prognosis [43]. Interestingly, there is a correlation between the expression of Mia40 and the activity of HIF-1α. Mia40 has been proposed to promote the hypoxic response required for adaptation and tumor angiogenesis. It has been demonstrated that Mia40 can stabilize HIF-1α, however the mechanism has not been elucidated. Three different indirect mechanisms could explain a stabilization of HIF-1α: 1) an overproduction of ROS species by the complex III of the respiratory chain [77]; 2) an increase of the consumption of oxygen by complex IV of the respiratory chain [78]; 3) an increased concentration of complex II substrate succinate [79]. If Mia40 is able to modulate the stabilization of HIF-1α in direct manner or indirectly with one of the three mechanisms proposed is currently object of study.

4. APE1/Ref-1

APE1/Ref-1 (Apurinic/apyrimidinic Endonuclease/ Redox factor 1) is the major apurinic/apyrimidinic endonuclease in mammalian cells [80]. APE1 is an essential and multifunctional protein that is ubiquitously expressed at high levels (10^4-10^5 copies/cell) in human cells [81], although it has a heterogeneous pattern of expression in different tissues and conditions [82]. APE1 principal functions within the cell are the maintenance of genome stability, acting in the BER pathway, and the redox-dependent transcriptional regulatory activity acting on several cancer-related transcription factors [81,82]. These two main functions are exerted by two different domains of APE1: the C-term domain possesses the endonuclease activity, while the redox activity is performed by the N-term domain [83] (Figure 13).

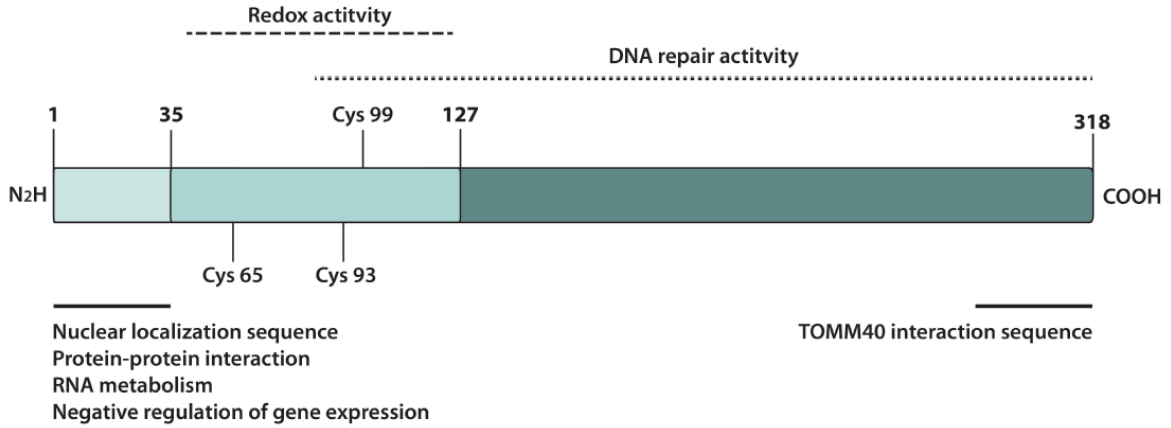

Figure 13 Schematic representation of APE1 structure: First 35 amino acids are responsible for the nuclear localization, the protein-protein interaction and RNA metabolism. The N-term domain that spans from a.a. 35 to a.a. 127 is responsible for the redox activity and the C-tern domain is responsible for the DNA repair activity. Recently in this last domain also an TOMM40 interaction sequence was found (Adapted from Tell et al. 2010)

Besides the endonuclease and the redox activities, other multiple functions were described for this protein (Figure 14). APE1 has a role in the RNA metabolism where it exerts endonuclease towards abasic RNA both *in vitro* and *in vivo* [84–87]. Another function of the protein is the binding activity and transcriptional regulation of nCaRE sequences in the promoter region of genes, as APE1 promoter itself [88]. An important role for the first 35 amino acids of APE1 was recently highlighted. This domain is essential for the protein-protein interaction with the majority of APE1 partners and for the modulation of its activities through different post-translational modifications [82,89,90].

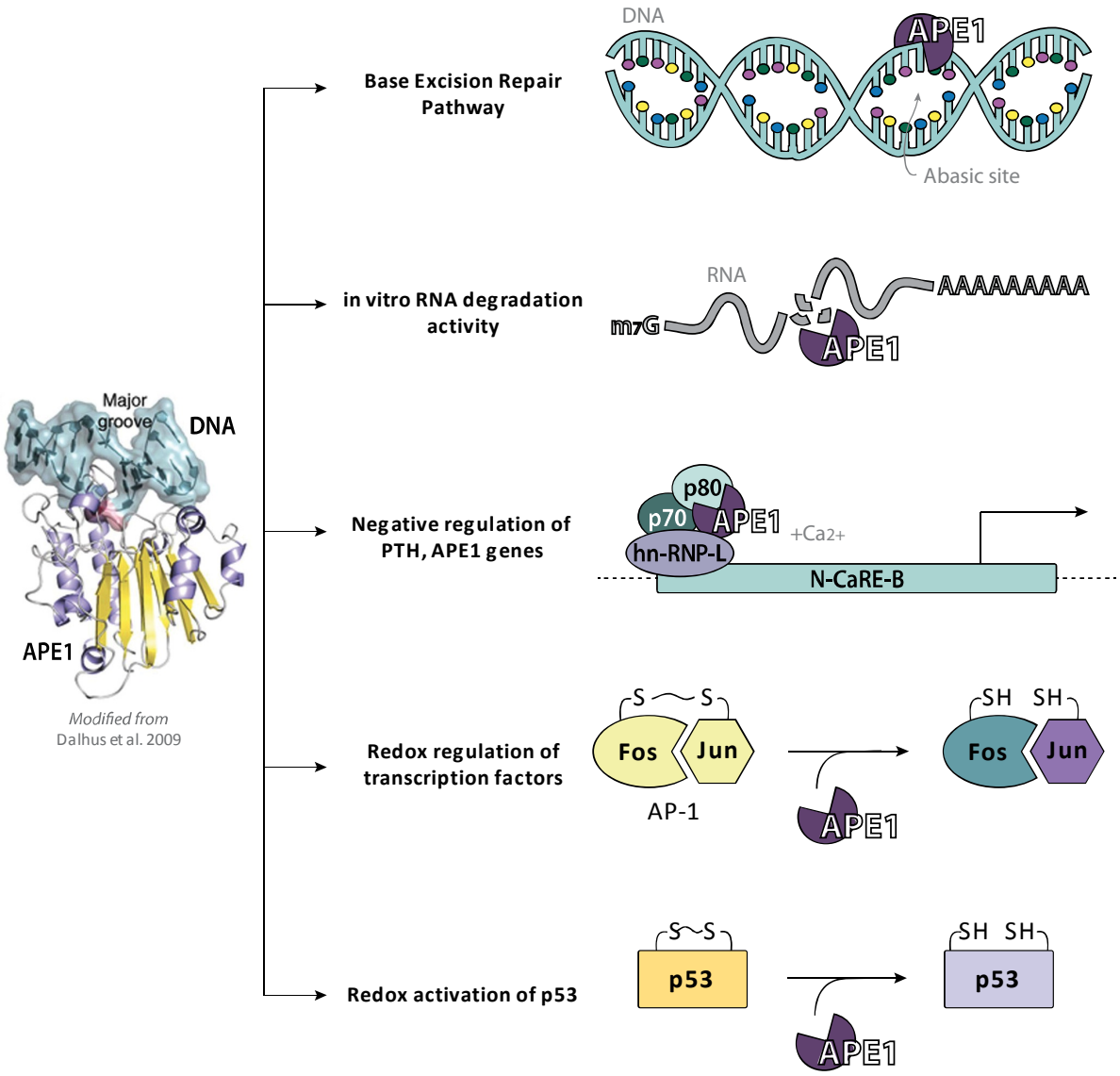

Figure 14: APE1 functions. First 35 amino acids are responsible for the nuclear localization, the protein-protein interaction and RNA metabolism. The N-term domain that spans from a.a. 35 to a.a. 127 is responsible for the redox activity and the C-tern domain is responsible for the DNA repair activity. Recently in this last domain also an unconventional mitochondrial localization sequence was found.

4.1 APE1 gene and transcriptional regulation

4.1.1 APE1 gene

APE1 is encoded by *HAP1* or *APEX* gene in human cells, it is located on chromosome 14q11.2-12 and it spans approximately 3 kb of DNA [91].

As shown in Figure 15, the gene consists of four introns and five exons, the first of which is not coding. The promoter region of the gene lacks a TATA box and only one CCAAT box is present, so a cluster of multiple transcription start sites is present in the proximal promoter region [92]. The first exon of the gene harbors several putative CpG regulatory elements and some recognition sites for several transcription factors such as Sp1, USF, AP-1, CREB and ATF [82]. Instead, in the distal promoter region, there are three nCaRE-B negative regulatory elements that can inhibit the APE1 gene transcription [93].

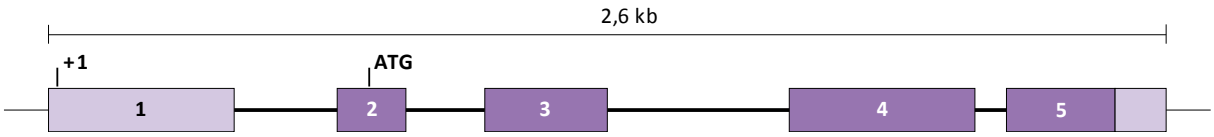

Figure 15: APE1 gene structure. APE1 gene spans 2,6 kb and consists of five exons and four introns. The first exon is non-coding (Adapted from Evans 2000).

4.1.2 Transcriptional regulation

Transcriptional regulation of APE1 gene is strictly correlated with the cell cycle. APE1 mRNA levels rise after G1-S phase thanks to the transcriptional activation of Sp1-2 that can bind APE1 promoter, in response to cell growth [94].

p53 has also been proposed by Bhakat *et al.* as a negative regulator of APE1, through the recognition of a p53 binding element presents in proximity to the CCAAT box. The mechanisms are not being fully elucidated, but it was proposed that APE1can indirectly recruit p53 to APE1 promoter through a physical interaction with Sp1-1 subunit of Sp1 and inhibit APE1 gene transcription [95].

APE1 gene contains other negative regulatory sites. As said before three nCaRE sequences are present in its promoter, one of type A and two of type B. Deletion of the nCaRE-B2 sequence strongly influences the negative regulation of APE1 gene. APE1 itself is able to bind this sequence suggesting the existence of an auto regulatory loop in which APE1 is able to bind its own promoter and inhibits its transcription (Figure 16) [96].

APE1 gene transcription can also be enhanced by an inducible activation. It has been demonstrated that stimulation with TSH (Thyroid-stimulating hormone) can activate APE1 transcription [97]. Subtoxic doses of ROS can also activate APE1 transcription probably through the binding of CREB and Egr-1 factors upstream the APE1 transcription start site [98].

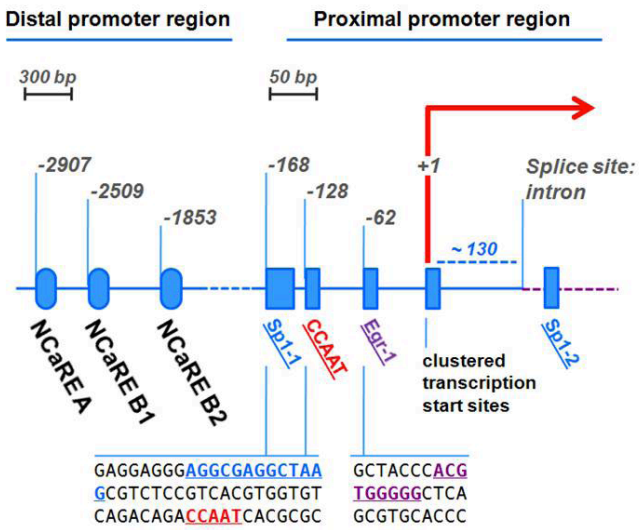

Figure 16: APE1 promoter. The distal promoter region of APE1 contains the nCa-RE sequences while the proximal promoter region contains binding sites for several transcription activator factors and the clustered transcription starting sites (Adapted from Tell et al. 2010).

4.2 APE1 structure

APE1 is composed by 318 amino acids, acts as a monomer inside the cell [91], and it is part of the EEP (endonuclease/exonuclease-phosphatase) family proteins, a divalent cation-dependent phosphoesterase superfamily [99].

APE1 has a globular structure that can be divided in two, partially overlapping, domains: the N-terminal domain and the C-terminal domain. Each domain is composed by six β-sheet strands surrounded by α-helices that together form an α/β sandwich [100] (Figure 17). Structurally and functionally, the N-terminal domain itself can be divided in two parts: the first 35 amino acids of this domain are non-conserved, completely unstructured and highly disordered [101]. This peculiar feature gave APE1 important functional advantages for damage sensing, post-translational modifications, and protein-protein interactions [89,102] . The remaining part of the N-terminal domain is part of the globular structure and provides the redox activity of the protein. The C-terminal domain, completely structured, contains the Mg^{2+} binding site and is responsible for the endonuclease activity exerted through the BER pathway.

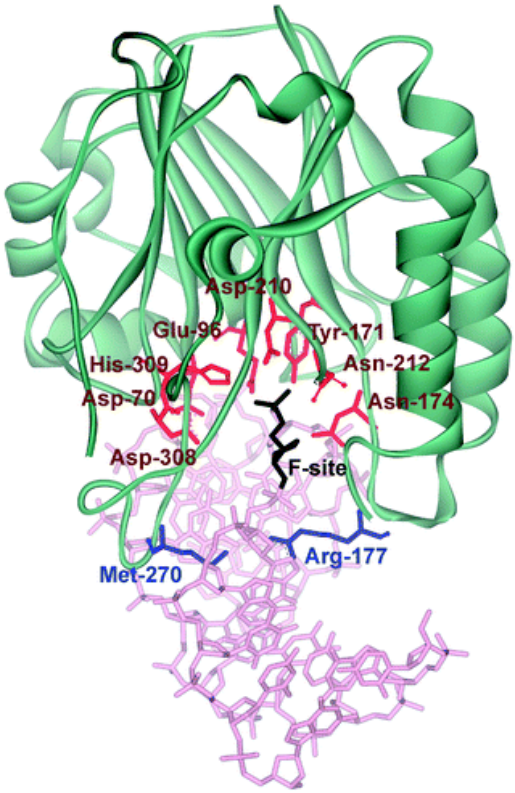

Figure 17: APE1 structure. Foundamental amino acids for the catalytic activity are highlighted in red and blue. The conserved four-layered α/β-sandwich structural core consists of two six-stranded β-sheets surrounded by α-helices, packed together (Adapted from Miroshnikova et al., 2016).

4.3 APE1 functions

4.3.1 The unstructured N-terminal domain

As mentioned before, crystallographic studies demonstrated that the first 42 residues of APE1 N-terminal domain are unstructured and highly disordered [101]. For its intrinsic structural plasticity, this domain could provide important functional advantages to APE1. This region contains the bipartite nuclear localization sequence (NLS) that direct APE1 to the nuclear compartment [104]. This domain is essential in mammals for the damage sensing and repair regulation through post-translational modifications. Indeed, the positively charged residues that are present in this region confer the capability to APE1, as other DNA binding proteins, to scan DNA for DNA damage [104].

Another important function of this domain is the ability to interact with other proteins as Nucleophosmin (NPM1), a nucleolar protein that is able to regulate the DNA repair and the RNA degradation of APE1 [86]. APE1's residues 27, 31, 32 and 35 are responsible for the binding with NPM1 and it has been demonstrated that during genotoxic stress this residues can be acetylated *in vivo*. This modification leads to a reduction of affinity for NPM1 and to an increase of the endonuclease activity. The result is a relocalization of APE1 from the nucleoli to the nucleoplasm where the protein can perform its DNA repair activity [105].

4.3.2 The N-terminal domain: transcriptional factors activation

The globular region of the N-terminal domain spans from amino acid 42 to amino acid 127 and is responsible for the redox activity of APE1 [82,106].

In 1992 APE1 was identified as a crucial activator of the DNA binding of transcription factors Fos and Jun subunits of the Activator protein 1 (AP-1) [107]. Then, APE1 was described as a redox activator of several others transcription factors involved in many different processes as cell cycle regulation, apoptosis, angiogenesis and differentiation. p53 [108], c-Jun [109], HIF1-α [110], NF-κB [111] are some of APE1 substrates that are activated via reduction of critical cysteine residues, as shown in Figure 18. Moreover, APE1 targets could also be tissue specific (e.g. TTF-1 and Pax proteins) and their activation could have opposite effects on cell fate [112].

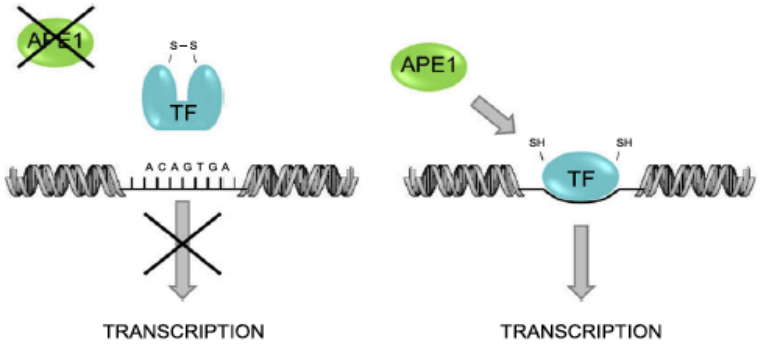

Figure 18: Schematic representation of transcriptional factors activator of APE1. If APE1 is not present the transcription factor remains in a oxidized state and it cannot bind its DNA target sequence so the transcription is blocked, while if APE1 is present, the transcription factor can be reduced and activated to bind the target sequence in the promoter and start the transcription (Adapted from Tell et al 2005).

The principal residues that are implicated in the redox activity of APE1 are Cys65, Cys93 and Cys99 [109,113]. Structural studies highlighted that Cys65 is located in a hydrophobic pocket of the core structure of the protein and therefore it is inaccessible to the solvent, as the other two cysteines. As a consequence the cysteine residues would be unable to interact directly with the target cysteine residue. A model was proposed in which APE1 may undergo to a conformational change that can "open" the globular structure and expose the cysteine residues to the solvent, creating in this way a binding site that can accommodate different transcription factors [114].

4.3.3 The C-terminal domain: DNA repair activity

The C-terminal domain of APE1 is involved in the repair of DNA lesions being an essential component of BER pathway. BER is committed to the removal of small, non-helix distorting base lesions, as oxidative (e.g. 8-oxoG) or alkylation lesions, restoring the chemical DNA integrity. These lesions, if not repaired, could determine the accumulation of mutations during the replication phase [115]. As shown in Figure 19, the first step in the BER pathway is the recognition of the damaged base by a glycosylase that removes the base and leaves an abasic site (AP-site). There are two major classes of glycosylases that can act in BER pathway: the monofunctional are able to remove the damaged base and present only this activity, while the bifunctional exhibit also a β-lyase activity [116]. The abasic site is recognised by APE1 which cuts in a Mg^{2+}-dependent mechanism the phosphodiester backbone at

the 5' end of the lesion leaving a 3'-hydroxyl group (3'-OH) and a 5' deoxyribose phosphate (dRP) at the upstream 3' end and the downstream 5' end, respectively [92].

APE1 catalytic domain possesses only one catalytic active site and has a positively-charged semi-rigid structure able to interact with the abasic DNA to which it has a very high affinity. Met270 and Arg177 residues are inserted in the minor groove and in the major groove respectively, creating a twist of the helix and retaining the product after the protein cut. Also the residues Asp70, Asn212, Asp283 and Asp308 are involved in the protein/DNA interaction, while residues Glu96, Tyr171, Asp210 and His309, are involved and essential in the catalysis of the reaction [82,100,117,118]. Asn212 is, in particular, the residue deputated to the recognition of the abasic site, mutation of this amino acid can disable APE1 to bind its substrate [93]. His309 and Asp283 in particular involved in the maintenance of the conformation of the active site. Substitution of the residue His309 with an asparagine residue leads to a loss of the catalytic activity of the protein in both DNA and RNA, maintaining the ability of the protein to bind the substrate, resulting in a dominant-negative form of the protein. [93,102]. Finally, to perform its endonuclease activity, APE1 needs two (Mg^{2+}) magnesium ions as cofactors. One of these residues is bound by residue Glu96 ensuring the stabilization of the enzyme structure and a high endonuclease activity. Mutation of this residue gives a partial loss of the endonuclease activity of the protein [119,120].

After APE1 activity on its substrate, the DNA is nicked and the repair can proceed with one of the two BER subpathways: the Short-patch (SP-BER) or the long-patch (LP-BER) pathways. The SP-BER is used by the cell for normal AP-sites, whereas, if several nucleotides are modified the LP-BER is used [93]. The termini that APE1 has generated are the substrate for the DNA polymerases. In the SP-BER, Pol-β (DNA polymerase β) is responsible for the insertion of the single nucleotide and finally the lesion is repaired by DNA ligase III and XRCC1. In the LP-BER there is a strand displacement that covers from two to several nucleotides surrounding the AP-site. In this case, Pol-δ, Pol-ε (DNA polymerase δ or ε) with the help of PCNA (proliferating cell nuclear antigen) and other factors are able to displace few nucleotides and to replace them. The 5' dRP terminus left by the previous step is removed by FEN1 (Flap endonuclease 1) and then the repair is completed by DNA ligase I that restores the phosphodiester backbone [93].

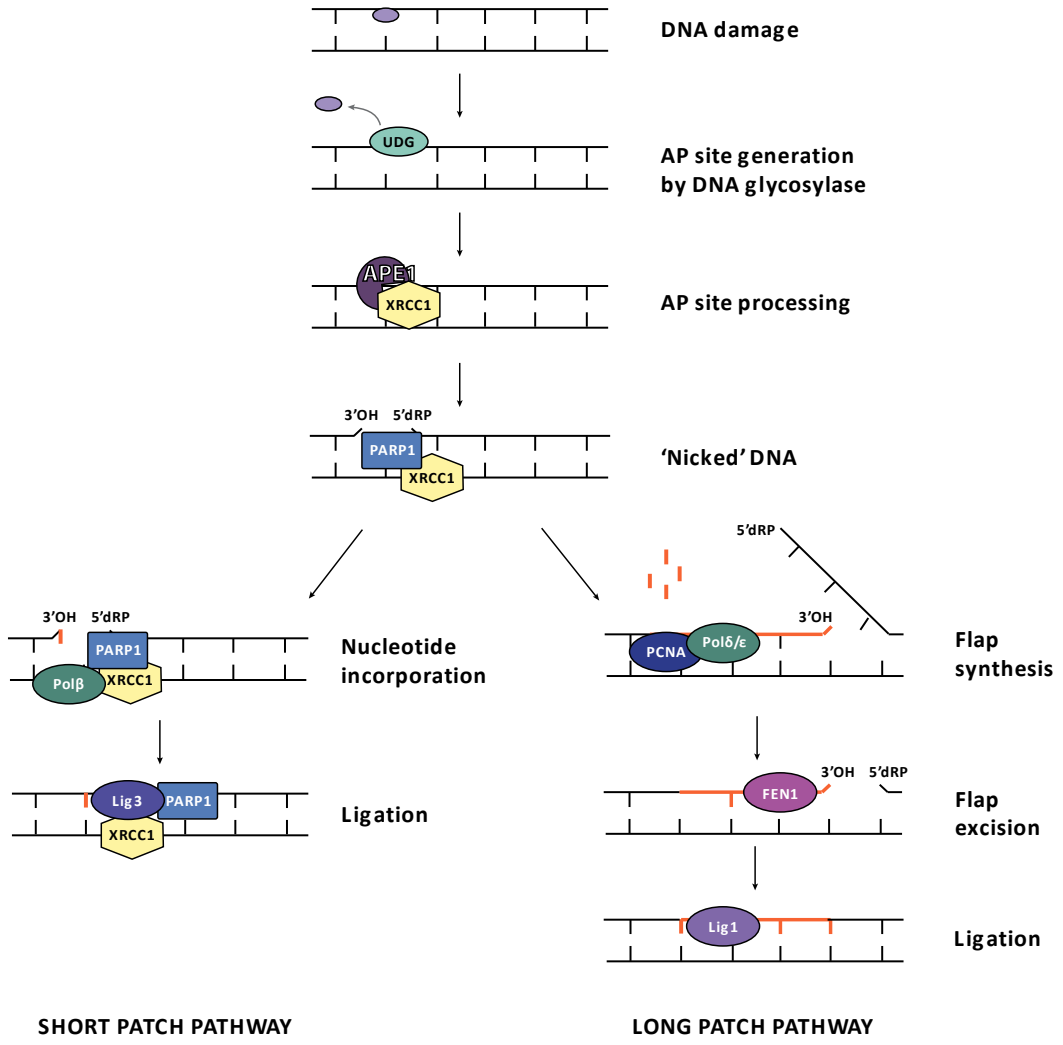

Figure 19: BER pathway. The repair process is initiated by the recognition and removal of the modified base by either a monofunctional or bifunctional DNA glycosylase to leave an AP site. Excision by either one of the monofunctional DNA glycosylases is followed by incision of the DNA backbone 5′ to the AP site by APE1. The resulting single-strand break will contain either a 3′ or 5′ obstructive termini. End processing is then performed by Pol β or APE1 depending on the specific nature of the terminus. When end processing has produced the necessary 3′-OH and 5′-P termini the following BER steps diverge into two subpathways, short-patch and long-patch. In SP-BER repair synthesis of the single nucleotide gap is by Pol β aided by the XRCC1 scaffold, and subsequent ligation by LIG3α finishes the repair. In LP-BER repair synthesis of the 2–13 nucleotide gap is by Pol β, and/or Pol δ/ε aided by PCNA. A resulting 5′ flap is removed by FEN1 and the final ligation step is performed by LIG1.

4.3.4 APE1 endonuclease activity on abasic RNA

Over the last few years emerging evidences indicate that certain DNA repair proteins are also involved in the RNA quality control processes, identifying damaged, chemically modified or oxidized RNA which may led to ribosomal malfunctioning, error-prone protein translation, and as a final consequence failed protein synthesis [121]. In this regard, the first demonstration of APE1 enzymatic action on RNA in vitro was the identification of its RNase H-like activity on a DNA/RNA duplex [122] and the capacity to cleave an AP site-containing ssRNA. It was found that APE1 can cleave AP sites contained in "pseudo-triplex" substrates designed to mimic stalled replication or transcription

intermediates, and configurations that resembles R-loop structures, suggesting a novel "cleansing" function that may contribute to the elimination of detrimental cellular AP-RNA molecules [123]. Next, Lee and colleagues identified APE1 as the endoribonuclease responsible of cleaving a specific coding region of the c-*myc* mRNA. In this study, using E96A and H309N mutants of APE1, it was demonstrated that the endoribonuclease activity for c-*myc* RNA shares the same active center with the AP-DNA endonuclease activity. They also demonstrate for the first time the ability of APE1 to affect mRNA half-life in HeLa cells and therefore supporting its role in RNA metabolism [124].
However, no further studies documented a similar activity toward other nuclear encoded messenger RNA. During the last decade, Tell and colleagues deeply investigated the uncanonical role of APE1 in RNA biology. In 2009 an interactomic study led at the identification and characterization of several novel APE1 partners which, unexpectedly, included a number of proteins involved in ribosome biogenesis and RNA processing [125]. As mentioned before, among the different interacting proteins identified there was also nucleophosmin (NPM1), a nucleolar protein implicated in a variety of cellular processes, including ribosome biogenesis [126]. It was demonstrated that APE1 is localized within the nucleolus and this localization depends on cell cycle and active rRNA transcription. NPM1 stimulates APE1 endonuclease activity on abasic double-stranded DNA (dsDNA) but decreases APE1 endonuclease activity on abasic single-stranded RNA (ssRNA) by masking the N-terminal region of APE1 required for stable RNA binding. Indeed, in APE1-knocked-down cells, pre-rRNA synthesis and rRNA processing were not affected but inability to remove 8-hydroxyguanine-containing rRNA upon oxidative stress, impaired translation, lower intracellular protein content, and decreased cell growth rate were found. These results supported the hypothesis that NPM1 exerted a fine-tuning control of APE1 endonuclease activity within nucleoli devoted to repair of AP damage on rDNA and the removal of oxidized rRNA molecules [125].
More recently, our knowledge about the enzymatic activity of APE1 toward RNA was extended demonstrating its ability to recognize and efficiently process an abasic or oxidised ribonucleoside 5'-monophosphate (rNMP) erroneously incorporated, and then damaged, into a DNA strand [84]. Finally, it is from last year the demonstration of the association of APE1 with the miRNA processing complex DROSHA and its active role in the processing of miR-221/222 [85].

4.4 Post-translational modifications

Several different types of post-translational modifications can occur *in vivo* for APE1 protein: acetylation, phosphorylation, ubiquitination, S-nitrosation and proteolysis [92].
APE1's acetylation is the most studied post-translational modification. Lys6 and Lys7 are the residues that targeted by the histone acetyl transferase p300 *in vivo* and *in vitro*. This modification is important for the binding of APE1 to the nCaRE sequences within the parathyroid hormone (PTH) promoter [127]. Also lysine residues 27, 31, 32 and 35 are subjected to acetylation *in vivo* and they are crucial for APE1 interaction with rRNA and NPM1, for controlling is catalytic activity on abasic DNA and for APE1 subcellular distribution in the nucleoli [89,105].
Several putative phosphorylation sites, located in both the nuclease and the redox regulatory APE1 domains, have been identified *in vitro* for a broad range of kinases, as Casein Kinase 1 and 2 (CK-I and CK-II), Glycogen Synthase Kinase 3 (GSK-III) and Protein Kinase C (PKC). Phosphorylation may occur on serine/threonine residues and might be responsible in controlling macromolecule (protein-protein and protein-DNA) associations involved in redox regulation and in DNA repair.
In 2009, Izumi and colleagues show that both *in vitro* and *in vivo* the E3 ligase MDM2 (murine double minute 2), a negative regulator of p53, ubiquitinates APE1 at one of the lysine residues 24, 25 or 27. Moreover, oxidative conditions can induce MDM2-mediated ubiquitination of APE1. Two years later, the same group gave further insights in the APE1 ubiquitination process, reporting an interesting

crosstalk between ubiquitination and phosphorylation of APE1 at Thr233. In particular, phosphorylation of APE1 may induce MDM2 activity, leading to augmented ubiquitination of APE1 [128].

A truncated form of APE1 lacking its first N-terminal 33 or 35 amino acids, lately named APE1 NΔ33, was first identified by Pommier *et al.* in 1998. To date, further studies are needed to elucidate the mechanisms responsible for the APE1 NΔ33 nuclear translocation, since the truncation leads to the loss of the nuclear localization signal. The truncation of the N-terminal of APE1 has been associated with different cell death programs. This irreversible posttranslational modification may represent a regulatory switch for controlling APE1 functions. Up to now, many unresolved question remain to be answered, regarding the identification of the proteases, the stimuli responsible for the generation of the truncated form and the effects of such modification on APE1 cellular translocation.

APE1 contains three redox-sensitive cysteine residues, two of which (Cys93 and Cys310) may undergo S-nitrosation after nitric oxide stimulus and are responsible for APE1 reversible shuttling from nucleus to cytoplasm in a non canonical CRM1-independent manner, connecting APE1 to nitric oxide physiological and pathological processes [129].

4.5 APE1 intracellular trafficking and localization

APE1 exerts both nuclear and extranuclear functions and therefore it is of the utmost relevance to elucidate the molecular mechanisms involved in the translocation of this protein within the different subcellular compartments.

Because of its function on the abasic DNA and as regulatory protein acting on several cancer-related transcription factors, APE1 has long been recognized as nuclear protein. In the 1998 the nuclear localization signal of APE1 was identified. The NLS is contained in the APE1 N-terminus and consists of a bipartite signal within the first twenty amino acids (residues 2-13) [130,131]. Stimuli as oxidative stress and other signalling molecules such as TSH or calcium have been shown to stimulate APE1 nuclear translocation [98,132]. Recently, Tell and co-workers showed a strong nucleolar pattern for APE1, maybe due to the protein–protein or protein-nucleic acids interactions in this compartment. [86].

Despite the nuclear targeting sequence, a large number of studies indicated that in some cell types, with elevated metabolic and proliferative rates, APE1 localize within mitochondria and endoplasmic reticulum [82,133]. Up to now a classic nuclear export sequence (NES) has not been found so the exact mechanism responsible for redirecting APE1 in the cytosol remains to be clearly elucidated. Recently, two different mechanisms were proposed to be responsible for the cytoplasmic translocation of APE1. S-nitrosation at Cys93 and Cys310 has been demonstrated to redirect APE1 in the cytoplasm in a CRM1-dependent manner [129] and a non-canonical mitochondrial targeting sequence has been found in the APE1 C-terminal domain (residues 289-318) [134].

Mitochondria are the main cellular source of ROS and mtDNA is vulnerable due to the lack of histones and the proximity to the ETC. Thus, it has not been surprising the observation of different groups regarding the existence of a DNA base excision repair (mtBER) within mitochondria [130,135,136]. Togheter with the mtBER apparatus, also APE1 has been found in mitochondria. One first study from Chattopardhay and coworkers hypothesized that the truncation of the N-terminal domain of the protein allows the protein to be imported in mitochondria, due to the lack of the NLS [137]. However, more recent studies show that in different cell types APE1 full length is imported within mitochondria [67,138].

All together, these data suggest that APE1's subcellular distribution is very dynamic process (Figure 20), and the purpose of this thesis is to elucidate the role of DRS in the trafficking of APE1 within the mitocohondrial compartment and the maintenance of mitochondrial DNA stability.

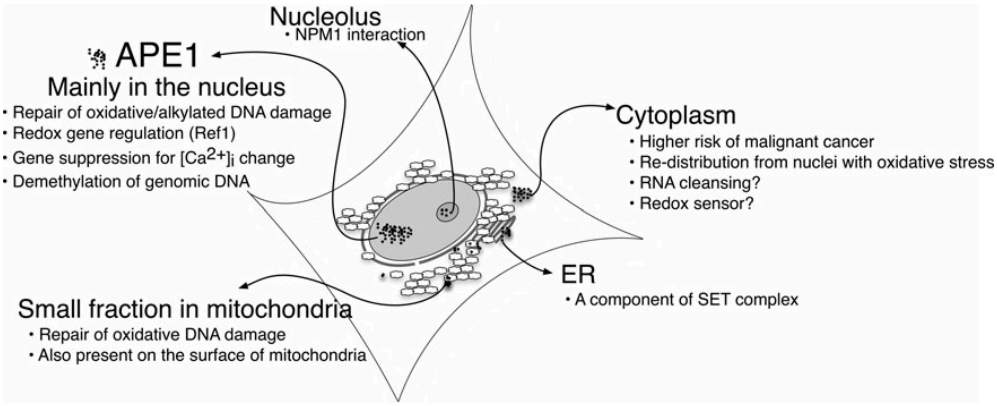

Figure 20: APE1 intracellular trafficking. APE1 subcellular distribution appears very dynamic. The main subcellular compartments where APE1 have been identified and its influence on cell physiology are highlighted. (Image from Scott et al. 2013).

4.6 APE1 in cancer

APE1 is a fundamental protein: deletion of both the alleles of Apex1 leads to embryonic lethality in mice [139] and triggers apoptosis in differentiated cells [140], suggesting its biological and clinical relevance in normal and tumoral cells. Defects in its activities have been linked to human pathologies, ranging from cancer to neurodegenerative diseases.

Accumulation of oxidative stress and inefficient base excision DNA repair have been described for several degenerative disorders, including neurophatologies as Alzheimer disease (AD), Parkinson disease (PD) or amyotrophic lateral sclerosis (ALS) [141,142]. Several observations suggest that an overexpression or an aberrant localization of APE1 is linked with cancer. APE1's deficiency could lead to augmented mutagenensis and carcinogen susceptibility, due to the lack of a proper endonuclease activity on the BER pathway. Moreover, dysregulation in terms of atypical subcellular localization or expression, have been found in many cancers types, including prostate, pancreatic, ovarian, cervical and colon type [92,143]. Indeed, APE1's cytoplasmic relocalization and/or overexpression is associated with more aggressive pathology, reduced sensitivity to chemotherapeutic agents and a poor prognosis for the patients [144]. The causes of this phenotype are still unknown. However, since one of the features of cancer cells is the high metabolic rate and the elevated amounts of ROS produced from the ETC, the hypothesis is that APE1 could have a role on the maintenance of the mtDNA integrity inside the mitochondrial compartment [145].

Nowadays, APE1 represents a predictive marker for sensitivity of the tumor toward radio- or chemotherapy and a promising target for pharmacological treatment. The studies to determine the effect of inhibiting either the DNA repair or redox regulatory functions are still ongoing, and several studies suggest that the increase of AP activity accompanying tumorigenesis could explain the therapy resistance of these pathologies. APE1's inhibitors could be used alone or in combination with other chemotherapeutic agent such as bleomycin, temozolomide or gemcitabine to enhance the cytotoxic effects [146]. Few compounds were already reported as APE1's redox (soy isoflavones, resveratrol and E3330) and DNA repair (CRT0044876, lucanthone, methoxyamine, compound 3 and 52) inhibitors [143,147]. Further studies are needed to identify new potent APE1 small molecule inhibitors, specific for one function of the protein, and to evaluate the side effects of combination therapies with APE1 inhibitors.

5. The nucleoid

Given their endosymbiotic bacterial origins, it is not surprising that the organization of DNA in mitochondria is similar to that of bacterial DNA. Bacterial genome is compacted by 104-fold of its volume to form the bacterial nucleoid and in a similar way the mitochondrial DNA is compacted and organized in discrete protein-DNA complexes distributed throughout the mitochondrial matrix [148].
mtDNA was first described in the 1960s [149] and completely sequenced in 1981 by Anderson [150]. Despite the differences between nucleoids in mammals and in yeast, most of the information on the structure and composition of the nucleoid comes from the studies on yeast that were fundamental and extremely informative in the understanding of the mammalian nucleoids. During the 1970s scientists were able to stain the mtDNA in vivo and notice sub-mitochondrial structures near the inner membrane, later called nucleoids, were the mtDNA was located. Each nucleoid can contain more than one mtDNA molecule and each mitochondrion can contain tens (for yeast) or hundreds (for mammalians) nucleoids. Moreover each nucleoid can be considered as the unit of genetic segregation in the mitochondria, as every nucleoid act as an independent genetic unit from the others.
Although the mtDNA is the principal component and the one of greater interest of the nucleoid, this is not the only molecule composing this unit. The mitochondrial nucleoid is composed of a range of proteins with a diverse variety of functions that have coevolved with mtDNA, from DNA packaging and transcription to factors with broader signalling functions facilitating mtDNA's integration into cell-wide metabolic and proliferative signalling networks. Moreover the mtDNA organization in nucleoids provides an efficient way to ensure that the mitochondrial genetic material is distributed throughout all the mitochondria in a cell and is responsive to cellular metabolic needs.

5.1 Mitochondrial genome

Mitochondrial DNA comprises 0.1-2% of the total DNA in most mammalian cells. There are several unique features of the mtDNA: in humans is circular, 16 kb long and inherited by the mother. It encodes two rRNAs, 22 tRNAs and 13 proteins, all of which are involved in the oxidative phosphorylation process (e.g. components of Complex I, Complex IV, Complex V and cytochrome *b*) [151]. As said before all others mitochondrial proteins are nuclear encoded. Another peculiarity of the mtDNA is its structure: mtDNA is double-stranded but the genetic information is not equally distributed between the two strands, most the information is contained in the heavy strand (purine rich) [152]. The intragenic sequence is almost absent or limited to a few bases [153] and moreover mtDNA do not have histones, instead is organised in nucleoids structures, as mentioned before.

5.2 mtDNA organization in nucleoids

The first evidence of the organization of the mtDNA in discrete foci within the mitochondrial network in mammals has come from DAPI staining of HeLa cells mitochondria in 1991 [154]. This observation was further proved a few years later with the use of Picogreen [155] and confirmed by FISH experiments for the specific detection of mtDNA sequences [156]. Another confirmation has come from time-lapse imaging experiments were it was possible to observe that larger-sized nucleoids were able to divide in smaller units [157,158] and bromodeoxyuridine (BrdU) incorporation experiments suggested also that replicating DNA can occur in these structures [157].
A large number of experiments showed that multiple copies of mtDNA could be found in each nucleoid, usually from 2 to 10 copies each, depending on the cell line studied [157]. However, quantitative analysis of the size and mtDNA content of the nucleoid in cultured mammalian cells suggests that an average nucleoid may contain 5-7 mtDNA molecules packed in a space of 70nm [157], similarly at what happens to the bacterial genome. The tight packaging of the mtDNA is achieved thanks to the proteins present in the nucleoid that will be described later on in this chapter. Another

similarity with the bacterial DNA comes from the fact that both genomes seem to be membrane-bound with the help of specific protein partners. In the case of the mtDNA the concept of that the DNA could be physically bounded to the membrane was introduced right after the mtDNA discovery [159] and a lot of work was done trying to identify the protein responsible for this feature.

5.3 Nucleoids protein composition

As said before nucleoids are discrete protein-DNA units. The principal proteins that compose the nucleoid structure are proteins specifically associated with the DNA.
Different studies have tried to identify the proteome of nucleoids in different cells lines, with different approaches [160]. The first attempt to do such an analysis was made by Bogenhagen et al. in 2003, in *Xenopus* oocytes and since then a plethora of studies have identified and classified nucleoid associated components through biochemical fractionation studies. A number of proteins have been characterized for their role in different steps of mtDNA metabolism. It remains, however, to be elucidated whether or not all proteins involved in the different processes are permanently associated with the nucleoid even if their function is not always required or if dynamic association and dissociation events can occur. Recently a "layered-structure" (Figure 21) of the nucleoid was proposed based on the work of Bogenhagen *et al*. [161]. In this study they adopted a different procedure for the isolation of nucleoids intended to identify proteins in close association with the mtDNA [162].
Cross-linking with formaldehyde allowed to identify a subset of proteins more closely in contact with the DNA such as mtSSB and TFAM as expected, but also other proteins such as DNA polymerase g, mtRNA polymerase and a small number of other proteins considered now the components of the nucleoid core [160,161]. Other components of the nucleoids were identified as associated with the DNA in native preparation, but not in the cross-linked preparation. The most interesting of these proteins is ATAD3 that seems to be the candidate for the attachment of the mtDNA to the inner membrane. A variety of other proteins were found to be in the nucleoid ranging over proteins needed for the mtDNA maintenance, replication and repair, to proteins belonging to mitochondrial transcription and translation processes. Transcription factors and replication related proteins, such as TFB1M, TFB2M mTERF, Pol g A, B and Twinkle, were found to be in native preparations, suggesting that the transcription of the mtDNA occurs in the core of the nucleoids [160,161]. Proteins involved in mitochondrial translation were found in both native and cross-linked nucleoids fraction suggesting a less tight interaction with the protein of the core, indeed some mitoribosomal proteins, initiation and elongation factors are part of the peripheral part of the nucleoids. mtDNA repair proteins are also part of the nucleoid proteome. Among those there are the endonuclease APE1, DNA ligase III, a set of DNA glycosylases (NEIL1, OGG1, NTH1), BRCA1 and quite a few others. More recently, Cockayne syndrome group B protein (CSB) has been suggested to take part in base excision repair and in anchoring a DNA repair complex to the inner mitochondrial membrane with possible association to nucleoids [160,162].
Overall, based on these results, they suggest that DNA replication and transcription can occur in the central core of the nucleoid, while RNA processing, translation and respiratory chain complexes assembly may occur in a peripheral zone [161]. This is also in accordance with more recent studies that have identified mitochondrial RNA granules as entities located in close proximity to the nucleoids were this last processes can take place (Figure 23) [163].

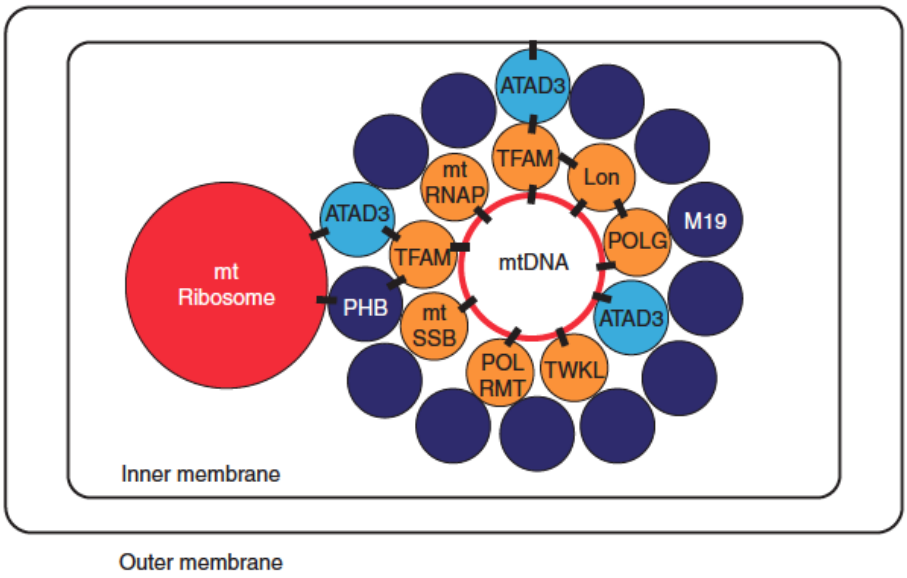

Figure 21. Schematic of interactions at the mitochondrial nucleoid. Core nucleoid factors (gold) have known mtDNA-binding activity. Peripheral factors (blue) do not directly interact with mtDNA, but associate with the nucleoid via protein–protein interactions. ATAD3 (light blue) associates with mtDNA, the mitochondrial ribosome, and the mitochondrial inner membrane. Shown protein–protein and DNA–protein interactions are designated by black rectangles [164].

Historically, the first protein identified in this context was Twinkle [165] that was discovered in 2001 and was shown to co-localize with mtDNA, while between the 70s and 80s the two principal proteins, tightly associated with the DNA were discovered: mtSSB and TFAM. This two proteins were the only two candidates resistant to high salt washes during the isolation of the mtDNA [166–170].

mtSSB is the mitochondrial counterpart of the SSB protein (single-stranded DNA binding proteins, the mammalian Rim1P homolog) [171] in the nucleus and of SSB protein in bacteria. It is able to bind the single-stranded filament of the DNA while is not complemented with the other filament, to protect DNA for any kind of injury. mtSSB is an essential protein of mtDNA maintenance as it was shown to stabilize the replication intermediates and the D-loop structure [172]. The presence of the protein in the nucleoids was showed in cell culture in mammals [173]. and was confirmed by mass spectrometry experiments [174].

The best-characterized and abundant protein binding duplex DNA is the HMG-box protein TFAM (Transcription factor A) that was identified as permanently associated with mtDNA [175].

TFAM is the only factor that plays a clear structural role in the mtDNA organization in the nucleoids, similar to the role of histones for the nDNA in the nucleus or to the role of the hisones-like proteins in bacteria [176,177]. This protein is probably the major factor responsible of the tight packaging of the mtDNA and thus plays a role in the mtDNA topology [178].

TFAM is able to bind the double helix of the DNA and act as a packaging protein, probably mostly on the central region of the mtDNA because the estimation of TFAM concentration is too low for the coverage of the entire mtDNA molecule [176,179,180]. From the first calculations was estimated that one molecule of TFAM can bind the DNA in regular intervals each 20 bp [181–183] but since the protein acts as a homodimer in the cell it was estimated that 2 molecules of TFAM bind the DNA each 35-40 bp [181,182]. However, it seems that TFAM can bind mtDNA with some sequence specificity allowing the interaction to be detected by DNase I footprinting [176,184]. Still a number of laboratories have quantified the stoichiometry of TFAM binding to mtDNA with very different results depending on the cell type

and organism studied. Some studies have suggested that there is sufficient TFAM to coat the mtDNA [185] while others have reported much lower levels. An interesting study by Bogenhagen *et al.* showed that the ratio TFAM/mtDNA is developmentally regulated in *Xenupus* oocytes, suggesting that immature oocytes that are actively replicating and transcribing DNA have a lower ratio TFAM/mtDNA. On the contrary, in mature oocytes where mtDNA replication and transcription is repressed there is an accumulation of TFAM with an increased TFAM/mtDNA ratio [186]. Somatic cell types generally require active transcription of mtDNA, so it is probable that they have a much lower TFAM/mtDNA ratio to provide subunits of the OXPHOS complexes and replication for mtDNA turnover [186]. TFAM has also a role in mtDNA transcription, in fact it markedly stimulates transcription initiation [187].

5.4 mtDNA damage and repair

Because of the lack of histones and chromatin structure and the proximity to the electron transport chain (ETC) the mtDNA is prone to the oxidative damage caused by the endogenous ROS produced by the ETC [188]. Mitochondrial DNA suffers damage from a greater extent than does nuclear DNA [189]. Because the mitochondrial membrane potential generates a negative charge on the matrix side of the inner membrane lipophilic cations, like many drugs and toxic chemicals, tend to accumulate inside mitochondria, specifically on mitochondrial membranes, so mitochondria import lipophilic cations from the cytosol and concentrate them up to 1000-fold becoming dangerous for mitochondria and cell survival [190].

Oxidative damage to mtDNA may occur in the form of base modification, abasic sites and other various types of lesions [191]. One of the most studied and common lesions due to the presence of ROS is the 8-oxoguanine (8-oxoG). 8-oxoG has been found to be a mutagenic lesion: mispairing of 8-oxoG with adenine results in a G-C to A-T transversion mutation during the subsequent round of replication. Early studies described 16-fold higher levels of 8-oxoG in mtDNA than in nuclear DNA [192] and that mtDNA damage is more extensive and persist longer than nuclear DNA damage in human cells following oxidative stress [193].

Initially it was thought that DNA repair mechanisms were either non-existent or very inefficient in mitochondria and that damaged molecules of mtDNA were just simply degraded and the undamaged copies serves as template for the new mtDNA synthesis [194]. However, recently studies have proved the presence of DNA repair pathways that can efficiently repair certain types of lesions [195]. Among these, the major repair pathway present in mitochondria is the BER pathway (mtBER). DNA repair enzymes belonging to the BER pathway isolated from mitochondria include several types of glycosylases, as OGG1, UDG, MUTY and NTH [196–200] the AP endonuclease APE1 [82,201] and DNA ligase III [135,202] (Figure 22). Other proteins necessary for mtDNA repair were discovered to be strictly involved in these mitochondrial pathways without a nuclear homolog as DNA helicase Twinkle and DNA polymerase γ (Polγ) [203].

In addition to the BER there are other pathways involved in the mtDNA repair such as Mismatch repair pathway (MMR) [204] and also the homologous recombination (HR) [205] and non-homologous end joining (NHEJ) [206] were described to be present in mitochondria.

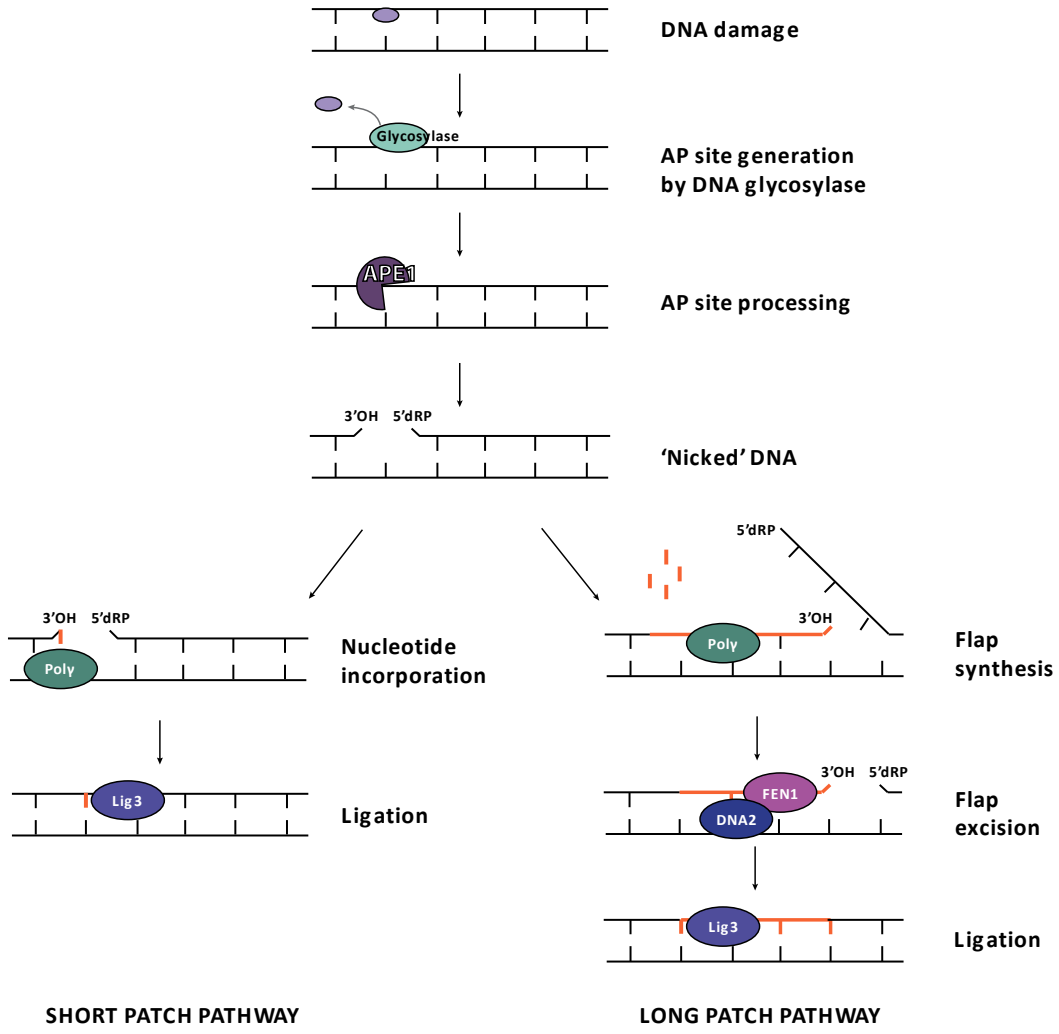

Figure 22: mtBER pathway. mtBER pathway resembles the nuclear one. Both the SN-BER and LP-BER subpathways are present in the mitochondria. All of the enzymes are nuclear encoded and imported into the organelle, some are common between the nBER and mtBER, like APE1, all the glycosylases and FEN1, others, like Pol γ DNA2 and DNA ligase III are specifically dedicated to the mtDNA repair (Adapted from Copeland et al. 2008).

6. The mitochondrial RNA granules (MRGs): regulation and coordination of mitochondrial gene expression

From their synthesis to their degradation mtRNA undergo several stages of maturation and modification for the correct production of mtDNA-encoded proteins. As mitochondrial DNA replication and transcription need to be spatiotemporal regulated to adapt to metabolic demand of the cell, the same must be for the basic stages of mitochondrial gene expression. To achieve this mitochondria have restricted mtRNA processing and maturation to dynamic nucleoprotein structures called mitochondrial RNA granules (MRGs), that may provide the regulatory function for the post-transcriptional processing allowing all the mtRNAs to be fully mature before release for use in protein synthesis [207,208].

6.1 Mitochondrial RNA granules protein composition

Experiments performed with 5-bromouridine (BrU) aimed at tracking the progress of the nascent RNA transcripts showed that newly transcribed mtRNAs are found in discrete foci situated in close proximity to mitochondrial nucleoids (Figure 23) [157,209,210]. To confirm and better understand the function of this structures in 2015 Antonicka et al. [211] characterized the proteome of the granules using GRSF1, a core component of the granule already described [209,210], as a bate. Some proteins found by the authors were already confirmed by the literature as RNaseP [210] and more interestingly the so called "mitochondrial degradosome" composed by hSUV3 and PNPase [212] confirming the hypothesis that MRGs are not only sites of RNA processing, but also of RNA degradation and turnover. Mass spectrometry analysis of the immunoprecipitated fraction showed a large number of proteins responsible for the post transcriptional processing of the primary polycistronic transcript as MRPP1, 2 and 3, RNA-modifying enzymes as TFB1M, PTCD3, and the mitochondrial poly-A polymerase.
Also proteins belonging to the mitochondrial translation machinery were present in the analysis as well as structural proteins of the small (mt-SSU) and large (mt-LSU) mitochondrial ribosomal subunits, aminoacyl tRNA synthetases, and factors involved in ribosome assembly and disassembly. These data suggest that MRGs are also involved in mitochondrial ribosome biogenesis and in mitochondrial translation regulation, with a function analogous to that of the nucleolus where initial steps of ribosomal assembly are performed [213,214]. Fractionation experiments suggested that nucleoids co-purify with mitochondrial factors involved in mtRNA metabolism, mitoribosome biogenesis and translation as well as with mitochondrial ribosomal proteins. As said before the latter has also been found in MRGs [161,215,216], so it has been suggested that early steps of mitoribosome assembly of MRPs occur in concert with mt-rRNA nucleotide modifications [217,218]. This protein content overlap between the nucleoid and the MRGs suggest an intimate association of these two entities.
It is possible that both mtDNA and its transcription products are portioned within non-membrane bound compartments to provide a greater degree of spatiotemporal regulation of mtRNA processing. It was in fact suggested by Jourdain and colleagues that immature RNA could be sequestered in the MRGs, away from mitochondrial translation process [219].
Also the last stage of the mtRNA life was suggested to take place in specific foci, called D-foci (degradation foci) composed mostly by the mitochondrial degradosome [212,220]. It has been shown that these foci co-localize with the MRGs, although it is still not clear whether they form a subset of MRGs or are separate entities with a distinct composition and purpose. Also several catalytic mitochondrial enzymes and other mitochondrial and non-mitochondrial proteins whose role remains to be established were found (Figure 23).

Figure 23: Rapresentation of nucleoids and mitochondria RNA granules in the mitochondrial matrix. mtDNA in contained in nucleoids, where also transcription of mt-mtRNA take place. Mitochondria RNA granules host the nucleolytic processing of the primary transcrtipt, maturation and modification of mt-mRNAs, mt-rRNAs and mt-tRNAs and mitoribosome assembly. Decay of mt-mRNA seems to take place in foci co-localized with MRGs called D-foci, in which the degradosome can degrade the used and eventually damaged RNA.

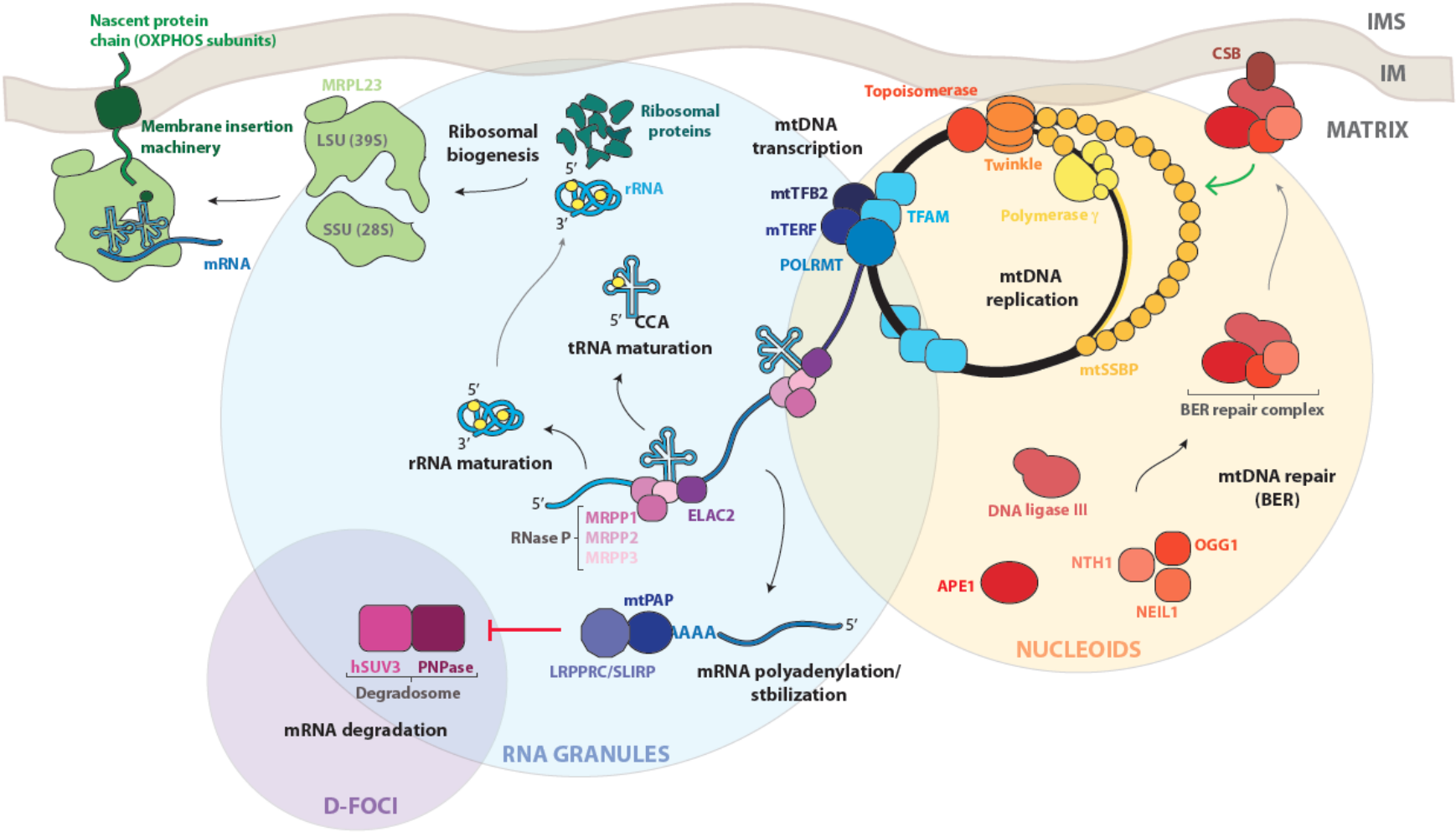
Nascent protein chain (OXPHOS subunits)
IMS
IM
MATRIX
CSB
Topoisomerase
Twinkle
Polymerase γ
TFAM
mtTFB2
mTERF
POLRMT
mtDNA transcription
mtDNA replication
mtSSBP
BER repair complex
mtDNA repair (BER)
DNA ligase III
APE1
NTH1
OGG1
NEIL1
NUCLEOIDS
MRPL23
LSU (39S)
SSU (28S)
Membrane insertion machinery
mRNA
Ribosomal biogenesis
Ribosomal proteins
rRNA
5′
3′
CCA
tRNA maturation
rRNA maturation
RNase P
MRPP1
MRPP2
MRPP3
ELAC2
mtPAP
AAAA
LRPPRC/SLIRP
mRNA polyadenylation/ stbilization
hSUV3
PNPase
Degradosome
mRNA degradation
RNA GRANULES
D-FOCI

7. mtRNA processing and metabolism

7.1 mtRNA transcription and regulation

mtDNA is transcribed as two unique, polycistronic molecules. Because both strands of the DNA contain genes, both strands are transcribed [153].

Since 1982 it was believed that transcription takes origin from the HSP1 and HSP2 (H-strand promoter 1 and 2) in the heavy-strand and from LSP1 (L-strand 1) in the light-strand [221,222]. The theory was that starting from HSP1, just upstream the mt-tRNA^{Phe}, only the two mt-rRNAs and two mt-tRNAs (Val, Leu) were transcribed from this point and the transcription was blocked at the mTERF1 sequence. Instead the majority of the molecule is transcribed from HSP2 that gives origin to a transcript that comprehends almost all the length of the mtDNA [223–225].

Indeed more recently was described a KO mouse for mTERF1 that does not present any defect in the H-strand transcription but tend to accumulate more antisense RNA species, meaning that mtTERF1 is probability used to terminates the L-strand transcript, preventing the formation of this antisense species [226]. Probably HSP1 and LSP1 only are responsible and sufficient for the transcription start.

Regarding the transcription of the light-strand, LSP1 is the unique site where the transcription can start, although the majority of initiation events from this site stop 200 bp downstream the promoter, at the CSB2 site (conserved sequence block 2) [227]. It seems that this short RNA strand is only used as an "RNA primer" by the polymerase to start the lagging-strand replication of the mtDNA [228].

The basal machinery for the mtDNA transcription has been well studied in mammals and it is composed by a single subunit of the RNA polymerase (POLRMT) [229,230] and the transcription factors TFB1M and TFB2M [231,232]. While the first one possesses a dimethyl-transferase function [233] , the second is needed for the transcription initiation [231,234]. In humans also TFAM and the transcription elongation factor TFEM are required for the process [231,235,236]. Also MRPL12, acting as a complex with POLMRT and TFEM, is needed for the processivity of the elongation phase and to prevent the termination of the transcription at CSB2 [236–238].

7.2 Transcript processing

The transcription of mtDNA gives rise to two polycistronic transcripts that must be somehow processed to release the different RNA species. As shown in Figure 24, most of the mRNAs and mt-rRNAs-coding regions are separated by mt-tRNAs. This RNAs are separated by each other according to the generally accepted mt-tRNA punctuation model [150,153].

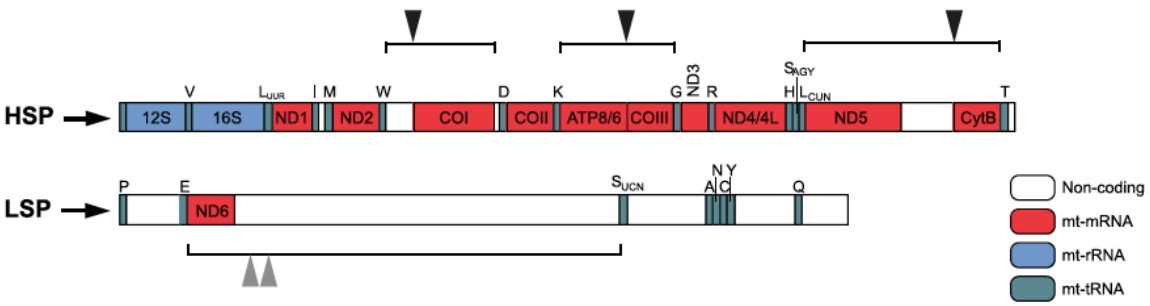

Figure 24: Schematic representation of the mitochondrial polycistronic transcript. mtRNA is transcribed in two polycistronic transcripts. The one transcribed from the HSP promoter contains 12 ORFs encoding 12 subunits of the OXPHOS complexes, the two ribosomal RNAS and 13 tRNAs, while the primary transcript transcribed from the LSP promoter encodes for only one

protein and 8 tRNAs. Black and grey triangles indicate the non-canonical junction between the gens that are not following the tRNA punctuation model (Image from Van Haute et al., 2015).

The mitochondrial RNA-processing machinery initiates the cleavage of the mt-tRNAs sequences freeing the mt-rRNAs or mt-mRNAs that they intersperse. However not all the mRNA and are flanked by a mt-tRNA coding sequence, as ATP6/8 and COIII or ND5 and Cyt B (Figure 24). Although it was reported the pentatricopeptide protein (PTCD2) seems to be involved in the processing of some of this RNAs as well as FASTKD5, the exact process by which these species are released is still unclear and object of study [211,240].

It has been recently proposed that the early stages of the mitochondrial transcription can take place co-transcriptionally inside the mitochondrial RNA granules. Indeed most of the proteins involved in the mt-RNAs processing were found to be part of the MRGs proteome [210,241,242].

In particular the 5'-end of the mt-tRNAs is processed by the protein complex RNaseP, composed by MRPP1, 2 and 3 that are found in the granules [210,243]. MRPP1 is a m^1G9-methylase, while MRPP2 is a dehydrogenase also involved in the other cellular functions [244]. These two proteins form a subcomplex that also participate in the tRNA modification [245]. MRPP3 is responsible for the hydrolysis of the phosphodiester bond [246]. The KO of any of this proteins cause an accumulation of the RNA precursor molecule, reducing the stedy-state levels of the mature form of mt-tRNAs and some mt-mRNAs (Figure 25) [247].

On the other hand RNaseZ or ELAC2 is responsible for the 3'-end processing of the mt-tRNAs, however this protein was not found to be part of the MRGs proteome [248,249]. It was then proposed that the primary transcripts undergo a first round of processing partially co-transcriptionally inside the MRGs, while a second part of the maturation takes place later and outside the granules. Also in this case the knockout of the protein can cause the accumulation of mt-RNAs precursors (Figure 25) [247,249].

Recently, other proteins were described in the MRGs that could have a function in the processing of the primary transcript. GRSF1 (G-rich sequence factor 1) is a RNA-binding protein, shown to co-localize with the newly synthesised mt-RNA and with MRPP1. The loss of the protein results in a decrease of the mature form of some transcripts [210,241]. PTCD1 is another protein implicated in the mt-RNA metabolism. It seems that this protein has a role in the coordination of the 3'-end processing and directly interacts with RNaseZ [247,250].

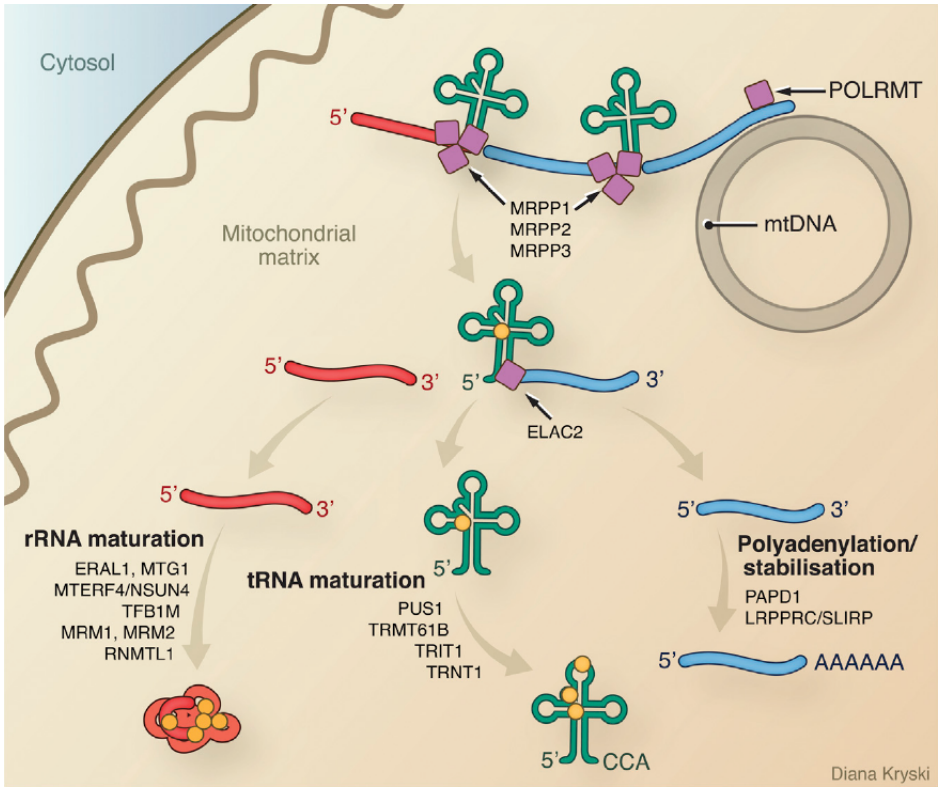

Figure 25: post-transcriptional maturation of mtDNA encoded RNAs. The primary transcript resulting from transcription is processed to release the individual mt-mRNAs, mt-tRNAs and mt-rRNAs. The mitochondrial RNaseP consists of three subunits (MRPP1, 2 and 3) and cleaves the primary transcripts at the 5'-end of tRNAs. tRNAs are then relased after cleavage of their 3'-end by RNaseZ (ELAC2). Yellow dots represent RNA modofications (Image from Hällberg and Larsson, 2014).

7.3 mt-tRNA processing and modification

mt-tRNAs released form the primary transcript need to reach their mature form and stabilised conformation to be used during the translation process. mt-tRNAs undergo a different variety of chemical modifications that can be divided in to two categories: the ones able to confer the tRNA the correct structural stability and folding and the ones that coordinate the proper tRNA function altering their interaction with other factors (Figure 26) [239].

One of the most important modifications found on the mt-tRNAs is found in the residues 34 and 37 that result modified in almost all the tRNAs studied so far. The residue 34, indeed, is one of the three that matches with the corresponding base in the mRNA that has to be translated. Because of the degeneracy of genetic code we know that multiple codons must be recognised by a single tRNA. Degenerate codons contain the same 1st and 2nd positions as the others but contain a different 3rd position. Base in position 34 is the one that will pair with the 3rd base of the codon in the mRNA, and to allow this recognition the interactions between this two bases are non-standard, so the base can "wobble" [239].

This position is often occupied by a U, which can pair with any of the four bases. However not always this is sufficient for the tRNA to correctly recognize the right codon, in some cases the presence of a purine or a pyrimidine in position 3 produces codons for different amino acids. The increase in the

discrimination by the wobble base required for accurate decoding is achieved through its post-transcriptional modification [252].

Several enzymes are imported into the mitochondrial matrix to modify these bases so that the mt-tRNAs can reach their mature form. GTPBP3 (GTP binding protein 3) [253], MTO1 (mitochondrial tRNA translation optimization 1) [254] and MTU1 (mitochondrial tRNA-specific 2-thiouridylase, TRMU) [255] that favour the base pairing with purines, preventing misreading phenomena.

For the correct achievement of the translation efficiency sometimes also base 37 of the t-RNAs should be modified. This base is substrate of different enzymes like TRIT1 (tRNA isopentenyltransferase 1) [256] and TRMT5 (tRNA isopentenyltransferase 5) [257] and then of CDK5RAP1 (Cyclin-dependent kinase 5 regulatory subunit associated protein 1) [258].

Another fundamental modification that tRNAs undergo to assure the correct aminoacylation in the acceptor helix are the modification of the discriminator base at the position 73 and the addition post-transcriptionally of the CCA codon by TRNT1 [259].

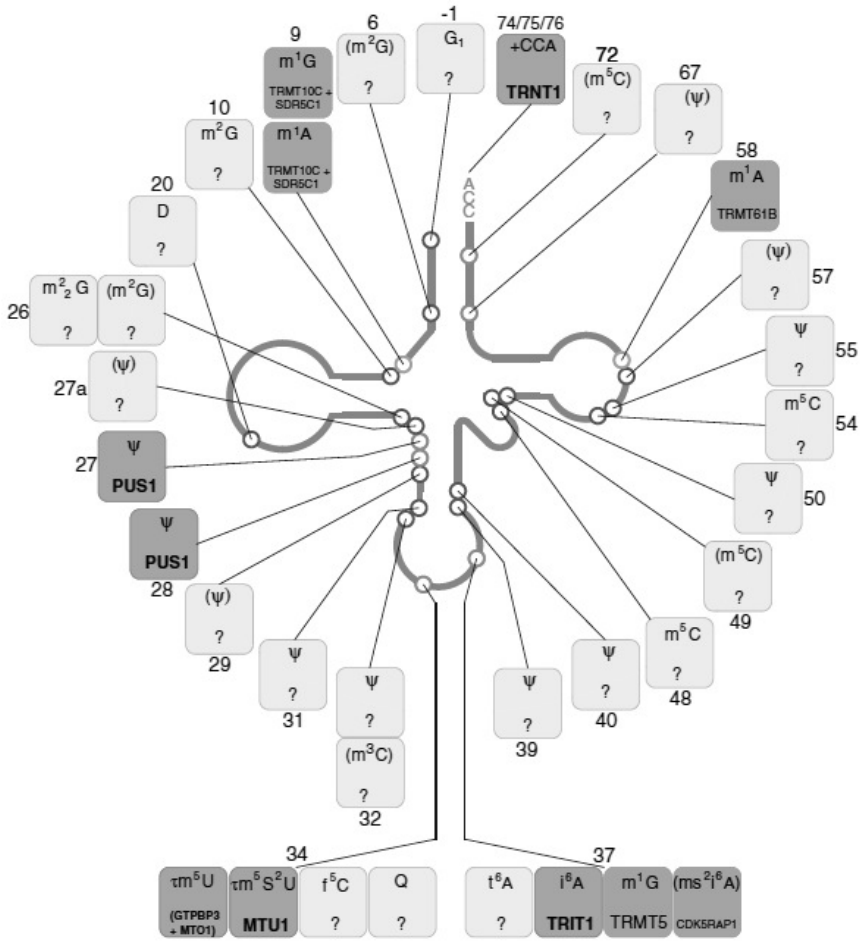

Figure 26: Post-transcriptional modification of mitochondrial tRNAs. An example of a tRNA is represented in its secondary structure indicating the post-tracriptionary modificated bases with a circle. The details of chemical modification and the enzyme responsible (if known) for each mt-tRNA position are given in boxes, indicating the base position number next to each box (Image from Van Haute et al., 2015).

7.4 mt-rRNA modification

The mammalian mitochondrial ribosome is composed, as the cytosolic one, by two subunits of different sizes, the small subunit 28S (mtSSU) and the large subunit 39S (mtLSU) [260–263]. Both of them are composed by the mitochondrial-encoded rRNAs 12S and 16S respectively, and the ribosomal proteins that are codified by nuclear genes and are imported to the mitochondrial matrix. As all the other rRNAs, mitochondrial rRNAs undergoe post-transcriptional modifications to be functional, but differently from the cytosolic ones, the range of modifications is less wide and they do not need any nucleolytic processing (Figure 27) [239,264,265].

7.4.1 Maturation of the 12S mt-rRNA

Only five nucleotide modifications were found in the 12S rRNA: methylation of one uracil base (m^5U429), methylation of two cytosine bases (m^4C839 and m^5C841), and dimethylation of two adenine bases ($m^6{}_2A963$ and $m^6{}_2A937$) [266]. However, until now only two of these modifications were characterized.

TFB1M is the enzyme responsible for the methylation of the two adenines that are located in the loop-structure (Figure 27, right part) [267,268]. In bacteria this part is responsible for the binding site of the large subunit [269], in humans the lack of this enzyme causes a decline of the mature levels of 12S, leading to a deficiency of assembled mtSSU and results in an impairment of mitochondrial translation [268].

NSUN4 (NOP2/sun domain containing family, member 4) is the enzyme that is responsible for the methylation of the cytosine residue in position 841 [270,271]. This modification is fundamental for the 12S folding in cooperation with the methylation in position 839.

The enzymes responsible for the methylation in position 429 and 339 have not been identified yet.

7.4.2 Maturation of the 16S mt-rRNA

As the 12S rRNA, also 16S rRNA do not need any nucleolytic cleavage to be fully functional, but 4 bases were found to be modified. Two methylation of guanosine (Gm1145 and Gm1370), one ribose methylation of uridine (Um1369) and one pseudouridylated base (Psi1397) were described [272,273].

Methylation on the 2'-O-ribose of Gm1145 is catalysed by MRM1 and this enzyme is part of the MRG proteome [242,274,275]. In yeast this methylation is fundamental for the stability of the large ribosomal subunit and for the ribosomal function [276].

The other two methylated sites are located in the A-loop that is an essential component of the peptidyl transferase centre in the large subunit, and are involved in the interaction with the aminoacyl site of the mt-tRNA [264]. G1370 and U1369 are modified by MRM2 and MRM3 respectively [242,274,275]. As in the case of MRM1, both these enzymes are localised in the MRGs and are crucial for the success of mitochondrial translation and OXPHOS function. Loss of one of these two enzymes result in an aberrant assembly of the LSU and consequent ineffective translation process [275].

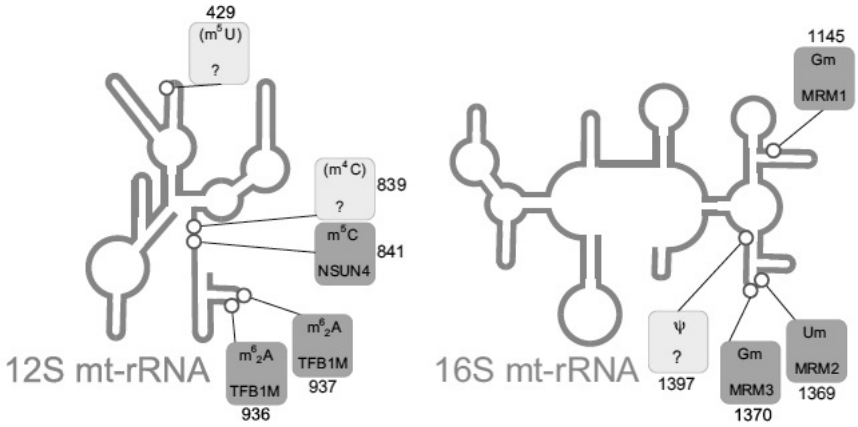

Figure 27: Post-transcriptional modifications of mitochondrial ribosomal RNAs. Schematics of the secondary structure of 12S and 16S mt-rRNAs indicating post-transcriptionally modified bases (circles) are shown. The details of chemical modification and the enzyme responsible (if known) for each mt-tRNA position are given in boxes, indicating the base position number next to each box (Image from Van Haute et al., 2015).

7.5 mt-mRNA processing and metabolism

mt-mRNAs are released from the primary transcript as described before, however, differently from the nuclear-encoded mRNAs, this molecules undergo a much simpler post-transcriptional modification. Stabilization of the mitochondrial mRNAs is very different and simpler than the stabilization process that take place for the nuclear-encoded mRNAs, while the degradation process have some hints that could remind the compartmentalisation and the degradation process that takes place in the cytoplasm [239].

7.5.1 mt-mRNA polyadenilation

The first difference that we can find between the maturation process of the nuclear-encoded mRNAs and the mitochondrial ones is the lack of 5'CAP modification as well as the absence of introns.

3'-end of mt-mRNAs is modified to have a poly-A tail much shorter than nuclear mRNAs that can go from 45 to 55 nucleotides, with some exceptions [277]. Indeed ND6 mRNA was found not to have a poly-A tail and is immediately competent for translation, while ND5 can be either oligo-adenilated or not adenilated at all [277].

Poly-A tails are synthesised by a non-canonical poly-A polymerase (mtPAP) that localize in MRGs suggesting again that the first maturation steps take place co-transcriptionally in the granules [278–281]. Knockdown of mtPAP or a decrease in the polyadenilation lead to an impaired mitochondrial translation and the disruption of the mitochondrial respiratory function [279].

The exact role of poly-A tail in mitochondrial transcripts is still unclear [282]. Seven out of 13 mt-mRNAs do not encode a complete stop codon for translation termination. Most of them are cut out when the mt-tRNAs are nucleolitically cleaved from the primary transcript often leaving a "U" or "UA". For this reason, it was suggested that the poly-A tail added after that cleavage has the function to complete the stop codons (Figure28) [150,153].

Although the classical role of the poly-A tail is to stabilise and increase the half-life of the transcripts, in the mitochondrial compartment this is not always the case. It was shown that poly-A tail could decrease the stability of COI, COII, COIII and ATP6/8, while it increases the stability of ND1, ND2,

ND3, ND4, ND4L, ND5 and Cyt. B. The mechanism by which this transcript-specific role of polyadenilation remains to be elucidated [283–285].

The phosphodiesterase 12 (PDE12), a mitochondrial 2' and 3' phosphodiesterase [283,286], is the protein responsible for the removal of the poly-A tail, but this activity was shown only *in vitro* and in cultured cells, after over-expression of the protein [283].

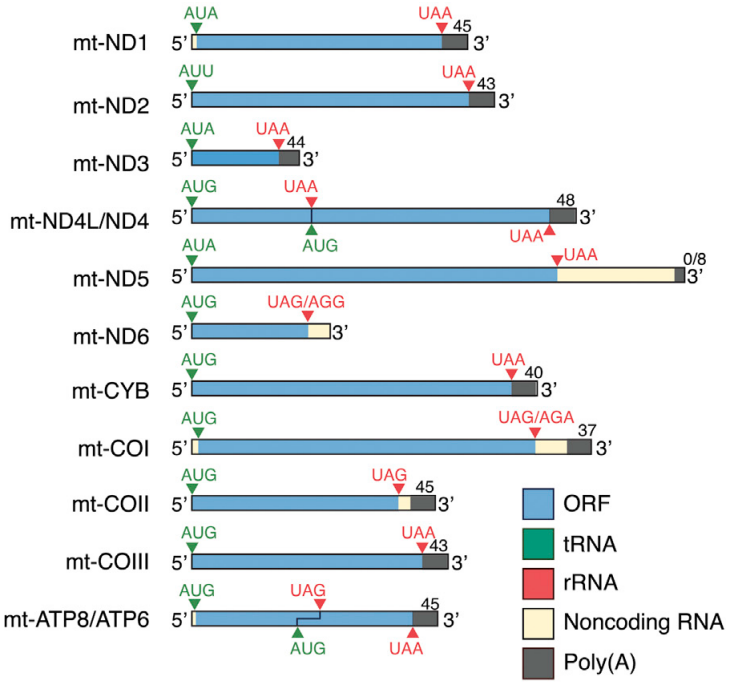

Figure 28: Messanger RNAs encoded by mitochondrial DNA. The mRNAs contains no or short 5' non-coding sequences (yellow) preceding the first translation initiation codon (AGA, AGG, UAA, UAG) and short poly-A tail. Two of the mRNAa (ND4/ND4L and ATP6/ATP8) are bicistronic, and each contains two partly overlapping ORFs. The structure of each human mRNA is shown (Image from Hällberg and Larsson, 2014).

7.5.2 mt-mRNA stability and decay

Regulation of mRNA stability and turnover are fundamental in the control of gene expression and are usually mediated by protein complexes. The best characterised protein complex that is involved in the mtRNA stability is the LRPPRC/SLIRP protein complex, which prevents the degradation of the mtRNAs.

LRPPRC is a leucin-rich pentatricopeptide repeat (PPR)-containing protein that binds RNA and is mainly present in the mitochondrial matrix [287]. Knockdown of LRPPRC in mice results in drastically reduced steady-state levels of mRNAs, but not of the mt-tRNAs of mt-rRNAs, and determining reduced polyadenilation and transcripts processing defects, and impaired translation [288–292].

LRPPRC is also able to block the action of PNPase (polynucleotide phosphorylase) that degrades RNA, while promoting polyadenilation by stimulating the activity of mtPAP [293].

The other protein that acts in a complex with LRPPRC to stabilize mRNAs is the stem-loop-interacting RNA binding protein (SLIRP) [294].

Knockdown of one of the two proteins cause the decrease in levels of the other, moreover SLIRP alone is not able to have an effect on polyadenilation of the transcript [291,293]. It was suggested that LRPPRC is able to stabilise a pool of translationally-inactive mt-mRNAs that are not associated with

the ribosome. It was also suggested that the LRPPRC/SLIRP complex could function binding the mRNA and preventing the formation of secondary structures, leaving the 3'-end of the mRNA available for the polyadenilation. This activity, as mentioned before, could also be involved in the suppression of the PNPase/hSUV3 mt-mRNAs degradation activity [291,293].

Once the mRNAs, tRNAs and rRNAs are used several times for the translation of proteins, they might be degraded in order to eliminate aberrant or damaged transcripts. The best characterised protein complex dedicated to the mt-mRNA degradation in the mitochondrial matrix is the hSUV3/PNPase complex [212].

hSUV3 is a NTP-dependent helicase that has more than one isoforms and at least one of these is localised in the mitochondrial matrix. This protein is able to unwind different DNA and RNA substrates. Szczesny et al. suggested that this helicase is involved in the degradation of the damaged mtRNAs and has a role in the decay of the properly processed RNA molecules [295–297].

The other protein acting with hSUV3 is PNPase that is a polynucleotide phosphorilase able of 3'-to-5' phosphorolysis and 5'-to-3' RNA polymerization [298]. For its role in RNA degradation PNPase is localized in the mitochondrial matrix, however some studies have recently shown the localization of the enzyme in the mitochondrial intermembrane space [299]. For this multiple localization PNPase has been attributed to different processes in the RNA metabolism. In the mitochondrial matrix it takes part in the degradation process on RNA and in the polyadenilation process, while in the intermembrane spece it seems to play a role in the import of different RNA species from the cytoplasm [212,299,300].

hSUV3/PNPase complex, also called "degradosome", has been shown to partially co-localise with the MRGs, although it has been suggested that RNA degradation can take place in specialized foci, called D-foci [208,239].

D-foci, besides containing the degradosome, also localize with newly-synthetized mtRNA, similarly to MRGs, suggesting that a subpopulation of MRGs can participate in RNA processing of degradation mediated by the degradosome [212].

Another protein potentially involved in the degradation of mtRNA is the RNA exonuclease REXO2. This 3'-to-5' exonuclease acts as a homotetramer and degrades oligonucleotides in the matrix. Again, as for PNPase, REXO2 seems to have a dual localization, in the mitochondrial matrix and in the mitochondrial intermembrane space [301].

It was suggested that, because the degradosome is expected to degrade RNA in small oligo-ribonucleotides, it is possible that they become the substrate for REXO2 to complete later stages of decay [301].

8. Translation process in mitochondria

8.1 Mitoribosome biogenesis and structure

Mitoribosme biogenesis pathway can be divided in 6 different steps, some of which have been already discussed in the previous chapters of this thesis. First, of all 12S and 16S RNAs have to be transcribed and released from the primary transcript (chapter 8.2) (1). Then, mitochondrial ribosome proteins (MRPs), that are all nuclear-encoded, need to be imported in the mitochondria and modified if necessary (2). rRNAs have be to post-transcriptionally modified to be fully functional (chapters 8.3.1 and 8.3.2) (3). 12S rRNA and SSU protein subunits must be assembled to form the small ribosomal subunit (4) and the same need to happen for the 16S rRNA and the LSU subunits (5). Finally, the two ribosomal subunits need to be assembled together (6) [217]. As mentioned before, the rNRAs modification steps are largely co-transcriptional and took place in the nucleoid/MRGs, so it was suggested that the biogenesis of the mitoribosome is initiated in the nucleoid and then completed in the MRGs [207,211,217].

The mammalian mitoribosome is composed by the LSU (39S) and the SSU (28S). The small subunit contains the 12S rRNA and 29 mitorobosome proteins, while the large subunit is composed by the 16S rRNA and 50 proteins [302]. Interestingly 15 of the SSU subunits and 20 of the LSU subunts have no bacterial homologues, meaning that the mammalian mitoribosome has a RNA:protein ratio much lower than the bacterial or eukaryotic cytosolic ribosome [303]. We know that the mitoribosome have bacterial origins and during evolution some of the rRNA segments were lost, probably substituted by ribosomal proteins. Besides the lack of bacterial homologs in the composition of the mitoribosome, it is likely that the structural and functional aspects have been conserved during evolution [251,304].

The two mitochondrial subunits are connected by 15 inter-subunit bridges and only six of them are conserved in the bacterial ribosomes [262,305]. In mitochondria these bridges are mainly made by protein-protein interactions, while in bacteria the interaction are mostly between rRNAs. It was also observed by Kaushal at al. that the mRNA that should enter the SSU can enter in the structure through an mRNA entrance site lined with conserved mitochondrial specific proteins [262]. Indeed, in mammals it is not known how the mt-mRNA is recognised and transported into this gate. However, it has been shown that differently from the requirements of bacterial and eukaryotic cytosolic RNAs, the addition of few nucleotides at the 5'-end can abolish the translation of mRNAs[306].

Another peculiar characteristic of the mitoribosome that is worth to be mentioned is that all the proteins that needs to be translated in the mitochondira are proteins of the respiratory chain and thus all of them are membrane proteins. Therefore mitoribosome have evolved to adapt and specialize for the translation of membrane proteins. Indeed, the mitoribosome seems to be normally bound to the inner membrane, avoiding the need to cycling between membrane-bound and unbound stages, which in contrast occur in bacteria and in the cytosol of eukaryotic cells [307]. Furthermore, it was also suggested that polypeptides are co-translationally inserted in the inner membrane [308]. The biogenesis of the mitoribosome includes the action of several enzymes to assemble the complete subunits. Many ribonucleoproteins (RNPs) are formed thanks to the action of GTPases and ATP-dependent RNA helicases [309]. Energy derived from this reactions can modulate the conformational changes needed to form the RNP. Moreover, GTPases could act as placeholders for proteins that will be added to the structure later in the maturation of the ribosome. Another important function of GTPases in this context is the sensor function they could have: GTPases are usually active in their GTP-bound state, so they sense the GTP/GDP ratio, and adapt the mitoribosome assembly to match the nutrient availability of the cell [207,310].

ATP-dependent helicases are necessary to unwind the RNA molecules, facilitating their interaction with the proteins or helping the displacement of the RNA from a ribonucleoprotein [311]. DDX28 and DHX30 have been recently identified to be both involved in mitoribosome assembly [213].

In the recent years a number of other factors were identified as important in the assembly and stability maintenance of the mitoribosome. For example, the enzyme mTERF3 that has a role in the mtDNA transcription has also a role in the biogenesis of the LSU [312] as for the Fas-activated serine threonine kinase family FASTKD2, the DDX28 helicase [211,213,313] and the mAAA-protease [314]. MALSU protein and GRSF1 instead have been found to have a role in the biogenesis and stability of the SSU [241,315,316].

8.2 The mitochondrial translation process

As for the cytoplasmic translation in eukaryotic cells the mitochondrial translation process can be divided in four steps: initiation, elongation, termination and recycling (Figure 29) [207,317,318]. Differently from the cytosolic translation, mitochondrial mRNAs have a different codon usage. In particular the UGA codon, which is usually recognized as a stop codon, is translated as a tryptophan, the AUA codon is translated as a methionine and AGA or AGG codons are not recognized by any mt-tRNA or protein factor [319,320].

The initiation step starts with the recruitment of the mt-mRNA and the mtSSU, which is bound to the initiation factor mtIF3 to inhibit premature re-association with the mtLSU. The entrance of the mRNA in the mtSSU channel is aid also by the mS39 protein [321,322]. AUG, AUA, AUU are the codons recognized by the mt-tRNA carrying the methionine in mitochondria and once the mt-tRNA^{Met} is recruited by mtIF2 bound to GTP, this complex can bind the mtSSU. Although the tRNAMet-mtSSU can form a complex also in absence of a mt-mRNA, this becomes stable only in the presence of a positive codon:anticodon match. At this point the interaction with the mtLSU can follow, and the formation of the monosome sets off the hydrolysis of the GTP bound to mIF2 into GDP in concomitance with the release of the initiation factors [306,323].

As mentioned before, mt-mRNAs present the start codon at the very beginning of the mature molecule, near to the 5'-end, and the efficiency of the translation strictly depends on the number of nucleotides positioned before the start codon [306]. Two of mt-mRNAs ND4L/ND4 and ATP6/ATP8 are bicistronic transcripts and each of them contains two open reading frames, partially overlapping. It is not known if the two ORFs are translated with only one mRNA/ribosome interaction or if the two ORFs are translated into two separate moments. Moreover, it is not known how the translation efficiency is maintained in the case of the second ORF of both transcripts, since the 5'UTR of this ORFs consist of the upstream coding sequence [317].

After the initiation the amino acid chain the elongation phase can start. In this step the mitochondrial elongation factor mtEF-Tu, a GTP molecule and a charged mt-tRNA form a ternary complex that enters the A-site in the mitoribosome. If there is no correspondence between the codon and the tRNA anticodon, the interaction between the complex and the mitoribosome is not stable and the complex dissociates. When there is the right correspondence the mitoribosome stimulates the hydrolysis of the GTP molecule in GDP and the consequent release of the mtEF-Tu factor [324]. At this point, the peptide bond is catalysed at the peptidyl transferase centre (PTC) in the large subunit. The deacylated tRNA, that is now in the P-site, must be released to free the space for the dipeptidyl-tRNA, while the dipeptidyl-tRNA that is positioned in the A-site, must slide in the P-site. This is achieved with the interaction of the elongation factor mtEF-G1 that binds to the mitoribosome, changing the conformational structure of the monosome and allows the slide of the two tRNAs, while the deacylated-tRNA can pass through the E-site before being released. The elongation process continues this way until a stop codon is positioned in the A-site [263,322].

During the termination phase the polypeptide chain is released from the tRNA and the mitoribosome must be recycled for another translation event. The termination codon in human mitochondria is recognised by the release factor mtRF1a that in the presence of a GTP molecule promotes the release of all 13 proteins from the mitoribosome [325]. As mentioned before, in human mitochondria codons UAA and UAG are used as stop codons. However, genes encoding COXI and ND6 do not terminate

with one of this codons, but with AGA and AGG, respectively [150]. Mapping of the codons present at A-site in the human mitochondrial ribosome showed that also these two genes are terminated by an UAG. A possible explanation is that there is a -1 frame shift downstream of the termination codon, probably driven by structured RNA [277,326].

Recently, another protein member of the mitochondrial release factors family, ICT1, was described to take part to the termination process. This protein has been suggested to take part in the termination of the synthesis of COXI and ND6. Besides, ICT1 is a component of the mitoribosome and it has been shown to have a hydrolase peptidyl activity on stalled ribosomes [327].

After the release of the polypeptide chain, the monosome must be dissociated into the two subunits, to allow another translation event. The two recycling factors mtRRF1 and mtEF-G2 are the enzymes that promote the dissociation of the ribosome, the release of the mt-mRNA and the release of the deacylated mt-tRNA [207,328,329].

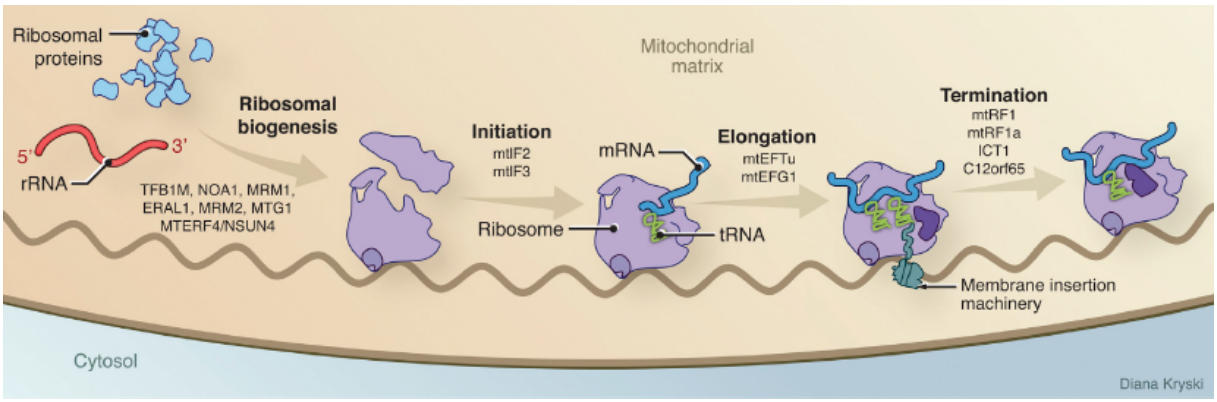

Figure 29: Biogenesis of the mammalian mitoribosomes and the translation cycle. The biogenesis of mitoribosome requires that the 12S and 16S rRNA are modified and assembled along with the ribosomal proteins. The large subunit of the mitoribosome is belived to be anchores with the mitochondrial membrane, and the translation cycle requires several factors for the initiation, elongation and termination. The membrane anchoring of the mitoribosome is belived to facilitate the insertion of the newly synthetized proteins into the inner mitochondrial membrane. Recycling of the mitoribosome is not shown (Image from Van Haute et al., 2015).

8.3 Regulation of mitochondrial translation

Considering the dual genetic origin of the OXPHOS complexes, there is the need of a tight coordination between the synthesis of the mitochondrial-encoded subunits and the synthesis of nuclear encoded subunits and their import into the organelle to prevent the accumulation of non-complete complexes into the inner mitochondrial membrane. Most of the studies in this context have been made in yeast. The mitochondrial translation adapts to the nuclear translation of the subunits and to their import, which is the limiting step in the assembling process. This adaptation is unidirectional, mitochondrial translation depends on the cytosolic one, but inhibition of mitochondrial protein synthesis does not affect the translation efficiency of the nuclear-encoded subunits [208,330,331].

Furthermore, yeast mitochondria possesses a variety of mitochondrial translation activators that can bind the 5'-UTR of the mt-mRNA. The exact mechanism by which these proteins can regulate the translation is still subject of study, but there are evidences that these activators can establish a

feedback loop whereby the absence of available subunits to form a complete OXPHOS complex can inhibit the translation of the associated transcript [207,208].

In human mitochondria one activator was identified, namely TACO1 [332]. This protein seems to have an effect on the translation of MTCO1 gene, which encodes for COXI protein. Indeed, TACO1 mutation result in complete absence of MTCO1 translation. However, the exact mechanism by which TACO1 coordinates the synthesis of COXI is not clear since MTCO1 has no 5'-UTR. It has been proposed that the protein can bind the start codon facilitating the initiation step or it could bind the nascent polypeptide chain stabilizing it [332].

The coordination between the mitochondrial synthesis and the import of the nuclear encoded subunits is essential for the coordination of OXPHOS complexes assembly. In human mitochondria the MITRAC (mitochondrial translation regulation assembly intermediate of cytochrome *c* oxidase) complex was identified as a key element in this step [333]. This complex seems to coordinate the assembly of the cytochrome *c* oxidase complex COX with the translation of the mitochondrial-encoded subunit COXI. As in the case of TACO1, the mechanism of this regulation is unclear but mutations in two of the MITRAC components, c12orf62 and MITRAC12, lead to the inhibition of COXI synthesis [334,335].

Mitochondrial translation can be also regulated by post-translational modification of its actors [336]. Mitoribosomal components can be phosphorylated or acetylated as a result of ATP, acetyl-CoA and NADH mitochondria levels. As mentioned before the mitoribosomal subunit mS29 can be found in association with GTP and the monosome [263,322]. This protein has more affinity for mtSSU than the monosome, suggesting a possible regulatory role of GTP hydrolysis on mS29 [337,338]. Formation of the monosome can also be influenced by mTERF4-NSUN4, which interacts with the small subunit, promoting the binding with the large subunit of the ribosome [270,339].

Finally several other mitochondrial subunits were found to be modified in proximity of domains crucial for translation such as the PTC or the PES (peptide exit site) [336].

9. mt-RNA processing, mt-translation and diseases

Mitochondrial diseases are a class of heterogeneous disorders characterized by mutations in mtDNA or nuclear DNA that cause severe effects on mitochondrial respiration. Most of the pathologies resulting from mutation in mtDNA or the enzymes involved in mtRNA maturation and mitochondrial translation can have very wide spectrum of symptoms, always due to the inefficiency of the OXPHOS function. Symptoms can vary from hearing impairment, epilepsy, retinal degeneration to loss of cognitive and motor function, cardiomyopathy lactic acidosis and developmental delay [340]. The affected patients are always heteroplasmic [341] and a fraction of 60% or more of mutated mtDNA is needed to have the impairment of mitochondrial translation and the clinical manifestation of symptoms [340,341]. Pathologies that results from these mutations are often lethal or with a neonatal or infantile onset and children with high levels of deleted mtDNA typically develop multisystem disease with more severe symptoms in respect to patients that have a less percentage of mtDNA mutations [342].
A variety of mainly autosomal recessive mutations that impair mitochondrial translation are known, and some examples of mutated genes include those that encode for mRNA stability and polyadenilation factors (LRPPRC and mtPAP), tRNA modification enzymes (PUS1, MTU1 and MTO1), enzymes that aminoacylate tRNAs (DARS2, RARS2 and others), mitoribosomal proteins (MRPS16, MRPS22, MRPS28, MRPL3, MRPL12 and MRPL44), translation elongation and termination factors (mtEFTu, mtEFG1, mtEFTs and C12ofr65) and translational activator factors (TACO1) [340,343].

LIST OF PUBLICATIONS

1. **Mitochondrial translocation of APE1 relies on the MIA pathway**
   Barchiesi A, Wasilewski M, Chacinska A, Tell G, Vascotto C.
   Nucleic Acids Res. 2015 Jun 23;43(11):5451-64. doi: 10.1093/nar/gkv433. Epub 2015 May 8.

   APE1 is a multifunctional protein with a fundamental role in repairing nuclear and mitochondrial DNA lesions caused by oxidative and alkylating agents. Unfortunately, comprehensions of the mechanisms regulating APE1 intracellular trafficking are still fragmentary and contrasting. Recent data demonstrate that APE1 interacts with the mitochondrial import and assembly protein Mia40 suggesting the involvement of a redox-assisted mechanism, dependent on the disulfide transfer system, to be responsible of APE1 trafficking into the mitochondria. The MIA pathway is an import machinery that uses a redox system for cysteine enriched proteins to drive them in this compartment. It is composed by two main proteins: Mia40 is the oxidoreductase that catalyzes the formation of the disulfide bonds in the substrate, while ALR reoxidizes Mia40 after the import. In this study, we demonstrated that: (i) APE1 and Mia40 interact through disulfide bond formation; and (ii) Mia40 expression levels directly affect APE1's mitochondrial translocation and, consequently, play a role in the maintenance of mitochondrial DNA integrity. In summary, our data strongly support the hypothesis of a redox-assisted mechanism, dependent on Mia40, in controlling APE1 translocation into the mitochondrial inner membrane space and thus highlight the role of this protein transport pathway in the maintenance of mitochondrial DNA stability and cell survival.

2. **Isolation of mitochondria is necessary for precise quantification of mitochondrial DNA damage in human carcinoma samples**
   Barchiesi A, Baccarani U, Billack B, Tell G, Vascotto C.
   Biotechniques. 2017 Jan 1;62(1):13-17. doi: 10.2144/000114491.

   The hepatocellular carcinoma (HCC) is the fifth most common cancer and the third cause of cancer mortality worldwide. Advances in diagnosis have improved the prognosis of HCC patients but it remains a fateful tumor because of its high rates of metastases and recurrence and the absence of an effective pharmacological therapy. Biomedical research relies on the use of animal models and human derived tissues for the study of human pathologies. Sub fractionation of cellular compartments, DNA isolation, and protein expression analyses are basic procedures in biomedical studies. However, the majority of protocols are specifically designed to carry out or genomic or proteomic studies. Here we describe a protocol that enables the simultaneous purification of nuclei and mitochondria from mouse liver, human healthy and HCC liver tissues suitable for proteomic analysis. In addition, genomic DNA was isolated from the nuclear fraction and used as a template for PCR. Mitochondrial DNA (mtDNA) was purified and its level of damage was evaluated in tumoral tissues. Generally, for the measurement of DNA damage the mtDNA is not separated from the genomic: we demonstrated the need of using a purified mtDNA to obtain reliable data of the levels of damage on human biopsies of HCC.

3. **DNA Repair Protein APE1 Degrades Dysfunctional Abasic mRNA in Mitochondria**
Barchiesi A, Oeljeklaus S, Jedroszkowiak A, Bazzani V, Borowski L. S., Szczesny R. J., Warscheid B, Chacinska A, and Vascotto C.
Submitted to EMBO reports

APE1 is a multifunctional nuclear/mitochondrial protein which plays a central role in the maintenance of genome stability and regulation of gene expression. Apart from these canonical activities, recent studies have demonstrated that APE1 is also enzymatically active on RNA molecules. The present study unveils for the first time a new role of APE1 in the metabolism of RNA in mitochondria. Our data demonstrate that APE1 binds and exerts endoribonuclease activity on abasic mitochondrial messenger RNA. Loss of APE1 determines the accumulation of damaged mitochondrial mRNA species determining impairment in protein translation and reduced expression of mitochondrial encoded proteins, finally leading to less efficient mitochondrial respiration. All these effects are rescued by the expression of a recombinant mitochondrial targeted form of APE1 protein. Altogether, our data demonstrate that APE1 has an active role in the degradation of the mitochondrial mRNAs and a profound impact on mitochondria well-being.

AIMS

Mitochondria are the main endogenous source of reactive oxygen species (ROS) production and its becoming apparent that ineffective functioning of respiratory complexes causes the progressive elevation in mitochondrial ROS. Like nuclear DNA, the integrity of mitochondrial DNA, as well as that of messanger (mRNA) and ribosomal (rRNA) RNAs, are also constantly threatened by exposure to damaging agents. Integrity of mitochondrial DNA and RNA is necessary for the cell survival under physiological conditions.

APE1 is an essential enzyme in the DNA BER pathway, which is responsible for repairing both the nuclear and mitochondrial DNA lesions caused by oxidation and alkylation agents. Apart from its effect on DNA, recent findings highlight a novel role of APE1 in RNA metabolism as proved by its interaction with RNA processing proteins, its ability to recognize and cleave abasic RNA, and the control of miRNA processing. Unfortunately, comprehensions of the mechanisms regulating APE1 intracellular trafficking are still fragmentary and contrasting.

The purposes of this thesis have been: i) to characterize the molecular mechanisms responsible for the translocation of APE1 into the mitochondria; and ii) to evaluate if APE1 exerts endoribonuclease activity on mitochondrial RNAs.

MATERIAL AND METHODS

1. Cell culture and treatments

HeLa and Huh7 cells were grown in DMEM (Dulbecco's modified Eagle's medium), JHH6 cells were grown in William's medium E, both supplemented with 10% foetal bovine serum (FBS), 100-U/ml penicillin and 10 mg/ml Streptomycin sulphate. One day before treatment HeLa cells were seeded 4×10^6 cells/plate. For mtDNA damage measurements HeLa and JHH6 cells were treated with 400 mM and 1.2 mM of H_2O_2, respectively, in medium without serum for 15 min, and then cells were grown for 1 h in the presence of 10% FBS before harvesting. For cell viability analysis 5×10^4 JHH6 and 10×10^4 Huh7 cells were seated on 96 multiwell plates and after 24 h treated with the reported amount of Methyl methanesulfonate (MMS) or H_2O_2 for 8 h in medium without FBS. For inducible silencing of endogenous APE1, HeLa cell clones were developed as described in Vascotto *et al* [67]: Scr-1 and shRNA-APE1 were grown in DMEM (Dulbecco's modified Eagle's medium) supplemented with 10% foetal bovine serum (FBS), 100 U/ml penicillin and 10 μg/ml Streptomycine sulphate, x Blasticidin and x Zeocin. For inducible siRNA experiments, doxycycline (Sigma) was added to the cell culture medium at the final concentration of 1 μg/ml, and cells were grown for 9 days. Stable clones expressing APE1-FLAG and Empty vector were grown in DMEM (Dulbecco's modified Eagle's medium) supplemented with 10% foetal bovine serum (FBS), 100 U/ml penicillin and 10 μg/ml Streptomycine sulphate, 3 μg/ml Blasticidin and 100 μg/ml Zeocin and 350 μg/ml Neomicin. For mRNA half-life calculations Scr-1 and shRNA-APE1 cells were seeded $4x10^6$ cells/plate 1 day before treatment and then treated with 500 ng/ml EtBr for 0,1,2,4 and 6 hours in DMEM supplemented with 10% foetal bovine serum (FBS), 100 U/ml penicillin and 10 μg/ml Streptomycine sulphate. After the treatment cells were harvested and RT-PCR was followed.

2. Transient transfection experiments

One day before transfection cells were seeded in 10 cm plates at the density of 1.2×10^6 cells/plate. Cells were then transfected with 100 nM of either shRNA Mia40 scramble, shRNA APE1 scramble or PNPase scramble (controls) and shRNA Mia40 or shRNA APE1 (encoding for siRNA against Mia40 or APE1 respectively) per plate using Oligofectamine Reagent (Invitrogen) according to the manufacturer's instructions. Cells were harvested 72 h after the transfection. For overexpression of APE1 and Mia40 proteins, 2.5×10^6 cells/plate were seeded 24 h before transfection. Cells were then transfected with 2 mg of pCMV5.1 FLAG, C65S, C93S, C99S, C65S+C93S, C65S+C99S, Mia40-HisTag, MTS-APE1-WT-FLAG, MTS-APE1-E96A-FLAG per plate using Lipofectamine Reagent (Invitrogen) according to the manufacturer's instructions. Cells were harvested 24 h or 48h after the transfection. For transient APE1 silencing HeLa cells were seeded at the density of 1.2×10^6 cells/plate. Then, cells were transfected with 6 mg of pSuper- scramble or pSuper-APE1, in order to obtain silencing of endogenous APE1, and with 6 mg per plate of pCMV 5.1 Empty, APE1WT, C65S or C93S to re-express APE1. Cells were harvested 48 h after the transfection.

3. Preparation of total cell extracts and anti-Flag affinity purification

For the preparation of total cell lysates cells were harvested by trypsinization and centrifuged at 250 × g for 5 min at 4°C. Supernatant was removed, and the pellet was washed once with ice-cold phosphate-buffered saline (PBS) and then centrifuged again as described before. Cell pellet was resuspended in lysis buffer [50-mM Tris-HCl (pH 7.4), 150-mM NaCl, 1-mM ethylenediaminetetraacetic acid (EDTA), 1% [wt/vol] Triton X-100, protease inhibitor cocktail (Sigma), 0.5-mM phenylmethylsulfonyl fluoride] at a cell density of 10^7 cells/ml and rotated for 30 min at 4°C. After centrifugation at 12 000 × g for 10 min at 4°C, the supernatant was collected as total cell lysate (WCE). The protein concentration was determined using Bio-Rad protein assay reagent (Bio-Rad). For affinity purification analysis total cell lysates were incubated with anti-Flag M2 affinity gel (Sigma) for 3 h at 4°C and then processed following the manufacturer's instructions.

Proteins were eluted by incubation with 0.15 mg/ml 3xFlag peptide in Tris-buffered saline and then subjected to western blot analysis.

4. Anti-Flag affinity purification from isolated mitochondria

For affinity purification analysis 1mg of mitochondria from APE1-FLAG expressing cells and and CTRL cells was lysed in 50mM Tris-HCl pH 8.0, 300mM NaCl, 10mM $MgCl_2$, 1mM EDTA pH 7.4, 0,5% NP-40. The lysates incubated with anti-Flag M2 affinity gel (Sigma) for 3 h at 4°C and then processed following the manufacturer's instructions. Proteins were eluted by incubation with 0.15 mg/ml 3xFlag peptide in Tris-buffered saline (TBS) and then subjected to MS or Western blot analysis.

5. Preparation of subcellular fractions

Subconfluent HeLa and JHH6 cells were collected and suspended in Grinding buffer (250-mM sucrose, 1-mg/ml bovine serum albumin (BSA), 2-mM EDTA, pH 7.4) with 1:100 protease inhibitor cocktail. Cell suspensions were sonicated on ice under mild controlled conditions to disrupt selectively plasma membranes (4-s sonication one time). The homogenates were then fractionated by differential centrifugation at 800 × g and 16 000 × g at 4°C, to obtain the enriched cytoplasmic, nuclear and mitochondrial fractions. Samples were then subjected to Bradford analysis for the evaluation of protein content before separation on sodium dodecyl sulphate-polyacrylamide gel electrophoresis (SDS-PAGE) and western blot analysis. Purity of mitochondria and nuclei was evaluated using specific marker proteins (LSD1 for nuclei and ATP 5A for mitochondria) to ascertain the absence of cross contamination between the two compartments.

6. Mitochondria isolation

$10*10^7$ cells expressing APE1-FLAG encoding or control vector were seeded one day before the procedure. After 24h cells were washed twice with PBS 1X and scraped. After an additional wash cells were centrifuged at 1200 rpm for 4' at 4°C. The cells were divided in two aliquotes and each aliquote was resuspended 6ml of MIB buffer (20mM HEPES pH 7.6, 1mM EDTA pH 7.4, 220mM mannitol, 70mM sucrose, 2mg/ml BSA, 0,5mM PMSF) and gently homogenized into a glass-glass potter with 20 strokes. The suspension was then transferred into a falcon tube and centrifuged at 650g for 5' at 4°C. The supernatant, containing mitochondria was removed and kept on ice while the pellet, containing nuclei and unbroken cells, was homogenized again with 10 strokes to increase the final yield. The suspension was centrifuged again at 650g for 5' at 4°C. The two supernatants were pooled together and centrifuged once again at 650g for 5' at 4°C. The supernatant was carefully removed and centrifuged at 14000g for 15' at 4°C while the pellet, containing mitochondria, was washed with MIB buffer supplemented with 1M KCl to remove proteins and nucleic acids attached to the outer membranes of mitochondria and then centrifuged 14000g for 15' at 4°C. Finally the mitochondria were washed with MIB buffer w/o KCl and BSA and centrifuged again as before, supernatant was removed and the pellet was resuspended in MIB buffer w/o KCl and BSA, keeping mitochondria as concentrated as possible. Samples concentration was determined using Bio-Rad protein assay reagent (Bio-Rad).

7. Western blot analysis

The indicated amounts of total, cytoplasmic, nuclear or mitochondrial extracts were electrophoresed onto a 12% SDS-PAGE. Then, proteins were transferred to nitrocellulose membranes (Schleicher & Schuell). Membrane were saturated by incubation with 5% non-fat dry milk in PBS-0,1% Tween 20 for 1 h at room temperature, and incubated with the specific primary antibody [anti-APE1 monoclonal (Novusbio): overnight 4°C, dilution 1:2000; anti-FLAG monoclonal (Sigma): 3 h at 25°C, dilution 1:3000; anti-Actin polyclonal (Sigma): overnight at 4°C, dilution 1:2000; anti-ATP 5A monoclonal (Abcam): overnight at 4°C, dilution 1:10000; anti-NDUFA1 polyclonal (Abcam): overnight at 4°C, dilution 1:5000; anti–NDUFS1 polyclonal (Abcam) overnight at 4°C, dilution 1:10000; anti–MT-ND5

polyclonal (Abcam) overnight at 4°C, dilution 1:1000; anti–CO2 polyclonal (Abcam) overnight at 4°C, dilution 1:1000; anti–COXVIB monoclonal (Abcam) overnight at 4°C, dilution 1:1000; anti–MRPS15 polyclonal (Abcam) overnight at 4°C, dilution 1:1000; anti–MRPL9 polyclonal (Novusbio) overnight at 4°C, dilution 1:1000; anti–TOMM20 polyclonal (Abcam) overnight at 4°C, dilution 1:1000; anti–PNPase polyclonal (Abcam) overnight at 4°C, dilution 1:1000); anti-Mia40 polyclonal (gift from the lab- oratory of Prof. Matthias Bauer) overnight at 4°C, dilution 1:1000; anti-HisTag polyclonal (Sigma): overnight at 4°C, dilution 1:2000]. Membranes were washed three times with PBS-0,1% Tween 20 and incubated for 2 h with the secondary antibody. After three washes with PBS-0,1% Tween 20 signals were detected with Odyssey CLx scanner (Li-Cor Biosciences). Normalization was performed with polyclonal antibodies anti-Actin or with anti-TOMM20. Blots were than quantified by using ImageStudio software (Li-Cor Biosciences).

8. DNA extraction and mtDNA damage measurement by quantitative PCR

After treatments cells were harvested by trypsin and high- molecular weight DNA was isolated with the QUIAGEN Genomic-tip 20/G and G2, QBT, QC, QF buffers (all reagents are distributed by Qiagen) as described by the manufacturer. Briefly cells were resuspended in G2 buffer supplemented with 400 mg of RNase A and 6 mAU of proteinase K and incubated at 50°C for 2 h in a water bath. Samples were then applied to equilibrated columns, washed three times with QC buffer and then eluted with 1 ml of QF buffer twice. DNA was precipitated overnight at −80°C with the addition of 700 ml of isopropanol and then centrifuged at 4°C, 15 000 × g for 1 h. DNA was washed with EtOH 75%, centrifuged again and resuspended in 100 ml of Tris-EDTA buffer pH 8. Quantification of DNA was performed with Quant.iT-Picogreen dsDNA reagent (Invitrogen) according to the manufacturer's instructions and DNA concentration was adjusted to 10 ng/ml. The number of mtDNA lesions was determined by Q-PCR. The following primers were used: Mitolong for 5'-TCT AAG CCT CCT TAT TCG AGC CGA-3' and Mito rev 5'-TTT CAT CAT GCG GAG ATG TTG GAT GG-3' which amplified an 8.9-kb mitochondrial fragment; and Mitoshort for 5'-CCC CAC AAA CCC CAT TAC TAA ACC CA-3' and Mito rev, which amplified a 221-bp mitochondrial fragment. DNA was amplified using Elongase enzyme mix (Invitrogen). The polymerase chain reaction (PCR) was initiated at 94°Cwith hot-start for the complete denaturation of DNA and allowed to undergo the following thermocycler profile: an initial denaturation for 1 min at 94°C followed by 19 cycles of 94°C denaturation for 1 min and 64°C annealing/extension for 11 min for the 8900 bp fragment and 60°C annealing for 45 s and 72°C extension for 45 s for the 221 bp. A final extension at 72°C was performed for 10 min for both fragments. To ensure quantitative conditions a sample with the 50% of template amount was included in each amplification and, as negative control, a sample without the template was used. PCR products were quantified in triplicate by using Quant.iT-Picogreen dsDNA reagent. The mitoshort fragment was needed to calculate the relative amount of mtDNA copies and to normalize the lesion frequencies calculated with the mitolong fragment.

9. RNA extraction and Real time-PCR

Total RNA extraction from cells was performed using the NucleoSpin RNA kit (Macherey-Nagel GmbH & Co., Germany). 1 mg of total RNA was reverse transcribed using the iScript cDNA synthesis kit (bio-Rad), according to the manufacturer's instructions. RT-PCR was performed with iQ5 multicolor real-time PCR detection system (Bio-Rad), according to the manufacturer's protocol. The following primers were used: APE1_for (5'- CAG CAA GAT CCG TTC CAA -3'); APE1_rev (5'- TTG TCA TCG TCG TCC TTG TAA -3'); 18S_for (5'- CTGCCCTATCAACTTTCGATGGTAG -3') and 18S_rev (5'- CCGTTTCTCAGGCTCCCTCTC -3'); ND1_for (5'- ACACTAGCAGAGACCAACCG -3') and ND1_rev (5'- CTGCGGCGTATTCGATGTTG -3'); CO2_for (5'- CGTCTGAACTATCCTGCCCG -3') and CO2_rev (5'- GGGATCGTTGACCTCGTCTG -3'); Cyt.b_for (5'- CCCACATCAAGCCCGAATGA

-3') and Cyt.b_rev (5'- AGTAATAGGGCAAGGACGCC -3'); ATP6_for (5'- AACCAATAGCCCTGGCCGTA -3') and ATP6_rev (5'- TATTGCTAGGGTGGCGCTTC -3'); NDUFA1_for (5'- CACTAACGGGGGCAAGGAAA -3') and NDUFA1_rev (5'- ATCAACTCCAGAGATGCGCC -3'); Cyt.c_for (5'- AAACGCATGGGGCTCAAGAT -3') and Cyt.c_rev (5'- TGACCACTTGTGCCGCTTTA -3'); COXVIB_for (5'- TGGTGTCTTTGCTGAGGGTC -3') and COXVIB_rev (5'- GTCTCCATGTCTTCCGCCAT -3'); GAPDH_for (5'-CCCTTCATTGACCTCAACTACATG -3') and GAPDH_rev (5'- TGGGATTTCCATTGATGACAAGC -3'); cDNA was amplified in 96-well plates using the 2X iQ SYBR green supermix (Bio-Rad) (100 mM KCl, 40 mM Tris-HCl [pH 8.4], 0.4 mM each deoxynucleoside triphosphate [dNTP], 50 U/ml iTaq DNA polymerase, 6 mM $MgCl_2$, SYBR green I, 20 nM fluorescein, and stabilizers) and 300 nM of the specific sense and antisense primers in a final volume of 15 µl for each well. Each sample analysis was performed in triplicate. As negative control, a sample without template was used. The cycling parameters were denaturation at 95°C for 10 seconds and annealing/extension at 60°C for 30 seconds (repeated 40 times). In order to verify the specificity of the amplification, a melting-curve analysis was performed immediately after the amplification protocol and PCR products were separated onto 2% agarose gel.

10. Expression and purification of recombinant proteins

pGEX-3X expression plasmids (Sigma) containing either wild-type APE1 or APE1 C65S, C93S, C99S, C65/93S, C65/99S mutants or pGEX-4T expression vectors (Sigma) containing wild-type Mia40, Mia40 C55S mutant or the empty vector were transformed into Escherichia coli BL21 (DE3) cells (Stratagene). Bacterial cells were grown at 37°C to an absorbance of 0.8 OD measured at 600 nm, and then protein expression was induced with 1 mM isopropyl-b-D- thiogalactopyranoside. Induction was carried out for 4 h for GST-APE1 and GST and for 2 h for Mia40 at 37°C and then cells were collected by centrifugation at 4000 × g for 20 minutes at 4°C. Cells were resuspended in Lysis buffer (20 mM Tris HCl (pH 8.0), 250-mM NaCl, 0.1% [v/v] Tween- 20) with protease inhibitor cocktail (Sigma), sonicated five times for 30 s and then centrifuged at 16 000 × g for 30 min. Recombinant proteins were purified from the clarified extracts on an AKTA Prime FPLC system (GE Healthcare) using GSTrap HP columns (GE Healthcare). To remove the GST tag from GST–APE1, WT and mutant proteins were further hydrolyzed with factor Xa (five factor Xa units per milligram of recombinant GST-fused protein) for 4 h at room temperature (RT). The protease was then removed from the sample using a benzamidine HiTrap FF column (GE Healthcare), and the proteins were then purified on a GSTrap HP column to purifyAPE1 from the GST tag. The quality of purification was checked by SDS-PAGE analysis. Accurate quantification of all recombinant proteins was performed by colorimetric Bradford assays (Bio-Rad) and confirmed by SDS-PAGE (Supplementary Figures S1 and S2).

11. GST pull-down assay

For GST pull-down experiments, 15 pmol of GST-Mia40 was added together with 15 pmol of APE1 WT or APE1 C65S, C93S, C99S, C65/93S, C65/99S mutants, to 10 ml of glutathione-Sepharose 4B beads (GE Healtcare). Binding was performed in Binding buffer (1XPBS, 50 mM Tris pH 8.0, 50% glycerol, 0.5% NP40 and protease inhibitor) for 3 h under rotation at 4°C. The beads were washed three times with Washing buffer (1XPBS, 0.1%NP40, 10% glycerol and protease inhibitor). Proteins were eluted for 10 min with Elution buffer (50 mM Tris pH 8.0 and 10 mM GSH). Then, samples were dissolved in reducing lamely buffer (250 mM Tris-HCl pH 6.8, 8% SDS, 40%, Glycerol, 0.08% Bromophenol Blue,20% b-mercaptoethanol) or non-reducing lamely buffer (250-mM Tris-HCl pH 6.8, 8% SDS, 40%,Glycerol, 0.08% Bromophenol Blue) and loaded onto 12% SDS-PAGE gels followed by western blot. The presence of APE1 and GST proteins was detected using anti-APE1 protein monoclonal antibody and GST mono- clonal antibody, respectively.

12. Endonuclease assay

Endonuclease assay was performed by carrying out enzymatic reactions in a final volume of 10 ml. After mitochondrial purification, the protein content was quantified by Bradford and 25 ng of mitochondrial protein extract was dissolved in AP buffer (50 mM HEPES, 50-mM KCl, 10 mMMgCl2,1 mg/ml BSA, 0.05% (w/v) Triton X-100, pH 7.5). Reactions were started by adding 100 nM of double- stranded abasic DNA substrate obtained by annealing a DY-782-labeled oligonucleotide [5'-AAT TCA CCG GTA CCF TCT AGA ATT CG-3'] (Eurofins MWG Operon), where F indicates a tetrahydrofuran residue, with the complementary sequence [5'-CGAATT CTAGAGGGTACC GGT GAA TT-3'] and incubated at 37°C for the reported amount of time. Reactions were halted by the addition of Stop solution (96% (v/v) formamide, 10 mM EDTA, Xylene cyanol and bromophenol blue), separated onto a 20% (w/v) denaturing polyacrylamide gel and analyzed on an Odyssey CLx scanner (Li-Cor Biosciences). mtAPE1 endonuclease activity of control and Mia40 siRNA was measured in all five biological replicates. The percentage of substrate converted to product was determined using the ImageStudio software (Li-Cor Biosciences). For each time point reported in the diagram of Figure 3C the percentage of product formation and SD were calculated as the average of the biological replicates.

13. Proximity ligation assay (PLA)

To monitor the interaction between ectopic APE1 and endogenous Mia40 in living cells, the in situ Proximity Ligation Assay kit (Olink Bioscience) was used. HeLa cells were seated into a glass coverslip in the amount of 8×10^4 per 24 X multiwell plate, and then transiently transfected with a FLAG-tagged form of APE1 WT, or mutants. Twenty four hours after transfection, cells were fixed with 4% (w/v) paraformaldehyde, permeabilized for 5 min with Triton X-100 0.25% in PBS 1X and incubated with 5% normal foetal bovine serum in PBS-0.1% (v/v) Tween-20 (blocking solution) for 30 min, to block unspecific binding of the antibodies. Cells were then incubated with the mouse monoclonal anti-FLAG FITC conjugated antibody (Sigma Aldrich) at a final dilution of 1:500 for 1 h an RT, in a humid chamber. After washing three times with PBS- 0.1% (vol/vol) Tween-20 (washing solution) for 5 min, cells were then incubated with a rabbit anti-Mia40 overnight at 4°C. PLA was performed following manufacturer's instructions. Technical controls, represented by the omission of the anti-Mia40 primary antibodies, resulted in the complete loss of PLA signal. Images were acquired using a Leica TCS SP laser-scanning confocal microscope (Leica Microsystems) equipped with a 488-nm argon laser, a 543-nm HeNe laser and a 63X oil objective (HCXPLAPO 63X Leica). At least 15 randomly selected cells per condition were analysed. PLA-spots present in each single cell were then scored using the BlobFinder software (Olink Bioscience). Anti-FLAG staining forAPE1 was used to identify cell nuclei. Cell viability assay Cell viability was measured through the CellTiter 96 Aqueous One Solution Cell Proliferation Assay (Promega) according to the manufacturer's instructions.

14. Mitochondrial translation evaluation

For the mitochondrial translation evaluation cells were seeded at a density of 1.7 x 10^6 in 6 mm petri dish the day before the experiment. After 24 h medium was changed with methionine/cysteine-free DMEM with the addition of FBS and Glutamine 1 mM and cells were placed in at 37°C for 1h. Then, emetine was added to the medium to a final concentration of 100 µg/ml and cells were further incubated for 10 minutes at 37°C. EasyTag™ EXPRESS^{35}S Protein Labeling Mix was added to the medium to the final concentration of 200 µCi/ml and the labeling was performed for 1h at 37°C. Cells were then washed twice with PBS, collected and resuspended in lysis buffer [PBS, protease inhibitor cocktail, PMFS 200 mM, 0.1% DDM, Viscolase, 1% SDS], incubated on ice for 15 minutes and then centrifuged for 20 minutes at 14000 x *g*. The supernatant was collected, protein content quantified with Bradford reagent and protein extracts separated on SDS-PAGE at 15%. Gels were dried and digital autoradiography was used for gel analysis with Typhoon FLA 9500 (GE Healthcare) followed by use of ImageQuant software (GE Healthcare).

15. BN-PAGE analysis

To test OXPHOS complexes stability, 500 mg of mitochondria isolated from Scr-1 and shRNA-APE1 cells were lysed in 1X NativePAGE Sample Buffer (LifeTechnologies) with 6mg/mg mitochondria of Digitonin (Calbiochem) in a final volume of 50 ml. Samples were incubated on ice for 15' and then centrifuged 20000g for 30' at 4°C. The supernatant was transferred in a new tube and stored at -80°C. 10 ml of NativePAGE 5% G-250 Sample Additive (LifeTechnologies) was added to the sample before electrophoresis. Electrophoresis was performed with the NativePAGE Novex Bis-Tris Gel System (LifeTechnologies) with 4-16% Bis-Tris gels, following manufacturer's instructions. After electrophoresis the gels were stained with Comassie R-250 stain or subjected to a Western-blot analysis.

16. mRNA accumulation and half-life calculation

To measure the extent of mitochondrial mRNA accumulation, one day before transfection Scr-1 and shRNA-APE1 expressing cells were seeded in 10 cm plates at the density of 4.5 x 10^6 cells/plate. After 24h cells were treated with 500ng/ml EtBr in complete DMEM for the indicated times (0,1,2,4 and 6 hours). After the treatment cells were collected and RNA extraction was performed using the NucleoSpin RNA kit (Macherey-Nagel GmbH & Co., Germany).

17. Northern blot analysis

Northern blot analyses were performed as reported by Szczesny and colleagues [220]. PCR products of the following mtDNA fragments: 3652-4029 (ND1) and 7586-7900 (COX2) were used as templates for preparing strand-specific [α-32P] UTP labeled riboprobes.

18. Analysis of mitochondrial mRNA half-life

To calculate mitochondrial mRNA half-life, control (Scr) and APE1 shRNA clones were seeded at the concentration of 4 x 10^6 cells in 10 mm Petri dish the day before the experiment and then treated with 500 ng/mL EtBr for 0, 1, 2, 4 and 6 hours in complete DMEM medium. After the treatment, cells were collected and RNA extraction was performed using the NucleoSpin RNA kit (Macherey-Nagel GmbH & Co.) and qRT-PCR was performed. Mitochondrial RNA stability was measured by metabolic labeling with 4-thiouridine as previously described by Borowski and colleagues [344].

19. OXPHOS efficiency evaluation

Oxygen consumption rate (OCR) was determined by direct measurement with a SeaHorse Extracellular Flux Analyzer XpE instrument (Seahorse Bioscience, Agilent Technologies, Santa Clara, CA, USA). The day before the measurement 6 x 10^4 cells and were seeded in XF cell culture microplates (Seahorse Bioscience, Agilent Technologies) in a volume of 100 ml and leaved under the hood for 1 hour in order to let the cells adhere to the bottom of the plate. Then the total volume of the wells were adjusted to 500 ml and the cells were leaved in the incubator O/N at 37°c and with 5% CO^2 pressure. The next day, cells were washed twice with PBS and incubated with XF assay medium supplemented with 10 mM glucose, 1 mM glutamine and 1 mM pyruvate (pH 7,4) and placed in a 37°C incubator without CO^2 for 1 hour. OCR for the mitochondrial stress test was determined following the manufacturer's instructions. Briefly, ports in the cartridge plate were loaded with 1 μM oligomycin (port A), 1 μM FCCP (port B) and, finally, a mixture of 0,25 μM Rotenone and 0,25 μM Antimycin A (port C). Real time OCR was averaged and recorded three times during each conditional cycle. Then, cells were collected, lysed and total proteins content was measured by Bradford to normalize the amount of cells for each well. For the statistical analysis all the values were normalized for the Scr-1 clone.

20. Mass spectrometric analysis of APE1-FLAG complexes.

Each lane from Control and IP samples were cut into nine slices of equal size. Subsequent sample processing including reduction and alkylation of cysteine residues and proteolytic in-gel digestion

using trypsin were performed as described before [345]. Peptide mixtures were analyzed by nano-HPLC/electrospray ionization-tandem mass spectrometry using an Orbitrap Elite mass spectrometer (Thermo Fisher Scientific) connected to an UltiMate 3000 RSLCnano HPLC system (Thermo Fisher Scientific). For protein identification, MS raw data were searched against the UniProt Human ProteomeSet including isoforms (downloaded 09/2015) and a database containing common contaminants using the software MaxQuant/Andromeda (version 1.5.2.8) [346,347] with default setting except that one unique peptide was required for protein identification; the option "match between runs" was enabled. Label-free quantification of proteins identified in APE1-FLAG and control IPs was based on normalized MS intensities. For normalization, the MS intensity of individual proteins was divided by the summed MS intensity of all proteins detected per sample and multiplied with 1,000. The ratio of normalized MS intensities of APE1-FLAG versus control samples was calculated to identify proteins enriched in the APE1-FLAG IP. For further analysis, only proteins with at least 3 MS/MS counts and a sequence coverage > 4% (in the APE1-FLAG IP each) that were detected exclusively in the APE1-FLAG IP or that have a ratio APE1-FLAG/control of > 5 were considered.. Assignment of proteins to mitochondria is based on Gene Ontology annotations (downloaded from UniProt, December 2017).

21. Immunofluorescence

For IF and PLA analyses, cells were seated into a glass coverslip in the amount of 8 x 10^4 per 24x multiwall plate. The day after, cells were fixed with 4% (w/v) paraformaldehyde for 20 minutes, permeabilized with Triton X-100 0.5% in PBS 1X for 5 minutes, and incubated with 5% goat serum in Duolink in situ solution A (Blocking solution) (Sigma Aldrich) for 1 h to block unspecific binding of the antibodies. Then, cells were incubated with primary antibody diluted in the Blocking solution in a humid chamber (anti-FLAG monoclonal (Sigma Aldrich): 2 h at RT, dilution 1:100; anti-APE1 monoclonal (Novus): 2 h at RT, dilution 1:400; anti-BrdU polyclonal (Thermo Fisher Scientific): o/n at 4°C, dilution 1:400; anti-PNPase (Abcam): o/n at 4°C, dilution 1:200). After washing three times with Duolink in situ solution A for 5 minutes, cells were incubated with secondary antibody conjugated with Alexa Fluor fluorophore (Thermo Fisher Scientific) 1h30' at RT, diluted 1:1000 in Blocking solution. Mitochondria were stained before fixation with Mito tracker Deep Red (Thermo Fisher Scientific) at a concentration of 100 nM for 15 minutes, followed by three washes in PBS before fixation.

22. AP-sites quantification

AP-sites were quantified following the protocol of Tanaka *et.al*, with some modifications. Breifly, 10 ug of total RNA were incubated with 2 mM ARP (N-(Aminooxyacetyl)-N'-biotinylhydrazine) in 50 mM Na acetate buffer pH 5.2 for 40 min, at 37 °C. As a loading control we used an in vitro synthesized RNA encoding Xenopus elongation factor 1α gene, biotinylated at the 5'-end, that was added to the total RNA after the derivatization. The RNA and then the RNA was precipitated by ethanol. After resuspention with 10 ul of deionized water, an aliquot of 2 ul was put aside for quantifying total transcripts, and the rest of RNA was incubated with streptavidin magnetic-beads for 20 min, at 60 °C. The beads were washed twice with solution A ((1M NaCl, 20mM Tris-HCl (pH7.5), 5mM EDTA, 1% NP-40), three times with solution B (2mM Tris-HCl adjusted pH7.5, 0.5mM EDTA, 1% NP-40) three times with solution C (4M urea, 10mM Tris-HCl adjusted pH7.5, 1mM EDTA, 1% NP-40) and 2 times with solution D (2mM Tris-HCl adjusted pH7.5, 1mM EDTA). Oxidized RNA was dissociated from beads by incubation of with 2.5 mM biotin solution at 90 °C, for 5 min, precipitated by ethanol and resuspended in deionized water. Precipitated and total RNA were used for cDNA synthesis (SuperScript™ III Reverse Transcriptase, Invitrogen). Complementary DNA was used for qRT-PCR (SYBR Green Master Mix from Biorad), according to the manufacturer's protocol.

The oxidation levels of mRNAs were determined based on ΔCq values between Cq of total RNA and oxidized RNA.

23. Statistical analyses

Statistical analyses on biological data were performed using the Microsoft Excel data analysis program for Student's t-test analysis. $p < 0.05$ was considered as statistically significant.

RESULTS

1. Role of MIA pathway in the mitochondrial internalization of APE1

APE1's localization is eminently nuclear although this protein is also present within the mitochondrial matrix, as an essential component of the mitochondrial BER (mtBER) pathway [67,348]. Notably, the mechanisms regulating APE1 intracellular trafficking are still largely unknown. Recent data from our lab confirm the presence of APE1 within mitochondria in its full-length form and that, during the trafficking from cytosol to the mitochondrial matrix tends to accumulate within the IMS [67]. Due to its molecular mass, APE1 must be imported in an active way into the organelle. In 2011 it was hypothesized that APE1 could be a substrate for the DRS pathway and the interaction of the two proteins was demonstrated to take place inside the mitochondria. The first part of this thesis focuses on the identification and characterization of the import machinery that mediates APE1 translocation into the mitochondrial compartment.

1.1 APE1 and Mia40 interact through disulfide bonds

In order to assess *in vivo* in a cell model the interaction between APE1 and Mia40, we transiently transfected HeLa cells with pCMV 5.1 plasmids expressing Mia40-HisTag, and APE1-FLAG (IP) or the empty vector as control (Mock). Then, APE1-FLAG was immunopurified and Mia40-HisTag protein was detected in the IP fraction (Fig. 30). To evaluate if the interaction between the two proteins involved the formation of a disulfide bond we produced recombinant Mia40 expressed in fusion with a GST tag at the N-terminus (rGST-Mia40) (Fig. 32), and recombinant APE1 (rAPE1) (Fig. 33) and quantified the interaction through GST pull-down assays. rGST-Mia40 was used as "bait" and rAPE1 was used as "pray", while GST protein alone was used as negative control. APE1 was able to interact with Mia40 (Fig 30 *left*, lane 2), and incubation with a reducing agent (DTT) let to an almost completely loss of APE1 signal in the pull-down fraction (lane 3). Data from literature identify the Cys55 of Mia40 as the catalytically active residue responsible for the formation of the disulfide bond with its substrates [29]. To verify if also APE1 formed the mixed disulfide bridge with Mia40 through this residue, we performed GST pull-down assays comparing APE1's binding activity of rGST-Mia40-WT with that of rGST-Mia40 C55S mutant form (Fig. 31). The mutant showed a significant reduction of affinity for APE1 (40±2%) but not a complete loss of binding as for other Mia40 substrates [52,65,349]. These data demonstrate that Mia40 interacts with APE1 through the formation of a mixed disulfide bridge involving Mia40 Cys55. Moreover, the partial persistence of interaction even when Cys55 is mutated support the hypothesis of a non-covalent contribution to the interactions between the two proteins.

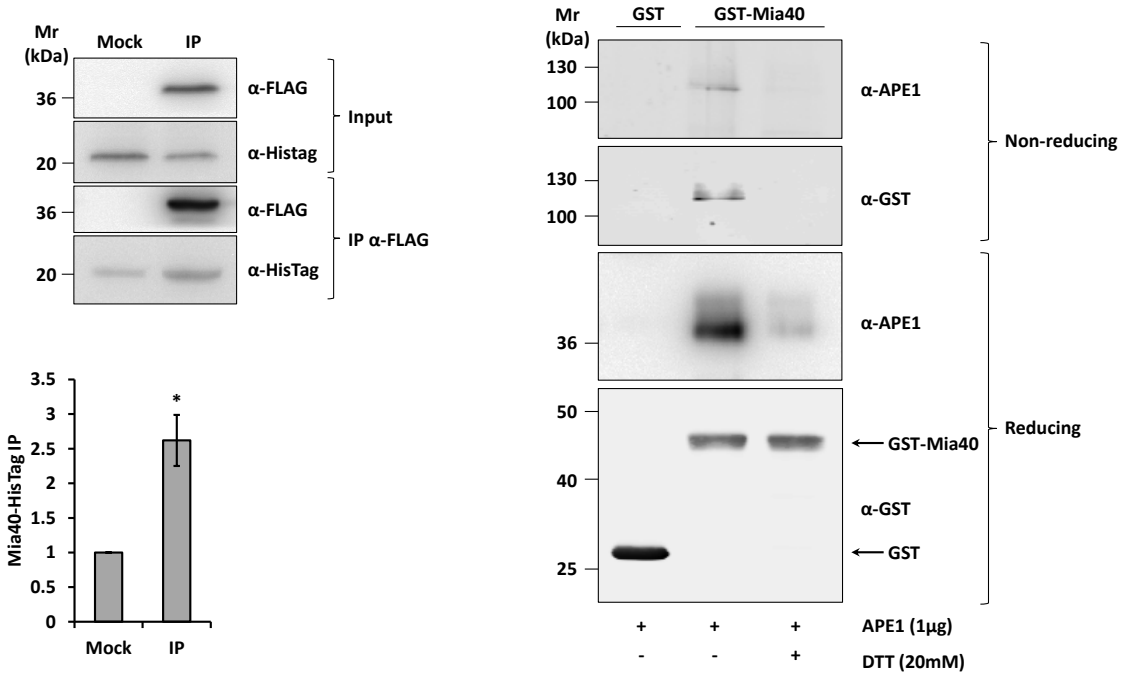

Figure 30. Mia40 Cys55 is responsible for the binding to APE1. (*left*) Western blot (*top*) and relative quantification (*bottom*) of the affinity purification analysis of HeLa cells expressing APE1-FLAG and Mia40-HisTag proteins. Control sample (Mock) and APE1-FLAG (IP) were immunoprecipitated under native conditions from total cell extracts, separated by 12% SDS-PAGE, and analysed by Western blot to evaluate the levels of each interacting partner by using specific antibodies (anti-APE1, anti-HisTag). Mia40-HisTag protein resulted enriched in IP fraction. **(*right*)** GST pull-down assay under reducing and non-reducing conditions. 15 pmoles of recombinant GST-Mia40 protein were used as bait, GST alone as control, and APE1 protein as prey. Interaction between the two proteins was disrupted after treatment with reducing agent (DTT 20 mM). Under non-reducing conditions the complex formed by APE1 and Mia40 is visible and is disrupted when proteins were incubated with DTT (*: $p<0.05$).

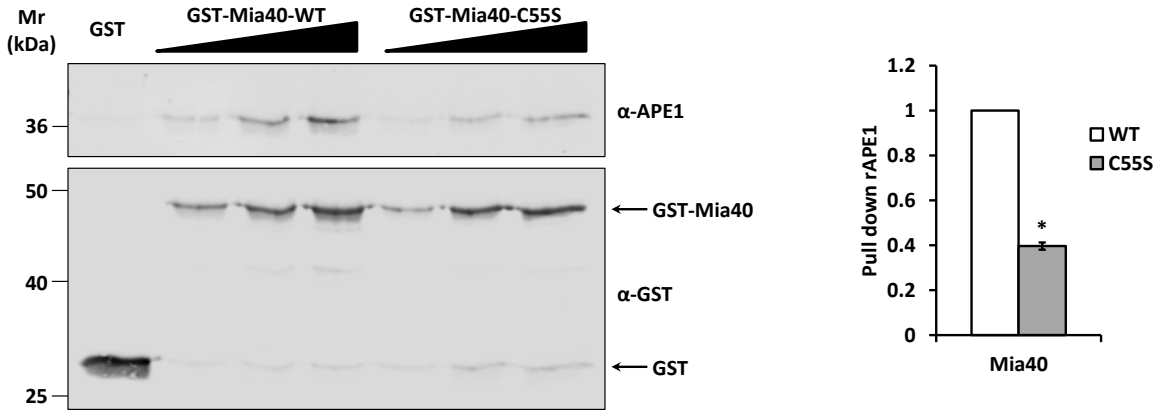

Figure 31. GST pull-down assay of WT and Cys55 mutant Mia40 with WT APE1. (*left*) Western blot analysis of GST pull-down assay with increasing amounts of WT and cys55 Mia40 mutant. **(*right*)** densitometric analysis of the GST-Mia40 bands. (*: $p<0.05$).

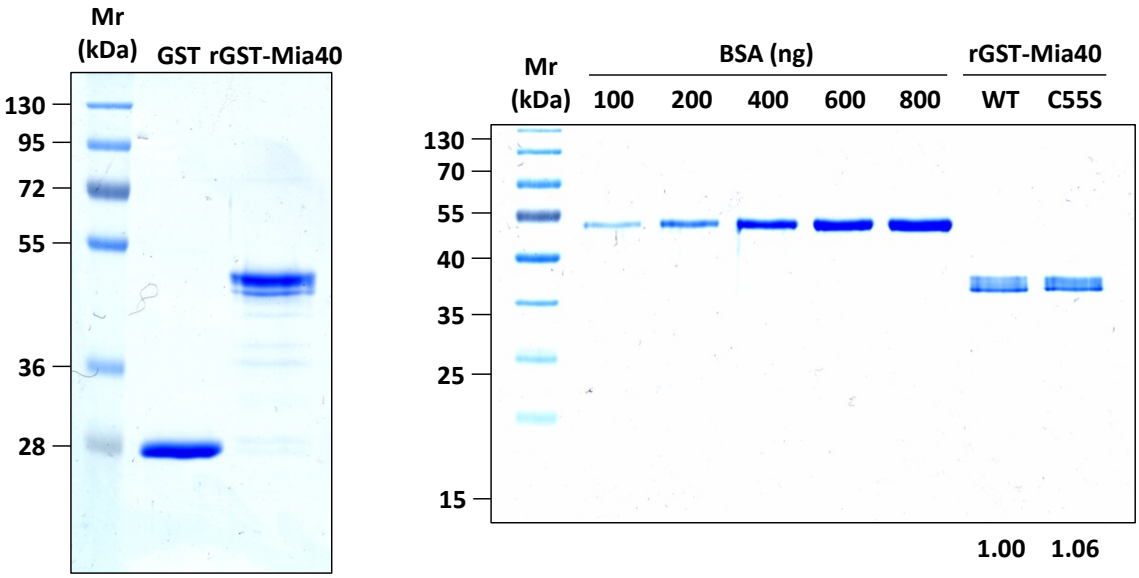

Figure 32. SDS-PAGE analysis of recombinant GST-Mia40 WT and C55S mutant proteins (*left*) 0.6 µg of recombinant GST and GST-Mia40 WT proteins were loaded and separated in a 12% SDS-PAGE gel and stained with Bio-Safe Coomassie (BioRad) to evaluate the absence of contaminants after chromatographic purification. **(*right*)** Recombinant GST-Mia40 WT and C55S mutant quantification. Proteins were quantified through Bradford assay and then 0.3 µg of each recombinant protein were loaded and separated in a 12% SDS-PAGE gel and stained with Bio-Safe Coomassie (BioRad). Reported amount of purified BSA were also separated and used for accurate titration of recombinant GST-Mia40 proteins. Image was acquired with Image Scanner (Amersham) and band intensity was measured with Image Quant TL (Amersham). Relative intensity of GST-Mia40 C55S is reported on the bottom.

After have verified the Mia40 cysteine responsible for the interaction with APE1, GST pull-down experiments were performed to identify which of APE1 redox cysteine formed a mixed disulfide bridge with Mia40. We expressed and purified recombi- nant APE1 single and double cysteine to serine mutants (C65S, C93S, C99S, C65S+C93S, C65S+C99S) (Fig. 33). As reported in Figure 5, the substitution of APE1 Cys93 and the substitution of both cysteine in position 65 and 93 with serine residues completely abolished the interaction of the two proteins confirming the residue Cys93 ofAPE1 to be primarily involved in the disulfide bond formation with Mia40. The substitution of Cys99 (single and double mutants with Cys65) did not alter the interaction with Mia40. Interestingly, the substitution of Cys65 alone determined a stronger interaction with Mia40 than the WT protein (Figure 34). To further investigate in vivo the interaction between APE1 and Mia40, we performed PLA assay overexpressingAPE1-FLAGWT, Cys65 and Cys93 to Ser mutants and quantified the interaction with endogenous Mia40 (Figure 35). Presence of PLA signals demonstrated that ectopic APE1 interacted with endogenous Mia40 which is known to be present only in the mitochondria IMS. As reported in the histogram of Figure 6, APE1 C65S had a stronger interaction with Mia40 than the WT protein, while the C93S mutant showed PLA signals similar to that of the control reaction (Ctrl) where the primary antibody for Mia40 was omitted. Interestingly, the stronger interaction of APE1 C65S was not accompanied by more efficient localization of APE1 in mitochondrial [67]. This behavior is reminiscent of the conditional mutant mia40-4 in yeast that binds client proteins but is defective in the completion of their oxidative folding and ultimately their mitochondrial accumulation [350,351].

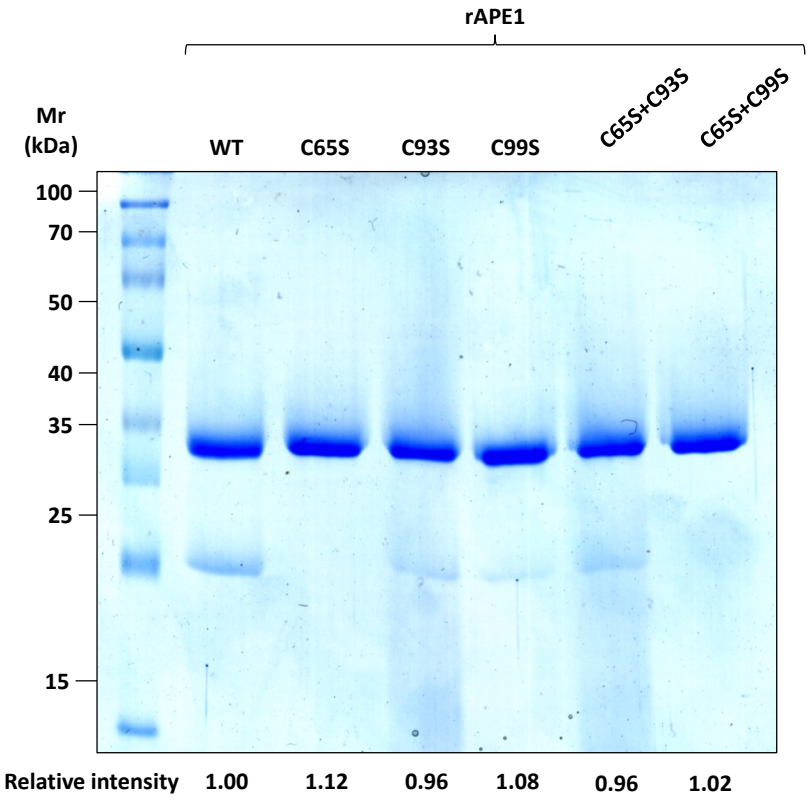

Figure 33. Recombinant APE1 WT and C65S, C93S, C99S, C65S+C93S, C65S+C99S mutants proteins. Proeins were quantified through Bradford assay and then 0.5 µg of each recombinant protein were loaded and separated in a 12% SDS-PAGE gel and stained with Bio-Safe Coomassie (BioRad) to evaluate the absence of contaminants after chromatographic purification. To calculate the relative intensity of each recombinant proteins respect to the WT, the image was acquired with Image Scanner (Amersham) and band intensity was measured with Image Quant TL (Amersham). Relative intensity of all mutants are reported on the bottom.

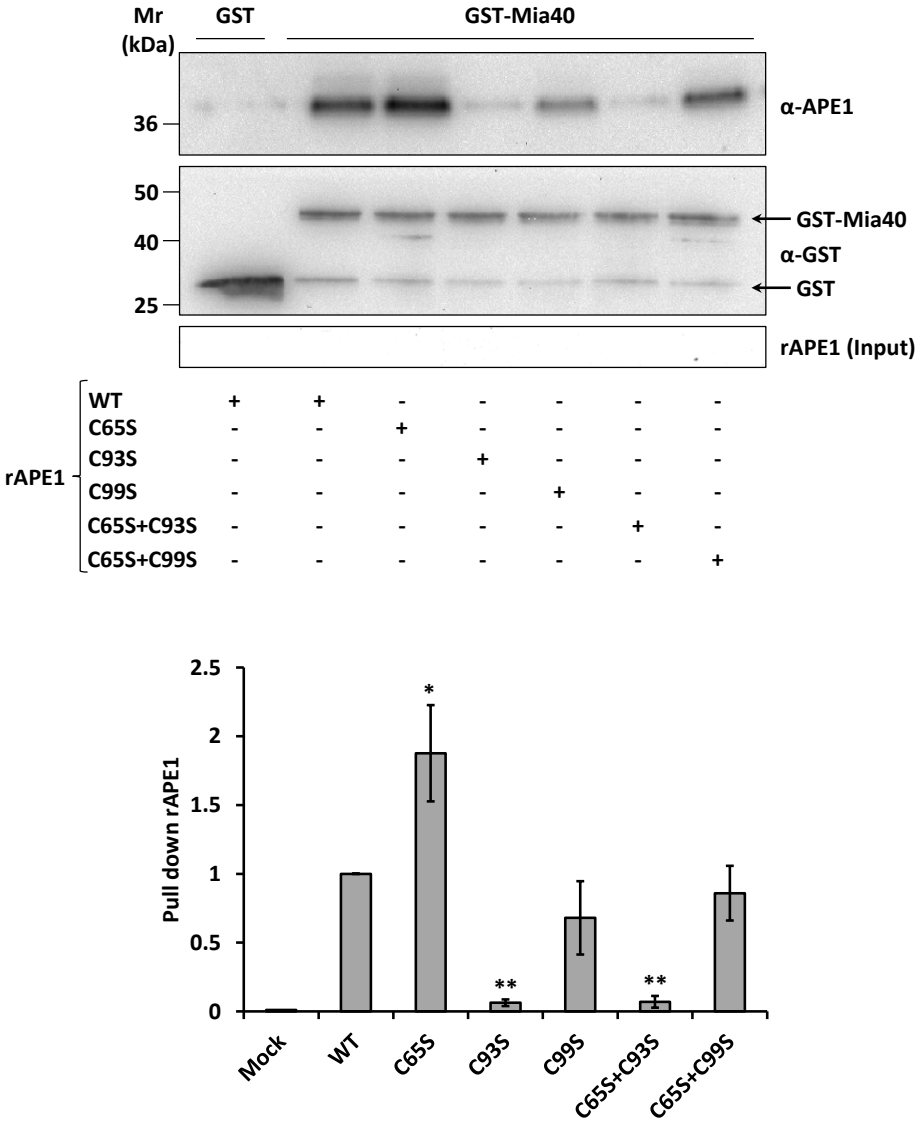

Figure 34. GST pull-down analysis of APE1 mutants and WT Mia40. (*top*) Western blot and **(*bottom*)** relative histogram of GST pull-down analysis of recombinant APE1 (15 pmoles) WT and redox Cys65, Cys93, Cys99, Cys65+Cys93, and Cys65+Cys99 to Ser mutants. GST-Mia40 (15 pmoles) was used as prey and GST (15 pmoles) alone as control. The binding of APE1 WT and mutants was normalized to the Western blotting signal of GST-Mia40 (*: $p<0.05$; *: $p<0.01$).

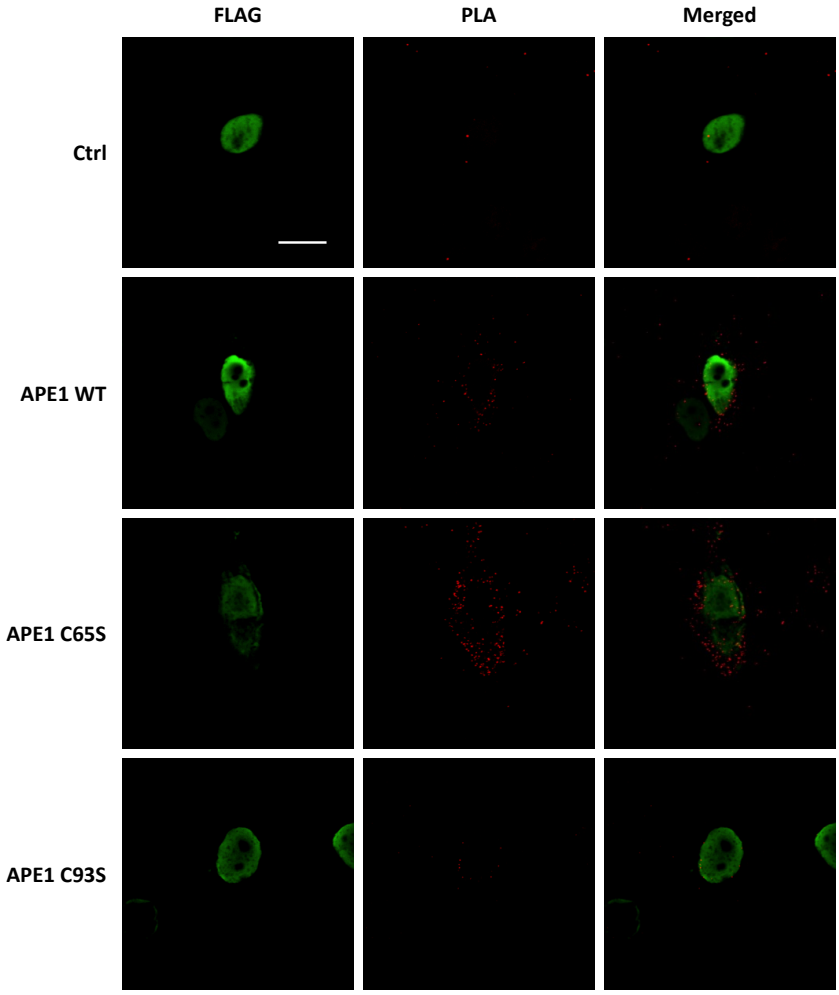

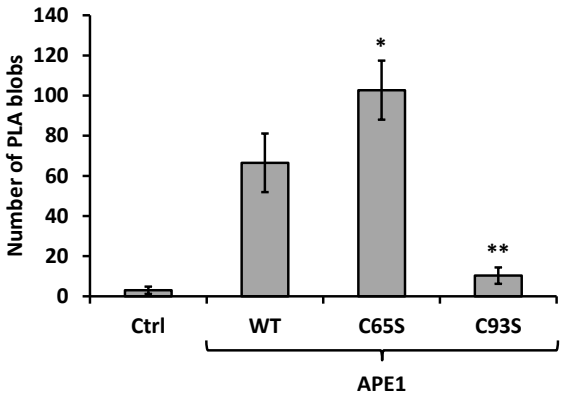

Figure 35. Representative immunofluorescence images (top) and histogram (bottom) of PLA analysis between ectopic flagged APE1 and endogenous Mia40. HeLa cells were transiently transfected with pCMV5.1-FLAG vector expressing APE1 WT, Cys65 and Cys93 to Ser mutants. APE1 expression was detected by using an anti-FLAG antibody (green), while PLA signal are visible as red dots. Control reaction was carried out omitting anti-Mia40 antibody and shows no or little PLA signal. White bar corresponded to 10 μm. Data reported in the histogram accounted for the average number of PLA signals of at least 15 randomly selected cells per condition.

We evaluated the effect of APE1's redox-active cysteine mutation on the stability of the protein, by transiently transfecting HeLa cells with pCMV 5.1 vectors express- ing APE1 WT, Cys65, Cys93, Cys99, Cys65+Cys93 and Cys65+Cys99 to Ser mutants. Expression levels of ectopic flagged APE1's mRNA were analyzed by RT-PCR not showing any major significant differences between the WT and all mutant forms (Figure 36, *top*). On the contrary, ectopic flagged APE1 protein levels in total cell extracts revealed a significant reduction of both the single C93S (33 ± 8%) and the double C65S+C93S (12 ± 8%) mutants, therefore supporting a pivotal role of Cys93 for the overall stability of the protein itself (Figure 36, *bottom*). Next, we assessed the effect of the expression of APE1's C65S and C93S mutants on the levels of mtDNA damage. To down regulate endogenous APE1's expression, we transiently transfected HeLa cells with a pSuper vector coding for an shRNA sequence that specifically target APE1's mRNA, as well as a scramble sequence as a control, and re-expressed shRNA resistant APE1 WT, Cys 93 and Cys56 to Ser mutant forms (Figure 37). Then, we evaluated the effect on the stability of the mtDNA of these mutants by measuring the levels of mtDNA damage through a Q-PCR assay that allowed us to calculate the relative number of mtDNA lesions [352]. As reported in the histogram of Figure 8, down regulation of APE1expression led to increased levels of mtDNA damage, while the re-expression of APE1WT rescued the phenotype. Remarkably, re-expression of the redox C65S mutant did not rescue the phenotype, while the C93S mutant showed even higher levels of mtDNA damage compared to silenced cells. In conclusion, we proved that APE1's Cys93 residue is necessary for the interaction with Mia40, and that the mutation of this residue determines the instability of the protein, inducing a mitochondrial stress condition that finally leads to the increase of mtDNA damage.

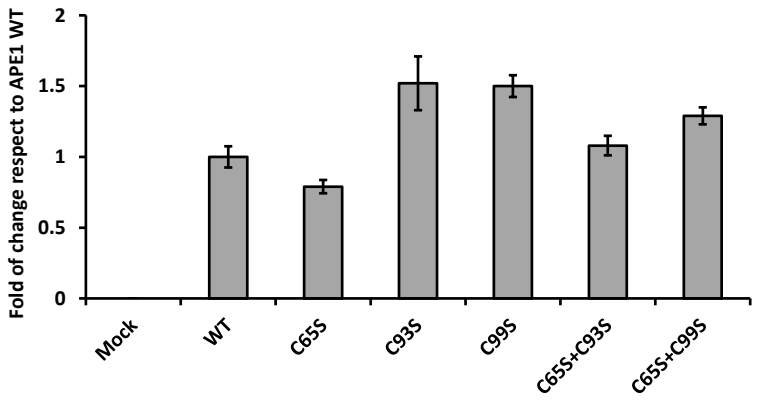

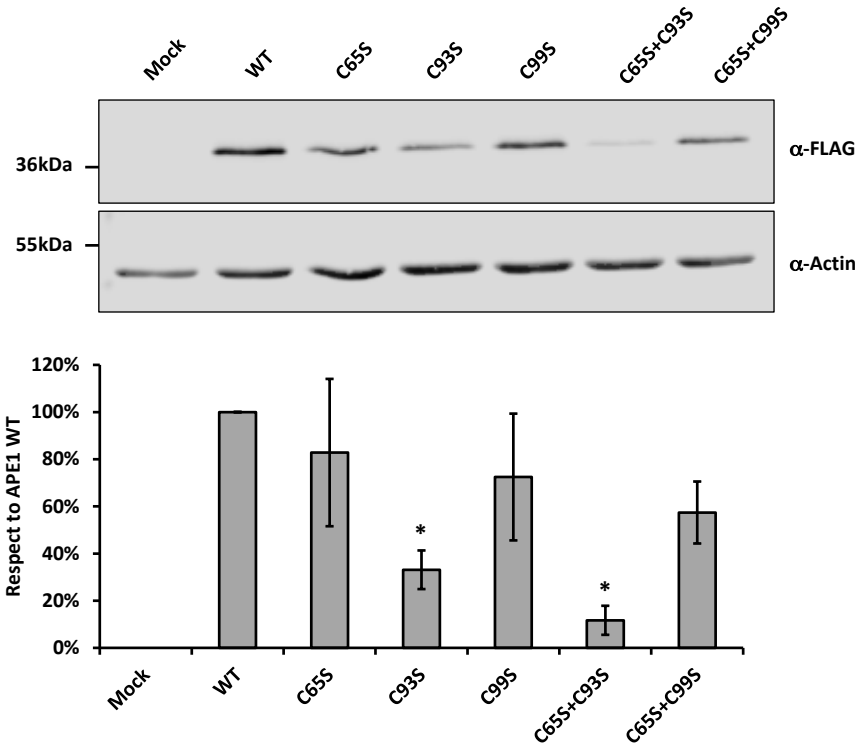

Figure 36. mRNA (*top*) and protein (*bottom*) expression analysis of APE1 redox mutants in HeLa cells. 10 µg of total cell extracts from HeLa cells expressing APE1 WT or redox mutant were analysed by Western blot to evaluate the effect of mutation on APE1 stability. Mutation of Cys93 significantly reduces the accumulation of the protein within the cell respect to the WT form. Actin was used as loading control to normalize APE1's signal intensity.

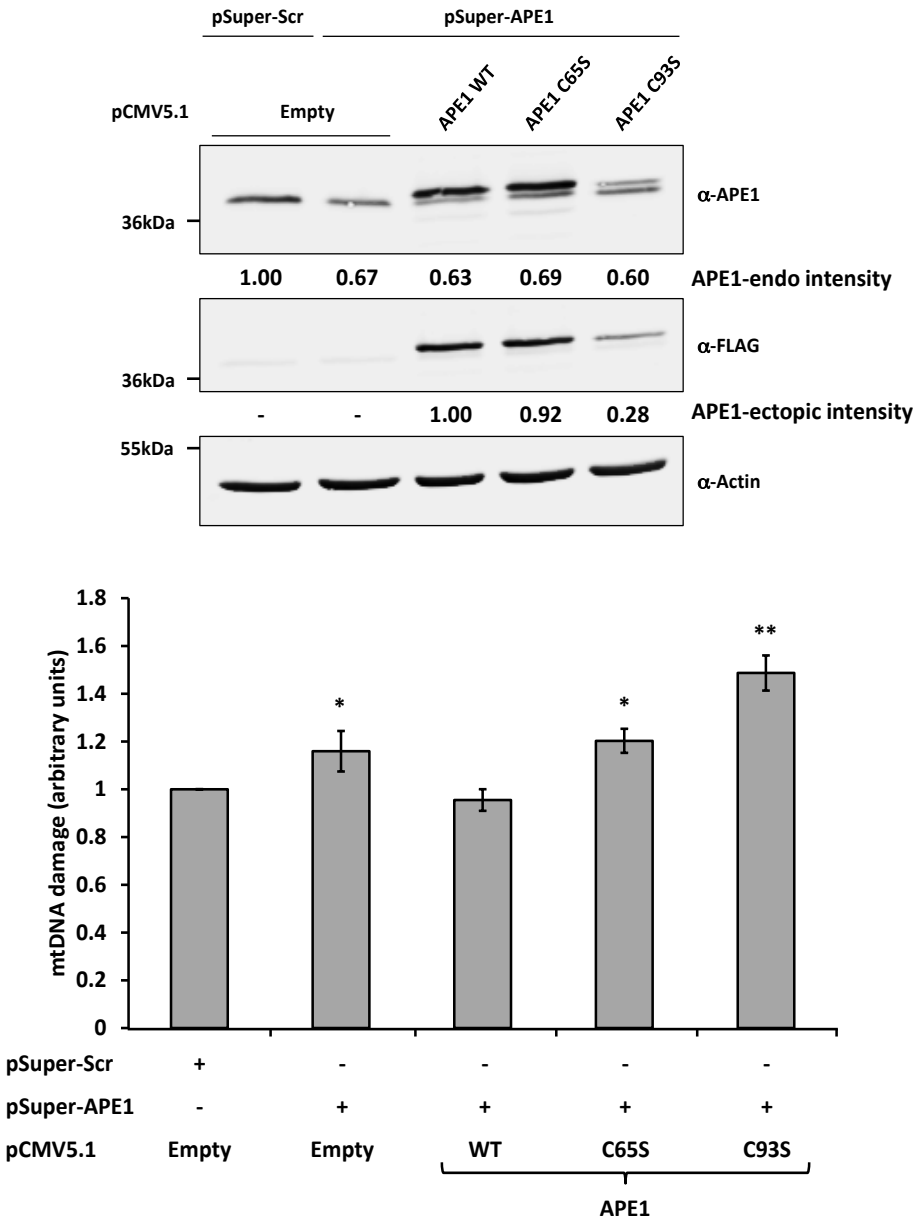

Figure 37. Western blot and mtDNA damage analysis of HeLa cells after endogenous APE1 silencing and re-expression of APE1 WT, Cys65, or Cys93 to Ser mutant proteins. (*top*) Endogenous APE1 protein is significantly reduced after transfection while exogenous APE1 WT, C65S and C93S proteins are expressed. Actin was used as loading control. mtDNA damage analysis of HeLa cells after endogenous APE1 loss of expression and re-expression of ectopic APE1 WT, Cys65, or Cys93 to Ser mutant proteins. **(*bottom*)** Silencing of APE1 leads to increased levels of mtDNA damage rescued by the re-expression of APE1 WT. APE1 C65S and C93S proteins are not able to rescue the damage after APE1 silencing.

1.2 Mia40 is required for mitochondrial translocation of APE1

Having demonstrated that APE1 interacts with Mia40, the next step was to test our hypothesis for an active role of this protein in controlling APE1's translocation into the mitochondrial IMS. First, Mia40 was overexpressed and the amount of APE1 within mitochondrial fractions was measured. A slight, but significant increase of the amount of mitochondrial APE1 form was observed (Figure 38). Next, to prove the biological relevance of the MIA pathway in controlling APE1 mitochondrial translocation, HeLa cells were transiently transfected with specific siRNA against Mia40 (Mia40) and the relative scramble control (Ctrl). Seventy-two hours upon transfection, cells were harvested, mitochondria and nuclei isolated and the amount of APE1 and Mia40 was evaluated through western blotting analyses. Mia40 levels were significantly reduced (up to 90%) and consequently, a significant reduction ofAPE1 levels (35 ± 7%) in mitochondria was observed, suggesting a direct role of Mia40 in controlling APE1's mitochondrial translocation. On the contrary, no significant variation in APE1's nuclear contents was observed (Figure 39). Then, to verify if the decrease of APE1 content resulted in a reduction of mitochondrial endonuclease activity, APE1's enzymatic activity on abasic DNA was measured. A tetrahydrofuran (THF) containing dsDNA probe was incubated with equal amounts of mitochondrial extracts from Ctrl and Mia40 siRNA-transfected cells for the reported times. A significant decrease of endonuclease activity was apparent upon Mia40 knock down due to the reduction of APE1 amount in the mitochondrial fraction (Figure 40). To further support the physiological relevance of Mia40 in controlling APE1 trafficking, we measured the level of mtDNA damage in Mia40 siRNA-transfected cells, and under basal conditions, loss of Mia40 expression did not significantly affect mtDNA damage levels. However, when cells were treated with H_2O_2, the degree of damage was significantly increased, suggesting that the reduction in mitochondrial APE1 amount, due to the loss of Mia40, affected the mtDNA repair capability and thus sensitizing cells to oxidative damaging agents (Figure 41). The same experiment was performed on the human hepatocellular carcinoma (HCC) cell line JHH6, by measuring the level of mtDNA damage in Mia40 siRNA- transfected cells upon H_2O_2 treatment. The data obtained were consistent with the previous results on the HeLa cell line, therefore supporting the generality of the mechanism (Figure 41). These data demonstrate, for the first time, a direct role of the Mia40 protein in the import of APE1 into the mitochondrial compartment and its indirect role in controlling the stability of mtDNA upon oxidative damage.

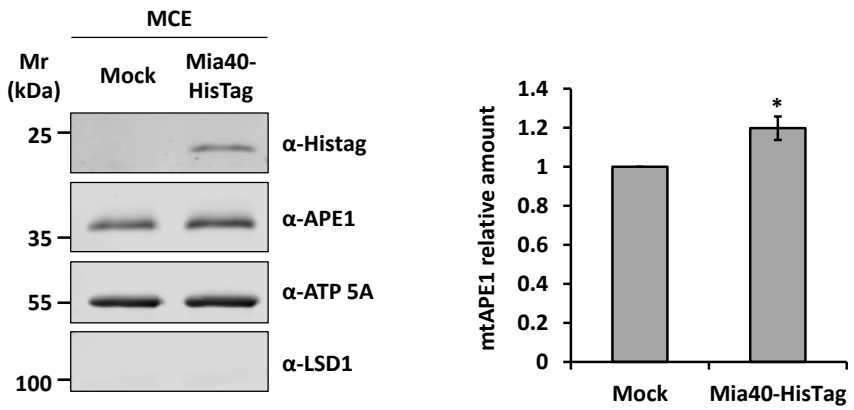

Figure 38. Western blot analysis of HeLa cells extract overexpressing Mia40. (*top*) Western blot analysis (top) of mitochondrial extracts from HeLa cells overexpressing Mia40-HisTag. HeLa cells were transiently transfected with pCMV 5.1 empty vector (Mock) or codifying for Mia40-HisTag protein. **(*bottom*)** Densitometric analysis of mitochondrial APE1 levels highlights a

statistically significant increase of APE1 content into the mitochondrial fraction as consequence of Mia40 overexpression. Data are the mean ±SD of three independent experiments.

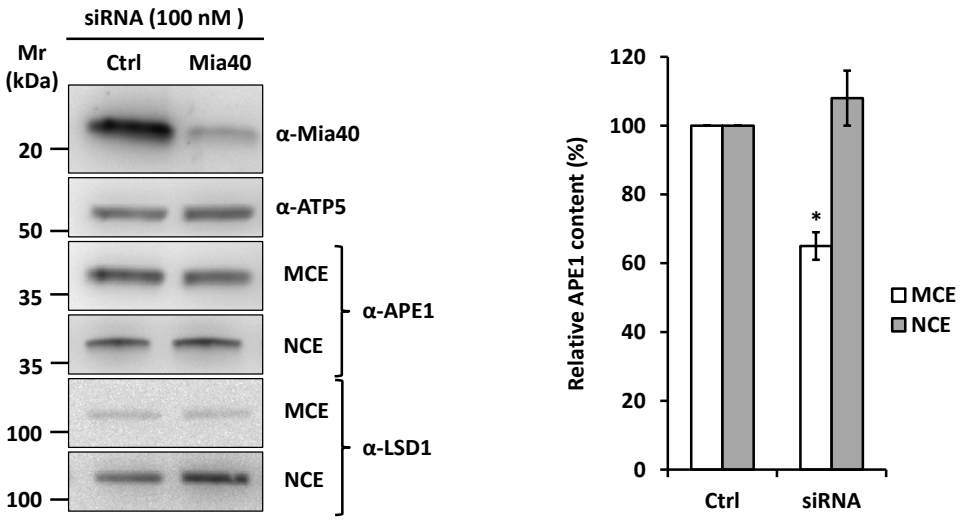

Figure 39. Western blot analysis of nuclear (NCE) and mitochondrial (MCE) HeLa cell extracts of Mia40 siRNA cells. Rapresentative image (*top*) and densitometric analysis (*bottom*) of mitochondrial and nuclear APE1 levels highlights a statistically significant reduction of APE1 content into the mitochondrial fraction as consequence of Mia40 loss of expression. Data are the mean ±SD of five independent experiments.

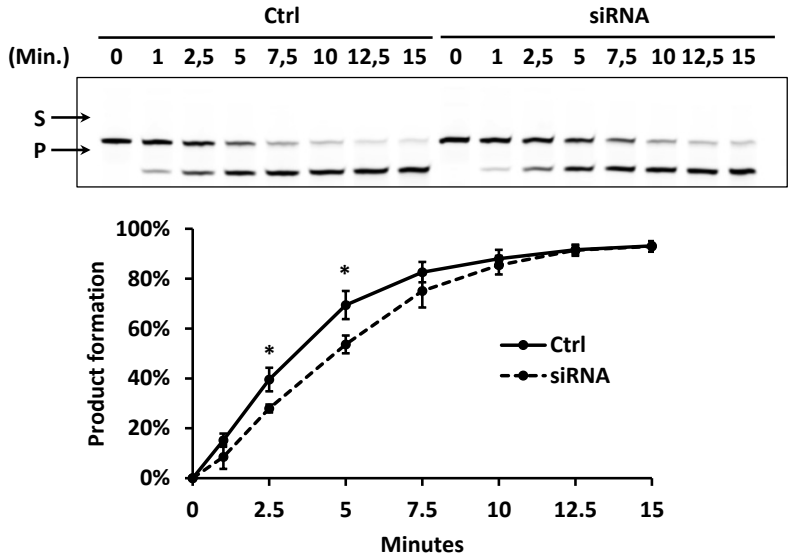

Figure 40. Endonuclease activity analysis of mitochondrial fractions from scramble (Ctrl) and Mia40-siRNA treated cells (siRNA). Data analysis reported in the diagram (bottom) shows that endonuclease activity is reduced after Mia40 silencing.

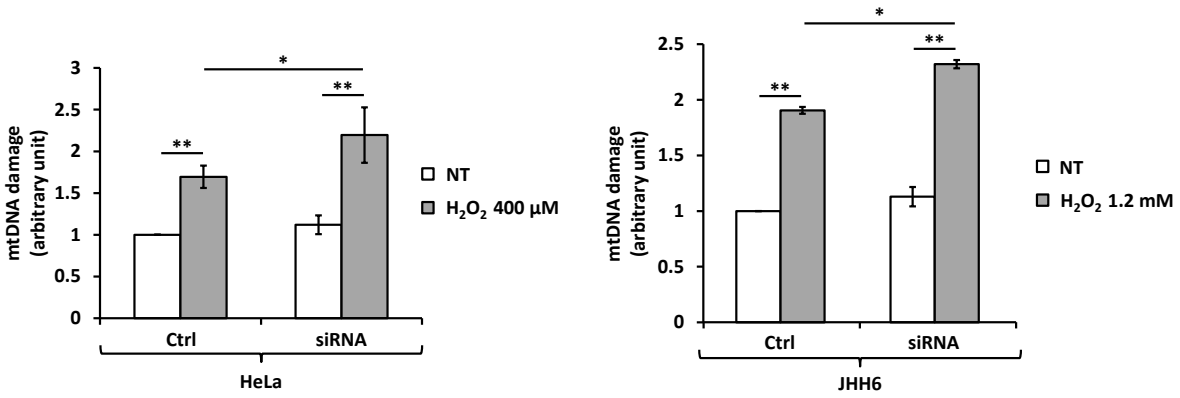

Figure 41. mtDNA damage analysis from HeLa cells (*left*) and JHH6 hepatic cell line (*right*) after Mia40 loss of expression under basal conditions and after H_2O_2 treatment (HeLa: 400 µM; JHH6: 1,2 mM). Silencing of Mia40 leads to an increase of mtDNA damage under oxidative stress conditions.

To prove that APE1 is necessary for the maintenance of the mitochondrial genome stability HeLa cells where endogenous expression of APE1 was knocked-down by siRNA technology in a conditional manner through a doxycycline-responsive promoter were used [102]. Control HeLa cells, obtained after stable transfection with a scrambled sequence (Scr-1), or silenced HeLa cells bearing the APE1 specific siRNA plasmid (shRNA), were treated with doxycycline for 10 days, mitochondria were isolated, and expression levels of APE1were evaluated by western blotting analysis. As re- ported in Figure 42 (left panel), APE1 mitochondrial expression in the shRNA expressing clone was strongly reduced, with protein levels less than 10% compared to the control. The endonuclease activity was also significantly reduced (Figure 42, right panel). The levels of mtDNA damage in the HeLa cell model upon APE1 knock down were then measured, and interestingly, lack of APE1 in shRNA expressing cells was sufficient to strongly increase the mtDNA damage under basal conditions (white bars) (Figure 43). Moreover, when cells were treated withH_2O_2 (gray bars) the mtDNA damage was significantly increased in shRNA expressing clone with respect to control. Altogether, our data support the essential role of APE1 for the repair of oxidative lesions and the repair of mtDNA.

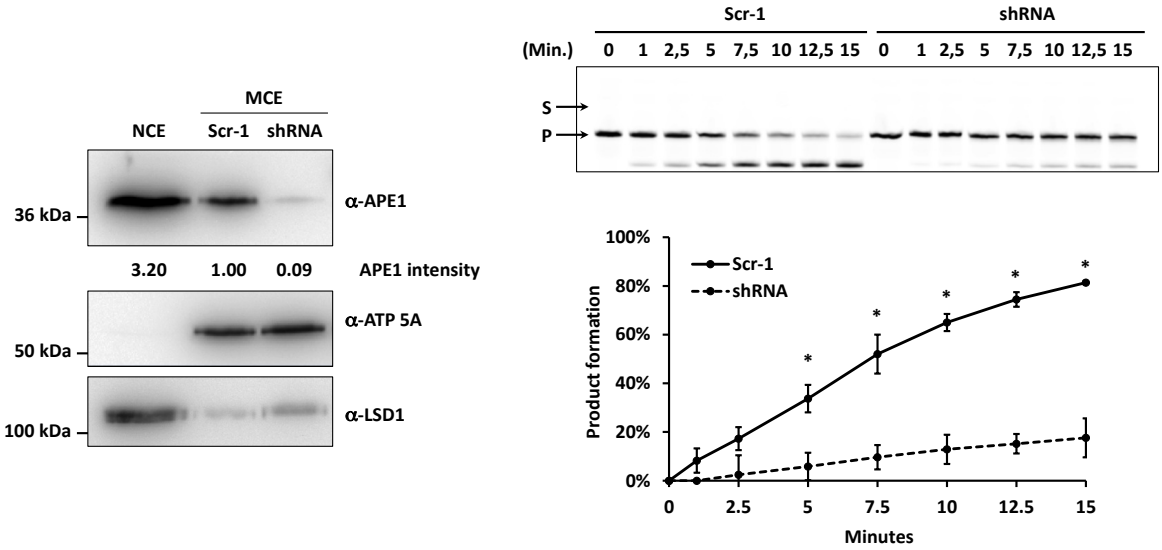

Figure 42. Western blot analysis and endonuclease activity of mitochondrial fractions (MCE) from control and APE1-shRNA stable clones. (*left*) APE1-shRNA cells show APE1 reduction up to 90% respect to the Scr-1 cells. ATP 5A and LSD1 were used as mitochondrial and nuclear markers, respectively. A nuclear extract from HeLa cells was used as control to exclude nuclear/mitochondrial cross contamination. **(*right*)** In the same way the endonuclease activity analysis of mitochondrial extracts from Scr-1 and shRNA cells showed that the activity is almost abolished upon loss of APE1 expression. The conversion of the fluorescent tetrahydrofuran-containing oligonucleotide substrate (S) to the shorter incised product (P) was evaluated for the reported times on a denaturing 20% (wt/vol) polyacrylamide gel. A representative image (top) and average values of incision percentage ±SD of three independent experiments (bottom) are shown.

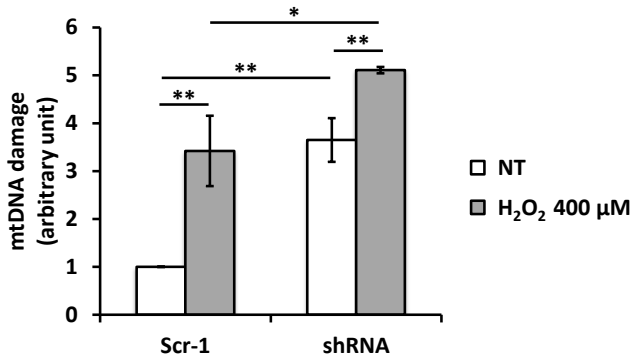

Figure 43. mtDNA damage analysis of Scr-1 and shRNA clones under basal conditions and after H_2O_2 treatment. Levels of mtDNA damage are increased in cells lacking APE1 both under basal and oxidative stress conditions.

APE1's extra-nuclear localization is a marker of poor prognosis in different cancers, such as hepatocarcinoma [353]. However, up to now, the role of this aberrant localization in tumor progression has been unknown. In order to determine whether a correlation exists between Mia40 expression levels and the amount of mitochondrial APE1 protein form in tumor cells, subcellular fractionation was performed on two hepatoma cell lines in which we previously demonstrated that the expression

levels of APE1were significantly different, particularly in the cytoplasmic compartment [353]: Huh7 (well-differentiated HCC) and JHH6 (poorly differentiated HCC). Western blot analyses highlighted the existence of a direct correlation between the expression levels of Mia40 and the amount of APE1 in the mitochondrial fraction of JHH6 cell extracts (Figure 44). To ascertain that the increased mitochondrial localization of APE1 was associated with increased resistance to genotoxic damage, both cell lines were treated with increasing amounts of the DNA alkylating agent MMS and cell viability was measured upon 8 h of treatment. As reported in Figure 16, JHH6 cells were significantly more resistant to the MMS treatment than Huh7 cells. The contribution of Mia40 to the increased resistance observed in JHH6 cells was verified. Down regulation of Mia40 expression by siRNA transfection in JHH6 cells caused a significant reduction of mitochondrial APE1's levels (Figure 45) and a concomitant increased sensitivity to MMS and H_2O_2 treatments than seen in the control cells (Figure 46). In conclusion, our data support the general hypothesis for an unexpected role of the MIA pathway in chemoresistance by directly controlling APE1 translocation into mitochondria and therefore influencing the stability of mtDNA upon genotoxic damage.

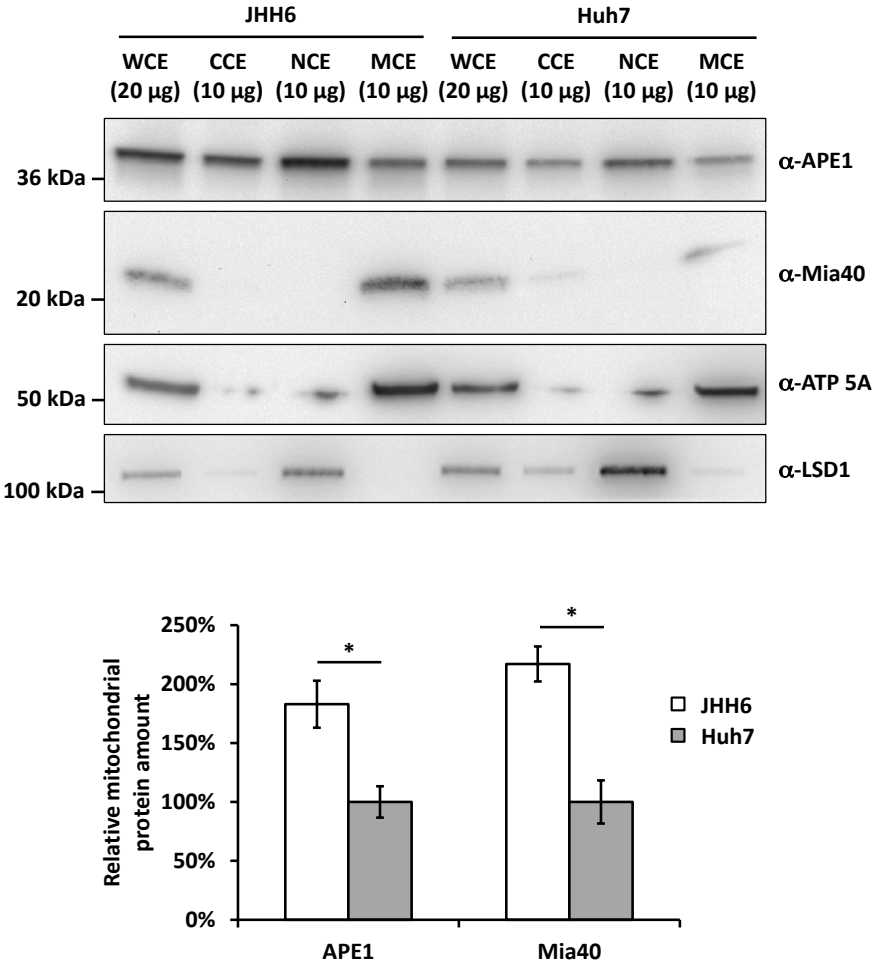

Figure 44. Loss of Mia40 expression sensitizes JHH6 cells to MMS and H_2O_2 treatment. (*top*) Western blot analysis of total (WCE), cytoplasmic (CCE), nuclear (NCE), and mitochondrial (MCE) cell extracts from JHH6 (lanes 1-4) and Huh7 (lanes 5-8) cell lanes. **(*bottom*)** Densitometric analysis shows a direct correlation between expression levels of Mia40 and APE1 (bottom). ATP 5A and LSD1 were used as mitochondrial and nuclear markers, respectively.

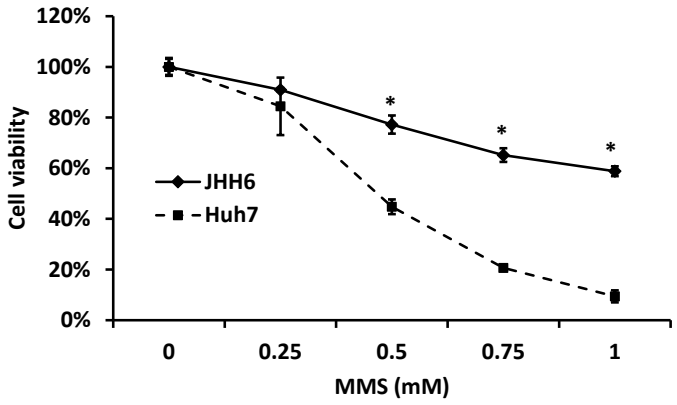

Figure 45. MTS cell viability assay on JHH6 and Huh7 cell lines. 8h MMs treatment of cells led to an increased sensitivity of Huh7 to the treatment.

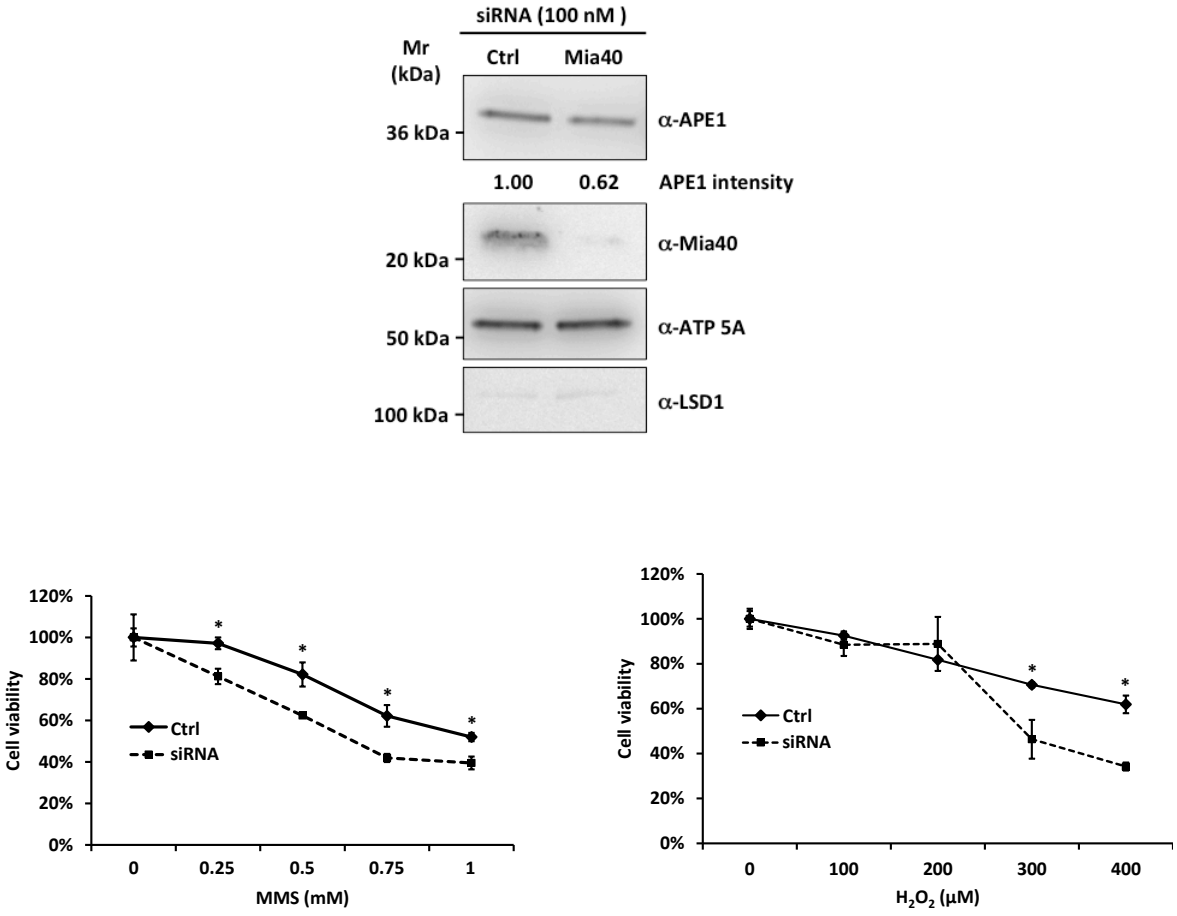

Figure 46. Western blot analysis of mitochondrial extracts of Mia40 siRNA and relative control from JHH6 cells. (*top*) Loss of Mia40 expression negatively affects the mitochondrial levels of APE1 protein. **(*bottom*)** MTS cell viability assay on control (Ctrl) and Mia40 siRNA JHH6 cells after 8 h of treatment with reported amounts of MMS (*left*) and H_2O_2 (*right*). Reduction of mitochondrial APE1 content as consequence of Mia40 silencing sensitizes cells to oxidative and alkylating treatments.

2. Uncanonical role of APE1 on mitochondrial messenger RNA

Having established that APE1 can enter the mitochondrial compartment interacting with Mia40 and using the DRS pathway, our research interest was then focused on how APE1 can enter the mitochondrial matrix, were it can exert its function on the mtDNA. To identify the inner membrane space translocator responsible for the transport of APE1 from the IMS to the matrix we performed an IP-MS analysis on isolated mitochondria expressing a FLAG tagged form of the protein aimed at detecting the mitochondrial interactome of APE1. Interestingly the analysis revealed, besides the expected interacting proteins, a significant percentage of proteins belonging to the mitochodndrial ribosome and enzymes involved in the metabolism of mtRNA and translation. On the basis of this unespected results and on the basis of the recent literature stating the APE1 can have a role on the metabolism of RNA, we decided to pursue this line of research, trying to understand the role of APE1 on the mitochondrial mRNA metabolism.

2.1 APE1 interacts with ribosomal and RNA processing proteins in mitochondria

To study the mitochondrial interactome of APE1 protein we used a HeLa based cellular model previously developed in our group [354] where it is possible to specifically re-express an ectopic siRNA resistant form of APE1 wild-type ($APE1^{WT}$) with a 3XFLAG at the C-terminal on an inducible APE1 siRNA background (Fig. 47). After nine days of doxycycline treatment to silence endogenous APE1 expression, mitochondria from the control shRNA sample (Mock) and $APE1^{WT}$ clones were isolated, and APE1 was immune-purified under native conditions. Then, eluates were subjected to the MS analysis for the identification of mitochondrial interacting partners of APE1 protein. Of all proteins identifies, 160 fulfilled the filter criteria and have been considered as mitochondrial interacting partners of APE1. Then, proteins were clustered for their function (Fig. 48) and, interestingly, many resulted to be involved in RNA translation (MALSU1, MRRF, TUFM, TFSM, ICT1, detailed described in Table 1), RNA processing (PTCD3, GRSF1, DHX30, FASTKD2, PNPT1, TFAM, detailed described in Table 2), or be components of the mitochondrial ribosome (Fig. 48). The interaction with two components of ribosomal small (MRPS15) and large (MRPL9) subunits was validated through the Western blot analysis of a co-immunoprecipitated material from an independent experiment (Fig. 49).

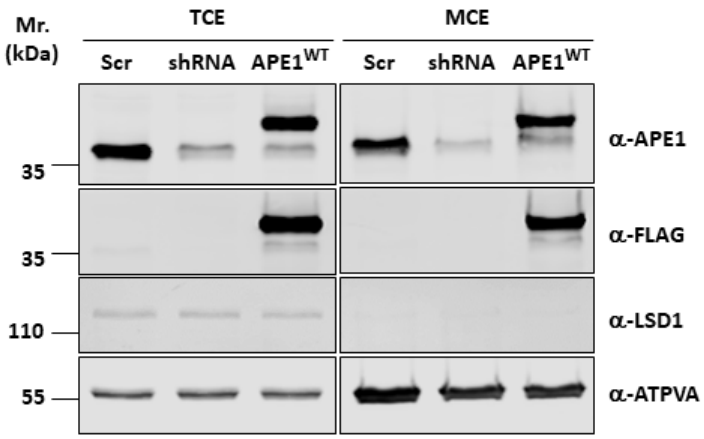

Figure 47. Western blot analysis of total (TCE) and mitochondrial (MCE) protein extracts of cell clones used. Control (Scr), APE1 shRNA (shRNA), and APE1 knock-in ($APE1^{WT}$) clones were treated with doxycycline for 9 days to silence endogenous APE1 protein and to express an ectopic FLAG-tagged recombinant siRNA resistant form ($APE1^{WT}$). Anti-APE1 antibody was used to detect both endogenous and ectopic APE1, while the anti-FLAG was used to confirm the presence of ectopic APE1 into the mitochondrial compartment. Anti-LSD1 antibodies and anti-ATPVA proteins were used as nuclear and mitochondrial markers, respectively.

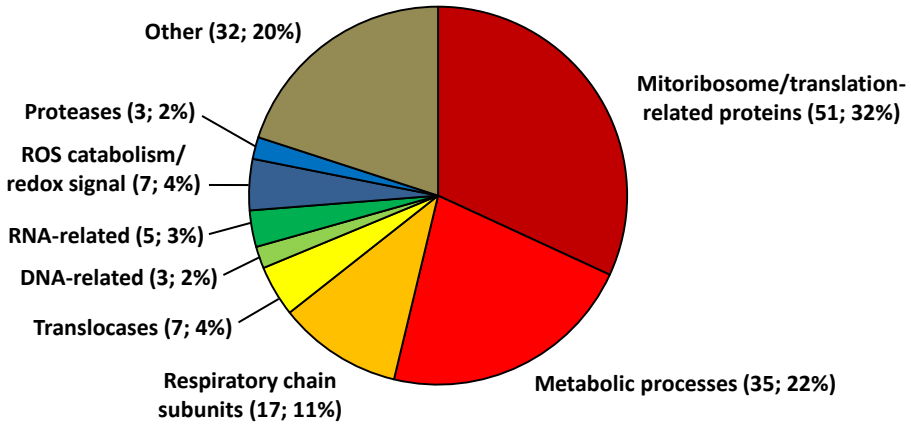

Figure 48. Pie chart of protein classes resulted from MS analysis to interact with APE1 in mitochondria: For each category numbers of proteins and percentage are reported.

Table 1: Mitoribosome/translation related proteins. Panel of proteins belonging to the mitoribosome/translation raleted proteins calss reporting the protein name, gene name, function, and molecular weight based on UNIPROT database description.

Protein name	Gene name	Function	IP/Ctrl ratio	MW
Mitochondrial assembly of ribosomal large subunit protein 1	**MALSU1**	May function as a ribosomal silencing factor. Addition to isolated mitochondrial ribosomal subunits partially inhibits translation. Interacts with mitochondrial ribosomal protein L14 (MRPL14), probably blocking formation of intersubunit bridge B8, preventing association of the 28S and 39S ribosomal subunits and the formation of functional ribosomes, thus repressing translation. May also participate in the assembly and/or regulation of the stability of the large subunit of the mitochondrial ribosome.	APE1-flag only	26,17
Ribosome-recycling factor, mitochondrial (RRF) (Ribosome-releasing factor, mitochondrial)	**MRRF**	Responsible for the release of ribosomes from messenger RNA at the termination of protein biosynthesis. May increase the efficiency of translation by recycling ribosomes from one round of translation to another.	APE1-flag only	36,962
Elongation factor Tu, mitochondrial (EF-Tu) (P43)	**TUFM**	This protein promotes the GTP-dependent binding of aminoacyl-tRNA to the A-site of ribosomes during protein biosynthesis.	2,15	49,541
Elongation factor Ts, mitochondrial (EF-Ts) (EF-TsMt)	**TSFM**	Associates with the EF-Tu.GDP complex and induces the exchange of GDP to GTP. It remains bound to the aminoacyl-tRNA.EF-Tu.GTP complex up to the GTP hydrolysis stage on the ribosome.	1,94	18,587
Peptidyl-tRNA hydrolase ICT1, mitochondrial (39S ribosomal protein L58, mitochondrial) (MRP-L58) (Digestion substraction 1) (DS-1) (Immature colon carcinoma transcript 1 protein)	**ICT1**	Essential peptidyl-tRNA hydrolase component of the mitochondrial large ribosomal subunit. Acts as a codon-independent translation release factor that has lost all stop codon specificity and directs the termination of translation in mitochondrion, possibly in case of abortive elongation. May be involved in the hydrolysis of peptidyl-tRNAs that have been prematurely terminated and thus in the recycling of stalled mitochondrial ribosomes.	6,98	21,905
Large ribosomal subunits (31 out of 50)				
Small ribosomal subunits (14 out of 31)				

Table 2: RNA related proteins. Panel of proteins belonging to the RNA related proteins class reporting the protein name, gene name, function, and molecular weight based on UNIPROT database description.

Protein name	Gene name	Function	IP/Ctrl ratio	MW
Transcription factor A, mitochondrial (mtTFA) (Mitochondrial transcription factor 1) (MtTF1) (Transcription factor 6) (TCF-6) (Transcription factor 6-like 2)	**TFAM**	Binds to the mitochondrial light strand promoter and functions in mitochondrial transcription regulation. Required for accurate and efficient promoter recognition by the mitochondrial RNA polymerase. Promotes transcription initiation from the HSP1 and the light strand promoter by binding immediately upstream of transcriptional start sites. Is able to unwind DNA. Bends the mitochondrial light strand promoter DNA into a U-turn shape via its HMG boxes. Required for maintenance of normal levels of mitochondrial DNA. May play a role in organizing and compacting mitochondrial DNA.	4,28	20,096
Polyribonucleotide nucleotidyltransferase 1, mitochondrial	**PNPT1**	RNA-binding protein implicated in numerous RNA metabolic processes. Catalyzes the phosphorolysis of single-stranded polyribonucleotides processively in the 3'-to-5' direction. Mitochondrial intermembrane factor with RNA-processing exoribonulease activity. Component of the mitochondrial degradosome (mtEXO) complex, that degrades 3' overhang double-stranded RNA with a 3'-to-5' directionality in an ATP-dependent manner. Required for correct processing and polyadenylation of mitochondrial mRNAs. Plays a role as a cytoplasmic RNA import factor that mediates the translocation of small RNA components, like the 5S RNA, the RNA subunit of ribonuclease P and the mitochondrial RNA-processing (MRP) RNA, into the mitochondrial matrix.	APE1-flag only	85,95
FAST kinase domain-containing protein 2	**FASTKD2**	Plays an important role in assembly of the mitochondrial large ribosomal subunit.	APE1-flag only	81,462
Pentatricopeptide repeat domain-containing protein 3, mitochondrial	**PTCD3**	Mitochondrial RNA-binding protein that has a role in mitochondrial translation.	14,16	78,549
Serine--tRNA ligase, mitochondrial	**SARS2**	Catalyzes the attachment of serine to tRNA(Ser). Is also able to aminoacylate tRNA(Sec) with serine, to form the misacylated tRNA L-seryl-tRNA(Sec), which will be further converted into selenocysteinyl-tRNA(Sec). ATP + L-serine + tRNA(Ser) = AMP + diphosphate + L-seryl-tRNA(Ser). ATP + L-serine + tRNA(Sec) = AMP + diphosphate + L-seryl-tRNA(Sec).	5,45	58,182

G-rich sequence factor 1	**GRSF1**	Regulator of post-transcriptional mitochondrial gene expression, required for assembly of the mitochondrial ribosome and for recruitment of mRNA and lncRNA. Binds RNAs containing the 14 base G-rich element. Preferentially binds RNAs transcribed from three contiguous genes on the light strand of mtDNA, the ND6 mRNA, and the long non-coding RNAs for MT-CYB and MT-ND5, each of which contains multiple consensus binding sequences.	2,50	36,613
Putative ATP-dependent RNA helicase DHX30	**DHX30**	Plays an important role in the assembly of the mitochondrial large ribosomal subunit. Required for optimal function of the zinc-finger antiviral protein ZC3HAV1 (By similarity). Associates with mitochondrial DNA.	2,70	130,55

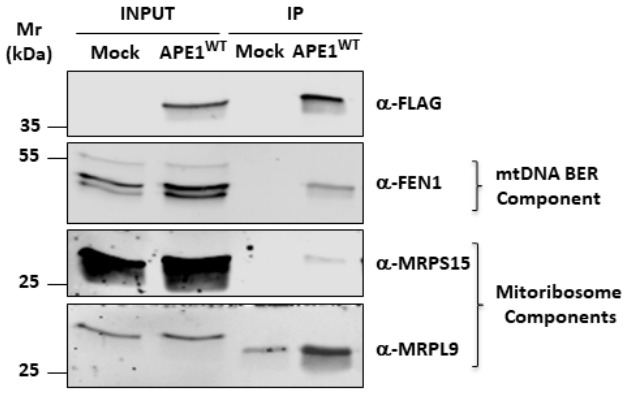

Figure 49. Western blot analysis of an immunoprecipitated material to validate the interaction with mitochondrial ribosome subunits. shRNA (Mock) and APE1^{WT} clones were treated with doxycycline for 9 days, then mitochondria were isolated and lysed under native conditions (Input) and immunoprecipitated with anti-FLAG (IP). The presence of small (MRSPS15) and large (MRPL9) subunit components were detected using specific antibodies. The interaction with mitochondrial base excision repair (mtBER) component FEN-1 was evaluated as the positive control.

2.2 APE1 binds and processes abasic mitochondrial RNA

Next, we assessed if, apart from interacting with mitochondrial proteins involved in RNA metabolism, the APE1was able to directly bind *in vivo* RNA molecules. Newly synthetized RNA was labeled *in vivo* with bromouridine (BrU) by 30-minute incubation of HeLa cells with 2.5 mM of BrU [355], while unlabeled cells (Bru-) were used as the control in PLA analyses (Fig 50). The presence of dots in the metabolically labeled cells (BrU+) confirmed the interaction between APE1 and RNA (Fig. 51). Moreover, to evaluate if the binding of APE1 increased upon oxidative stress, the cells labeled with BrU were treated with Antimycin A (AMA) at the final concentration of 25 μM for 30 minutes. AMA

is an inhibitor of the mitochondrial electron transport chain complex III which inhibition specifically induces mitochondrial oxidative stress [356]. As for DNA, also RNA can undergo oxidative damage and the prevalent oxidized base in RNA is 8-hydroxyguanosine (8-OHG) which could be released leaving AP sites [357]. The analysis has demonstrated that APE1 constitutively binds to RNA (70±21 PLA dots/cell) and that this binding is significantly enhanced by the induction of mitochondrial oxidative stress (179±24 PLA dots/cell). These data open up the possibility that APE1 could bind and exert endoribonuclease activity on abasic RNA (AP-RNA) (Fig. 51). To verify this hypothesis, we measured the extent of oxidative base loss in mitochondrial RNA as a function of APE1 expression using an aldehyde-reactive probe (ARP) [358]. Oxidatively depurinated/depyrimidinated RNA species were specifically labeled with ARP, isolated with streptavidin magnetic-beads, and qRT-PCR was performed to evaluate the amount of ND1 and COX2 mRNAs. Loss of APE1 expression (shRNA) was associated with a significant increase in damaged mitochondrial RNA, while re-expression of wild-type APE1 ($APE1^{WT}$) reverted this effect (Fig. 52, top). To support the specificity of the assay, the cells treated with AMA showed a higher amount of damaged RNA (Fig. 52, bottom). Altogether, these data support a new role of the mitochondrial form of APE1 protein in the metabolism of damaged mitochondrial RNA.

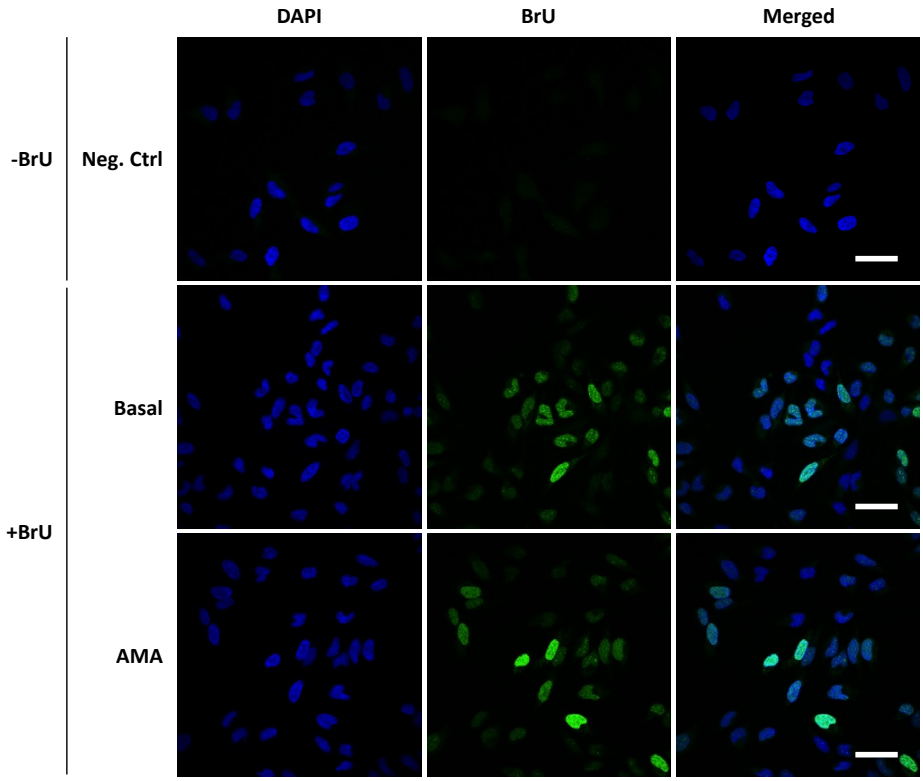

Figure 50. *In vivo* RNA labeling with boromouridine. Immunofluorescence analysis of HeLa cells unlabelled (-BrU) or labelled (BrU) with bromouridine in vivo and treated (AMA) or not (Basal) with Antimycin A, 25 μM for 30 minutes. Nuclei were stained with DAPI, and BrU incorporation was detected using a polyclonal primary antibody anti-BrdU followed by incubation with a secondary antibody anti-Rabbit conjugated with an Alexa Flow 488 dye. The specificity was confirmed by the absence of any signal in unlabeled cells (Neg. Ctrl). Moreover, in the image is also visible how treatment with AMA did not affect the signal of BrU. White bars indicates a measure of 10 μm.

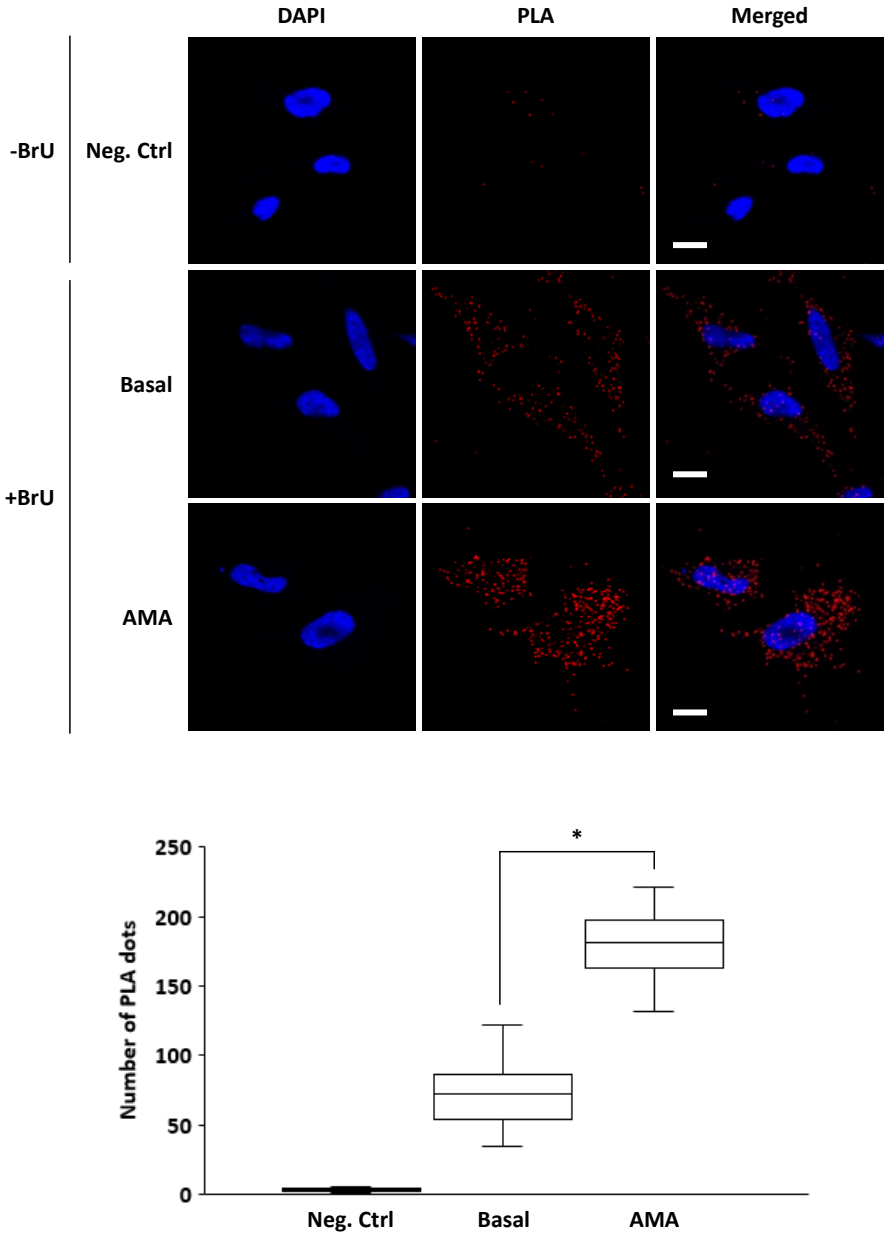

Figure 51. Proximity ligation assay analysis between APE1 and RNA. (*top*) Rapresentative image of PLA analysis performed to evaluate the interaction between APE1 and RNA under basal condition and upon induction of mitochondrial oxidative stress. HeLa cells unlabeled (-BrU) or labeled (BrU) with bromouridine in vivo were treated (AMA) or not (Basal) with Antimycin A to induce mitochondrial oxidative stress. PLA was performed using anti-APE1 and anti-BrdU antibodies. **(*bottom*)** Box plot reports the number of PLA dots counted in an average of 35 cells for each condition and the differences were found significant at a p-value of 0.01x10-15. White bars indicate a measure of 10 µm. (*: $p<0.05$).

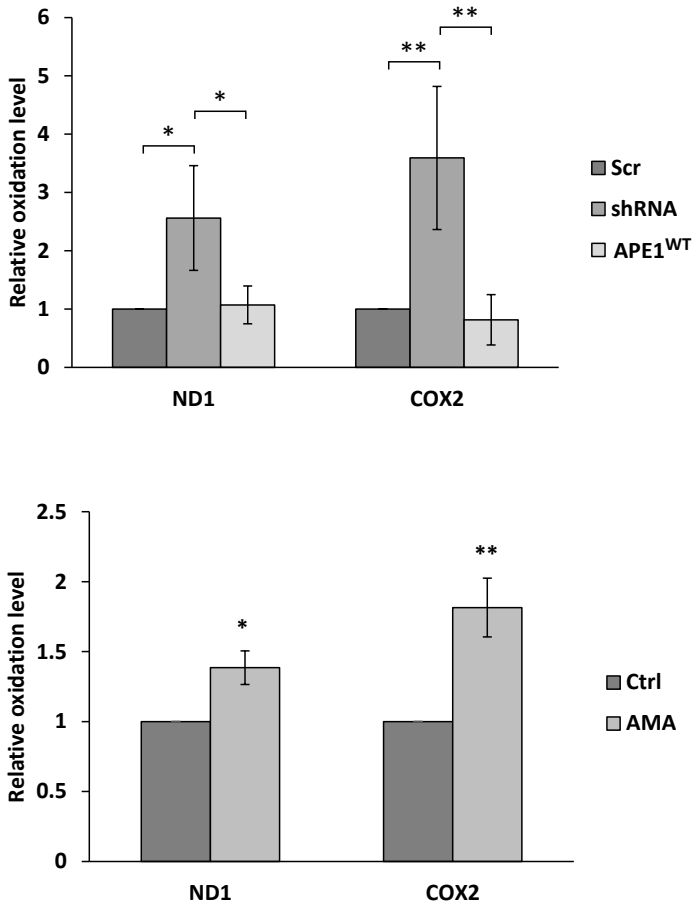

Figure 52. Quantification of abasic sites in mitochondrial RNA. (*top*) Quantification of abasic sites in mitochondrial RNA of ND1 and COX2 messengers in control (Scr), APE1 shRNA, and knock-in ($APE1^{WT}$) clones. Precipitated AP-RNA and total RNA were subjected to qRT-PCR and levels of mitochondrial RNA damage were determined based on the difference in Ct value between oxidized and total RNA. **(*bottom*)** Quantification of abasic sites in mitochondrial RNA of ND1 and COX2 messengers in HeLa cells treated with AMA. As positive control of the assay used to evaluate the levels of mitochondrial mRNAs oxidation as consequence of APE1 loss of expression (Fig. 2B), HeLa cells were treated for 3 h with 100 μM of AMA to induce mitochondrial oxidative stress. Isolated RNA was derivatized by treatment with ARP, followed by purification with magnetic beads. Precipitated AP-RNA and total RNA were subjected to qRT-PCR for ND1 and COX2. Levels of mitochondrial RNA damage were determined based on difference in Ct value between oxidized and total RNA. (*: $p<0.05$; **: $p<0.01$).

2.3 Mitochondrial mRNA half-life is dependent on APE1

Having established that APE1 binds RNA and that loss of mitochondrial APE1 expression determines the accumulation of AP sites on mRNAs, we used qRT-PCR to measure the levels of mitochondrial (ND1, CytB, COX2, ATP6) and nuclear (NDUFA1, CYC1, COX6B, ATPVA) encoded mRNAs codifying for proteins of the complexes I, III, IV, and V, respectively. While the expression of APE1 did not affect the levels of the nuclear encoded mRNAs, all mitochondrial encoded primary transcripts (mt-mRNA) were significantly upregulated in APE1 shRNA clone (Fig. 53). In order to exclude the

possibility that the effect observed was due to the use of stable cell clones, HeLa cells were transiently transfected with a different APE1-specific siRNA. Also in this case, APE1 depletion was followed by a significantly increased expression of mitochondrial encoded mRNAs (Fig. 54). To establish if the observed rise in mt-mRNA levels was the consequence of an enhanced expression or of an impairment in the RNA degradation processes, mitochondrial gene transcription was specifically inhibited by treating cells with low concentrations of ethidium bromide (EtBr) [359]. While control cells (Scr) showed a linear reduction of mRNA levels, in APE1 deficient clone (shRNA) mRNAs appeared to be more stable, thus confirming the hypothesis of an impairment in the mitochondrial RNA degradation processes in the absence of APE1 (Fig. 55). To further support these data, mitochondrial RNA stability of ND1 and CytB primary transcripts was measured by metabolic labeling with 4-thiouridine (4sU) as previously described by Borowski *et al.* [344]. In accordance with the previous results, RNA half-life of ND1 (1.67±0.06 hours) and CytB (1.50±0.03 hours) of the control clones was significantly increased upon APE1 loss of expression ND1: 2.34±0.36 hours; Cyt.B (2.14±0.31 hours) (Fig. 56).

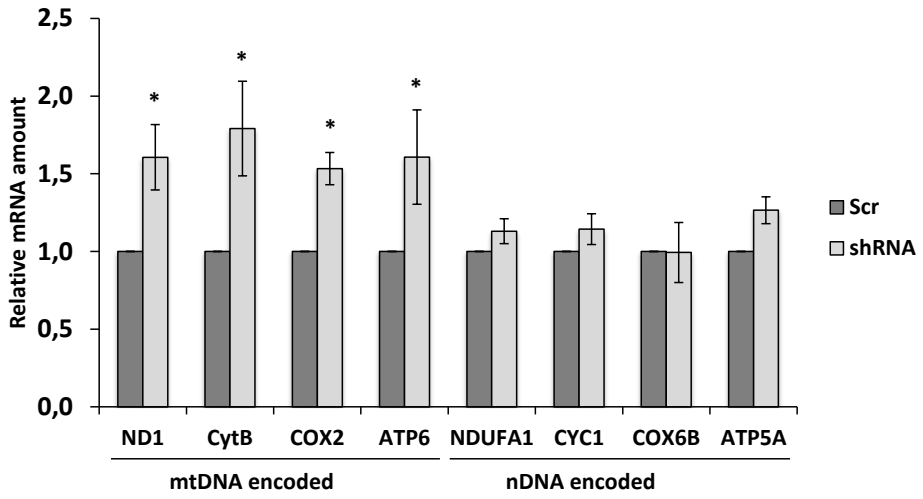

Figure 53. qRT-PCR analysis of mitochondrial DNA (mtDNA) and nuclear DNA (nDNA) encoded mRNAs. mRNA levels of mtDNA encoded genes ND1, CytB, COX2, ATP6 and nDNA encoded genes NDUFA1, CYC1, COX6B, ATP5A were measured on control (Scr) and APE1 shRNA clones using specific primers. (*: $p<0.05$).

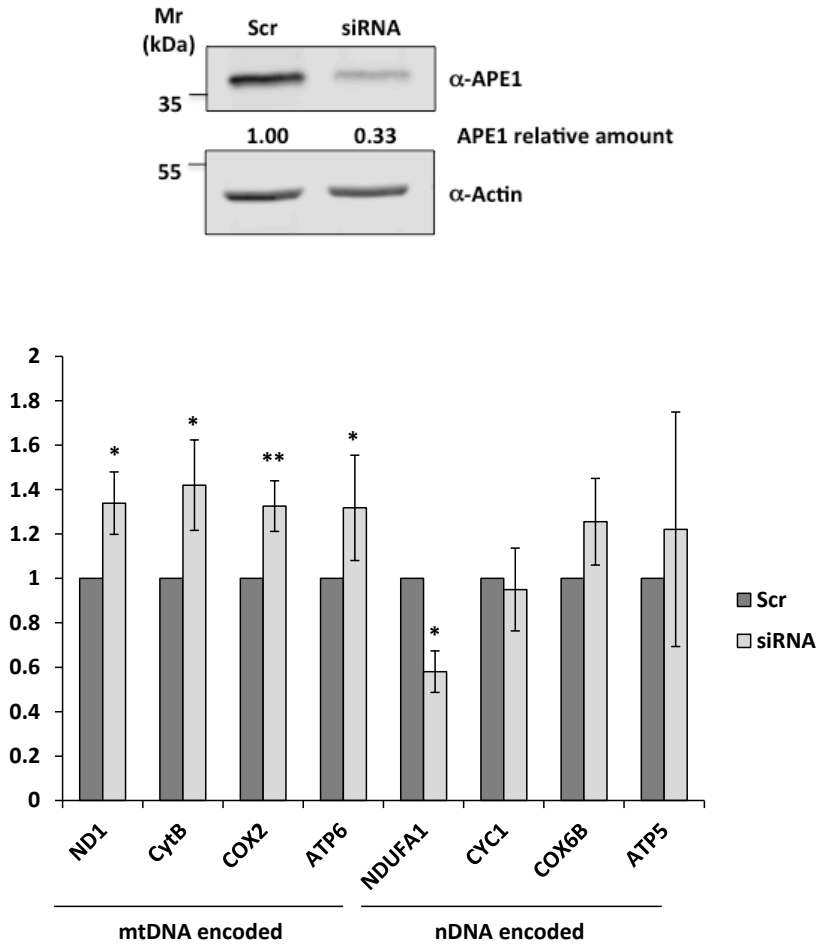

Figure 54. Effect of transient APE1 downregulation on mitochondrial mRNA expression. (*top*) Representative Western blot analysis of total cellular extract of HeLa cells transiently transfected with control (Scr) and specific siRNA for APE1. Protein expression was evaluated using anti-APE1 antibody, while anti-Actin was used as loading control. **(*bottom*)** qRT-PCR analysis of mitochondria (mtDNA) and nuclear (nDNA) DNA encoded mRNAs expression of HeLa cells where APE1 protein was transiently silenced by siRNA transfection. As in the stable clones, while the expression of APE1 did not affect the levels of the nuclear encoded mRNAs, all mitochondrial encoded primary transcripts resulted significantly upregulated as consequence of APE1 loss of expression. Data reported are the mean±SD of three independent biological replicates. (*: $p<0.05$; **: $p<0.01$).

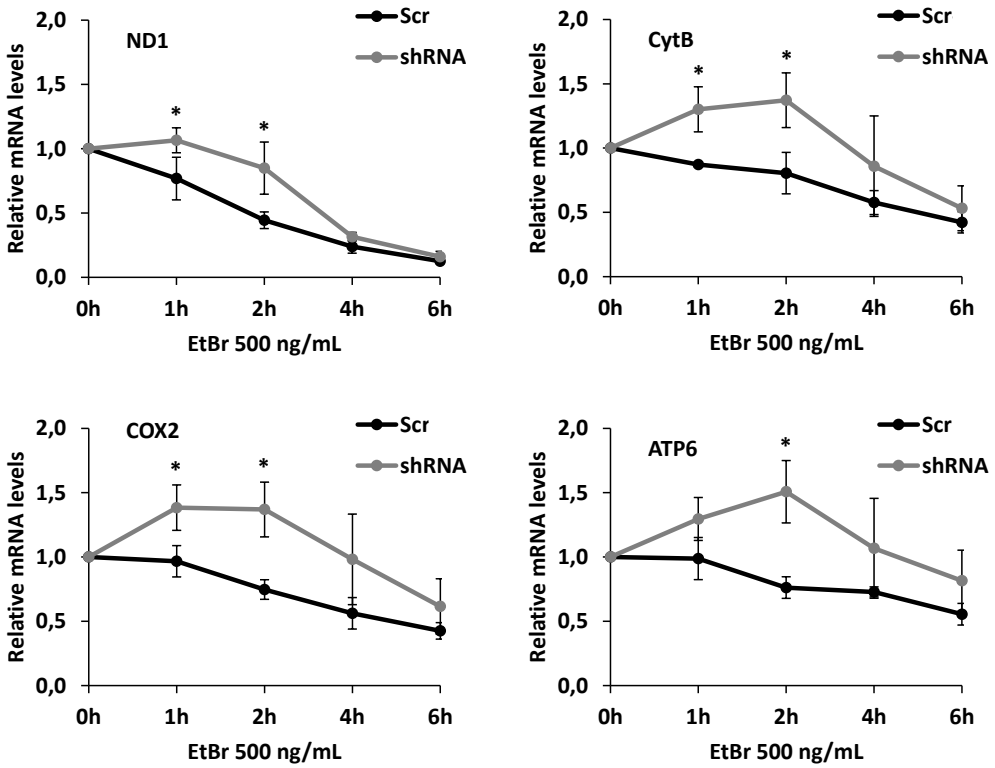

Figure 55. qRT-PCR analysis of mitochondrial encoded mRNAs ND1, CytB, COX2, and ATP6 to measure mRNA half-life. Cells were treated with ethidium bromide to inhibit mitochondrial gene transcription and to measure the effect of APE1 expression on mt-mRNAs half-life. (*: $p<0.05$).

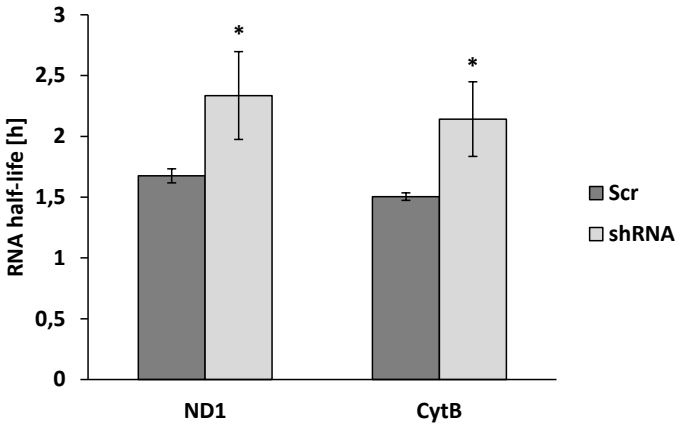

Figure 56. Histogram represents the ND1 and CytB mRNA half-life. Half-life was calculated by metabolic labeling with 4-thiouridine (4sU). (*: $p<0.05$).

2.4 APE1 mutant E96A is not able to exert enzymatic activity on mitochondrial mRNA species

The majority of APE1 is localized within the nucleus where the protein exerts endonuclease activity on abasic DNA but also regulates in a redox-dependent manner the activity of several transcriptional factors such as NF-κB, HIF-1α, and p53. To confirm that the effects observed on mt-mRNAs were due to the absence of the mitochondrial APE1 rather than to its nuclear counterpart, we transiently re-expressed on the background of APE1 shRNA clone an ectopic siRNA resistant APE1 form where the NLS at N-terminus was replaced by the mitochondrial targeting sequence (MTS) of MnSOD2 [131]. The Western blot analysis confirmed the expression of the two chimeric proteins, the enzymatically active MTS-APE1^{WT} and the nuclease defective mutant MTS-APE1^{E96A} [122] (Fig 57, top), while through the immune fluorescence analysis we proved that substitution of NLS with MTS led to the exclusion of the recombinant proteins from the nuclear compartment and their accumulation within the mitochondria (Fig. 57, bottom). Then, we measured the levels of mitochondrial mRNAs in APE1 shRNA cells after the re-expression of the two ectopic recombinant forms of APE1 (Fig. 58). While the expression of the APE1^{WT} was able to revert the phenotype reducing the levels of mt-mRNAs, the nuclease defective APE1^{E96A} mutant only partially rescued the phenotype supporting the conclusion that APE1 exerts endoribonuclease activity on AP-RNA in mitochondria. qRT-PCR data were further validated by Norther blot analyses using specific probes for ND1 and COX2 mRNAs. In accordance with qRT-PCR analyses, mRNA levels were higher in APE1-deficient cells and the phenotype was restored by sole re-expression of APE1^{WT} within the mitochondrial compartment. As before, the rescue effect was lost when the endonuclease defective form APE1^{E96A} was expressed (Fig. 59).

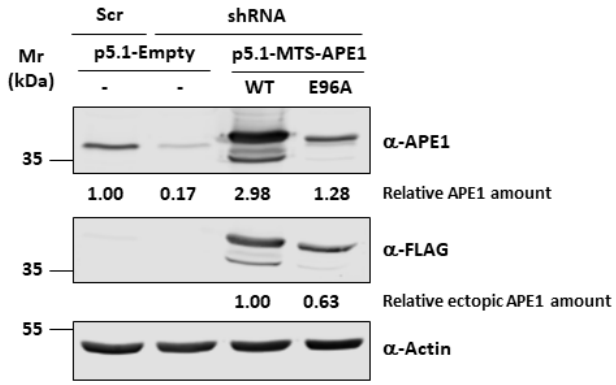

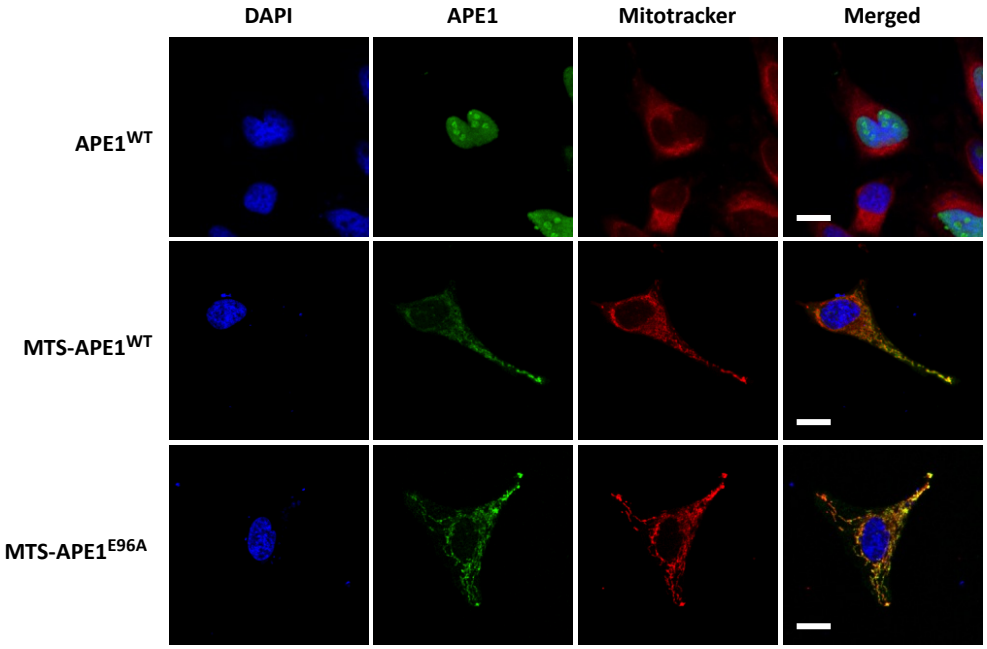

Figure 57. Western blot analysis and immunofluorescence analysis of control (Scr) and APE1 shRNA clones. (*top*) Western blot analysis of clones treated with doxycycline and transiently transfected with empty vector (p5.1-Empty) or FLAG-tagged expression plasmids codifying for siRNA-resistant APE1 forms MTS-APE1^{WT} and MTS-APE1^{E96A}. Anti-APE1 and anti-FLAG antibodies were used to detect endogenous and ectopic APE1 expression, respectively. Anti-Actin was used as loading control. **(*bottom*)** Representative image of immunofluorescence analysis of APE1 shRNA clone transiently transfected with FLAG-tagged expression plasmids. shRNA clone was transfected with plasmids codifying for siRNA-resistant APE1^{WT} and mitochondrial targeted mutants MTS-APE1^{WT} and MTS-APE1^{E96A}. Nuclei are stained with DAPI, APE1 with anti-FLAG conjugated with 488 dye, and mitochondria with Mitotracker DeepRed. White bars indicate a measure of 10 μm.

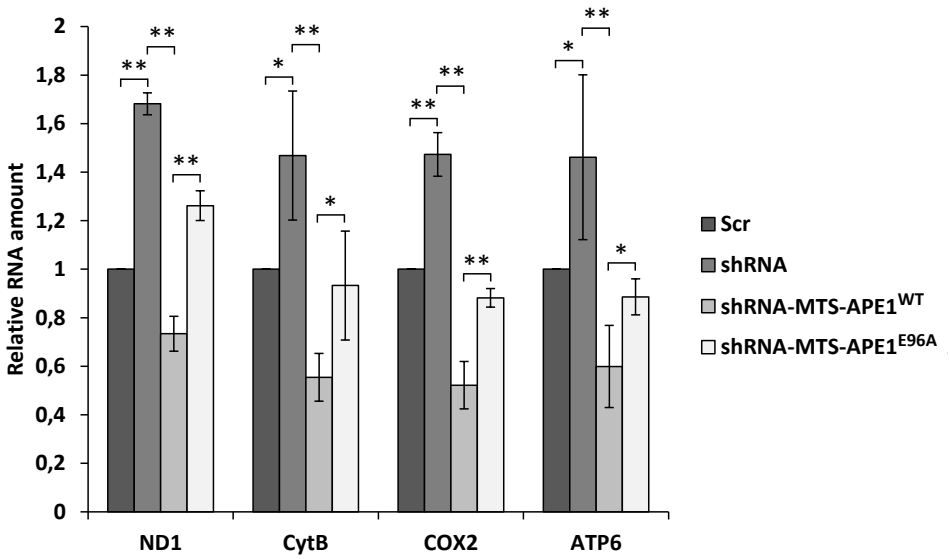

Figure 58. qRT-PCR analysis of mitochondrial DNA encoded genes. ND1, CytB, COX2, ATP6 measured on control (Scr) and APE1 shRNA clones treated with doxycycline and transiently transfected with empty vector (p5.1-Empty) or FLAG-tagged expression plasmids codifying for siRNA-resistant APE1 forms MTS-APE1^{WT} and MTS-APE1^{E96A}. (*: $p<0.05$; **: $p<0.01$)

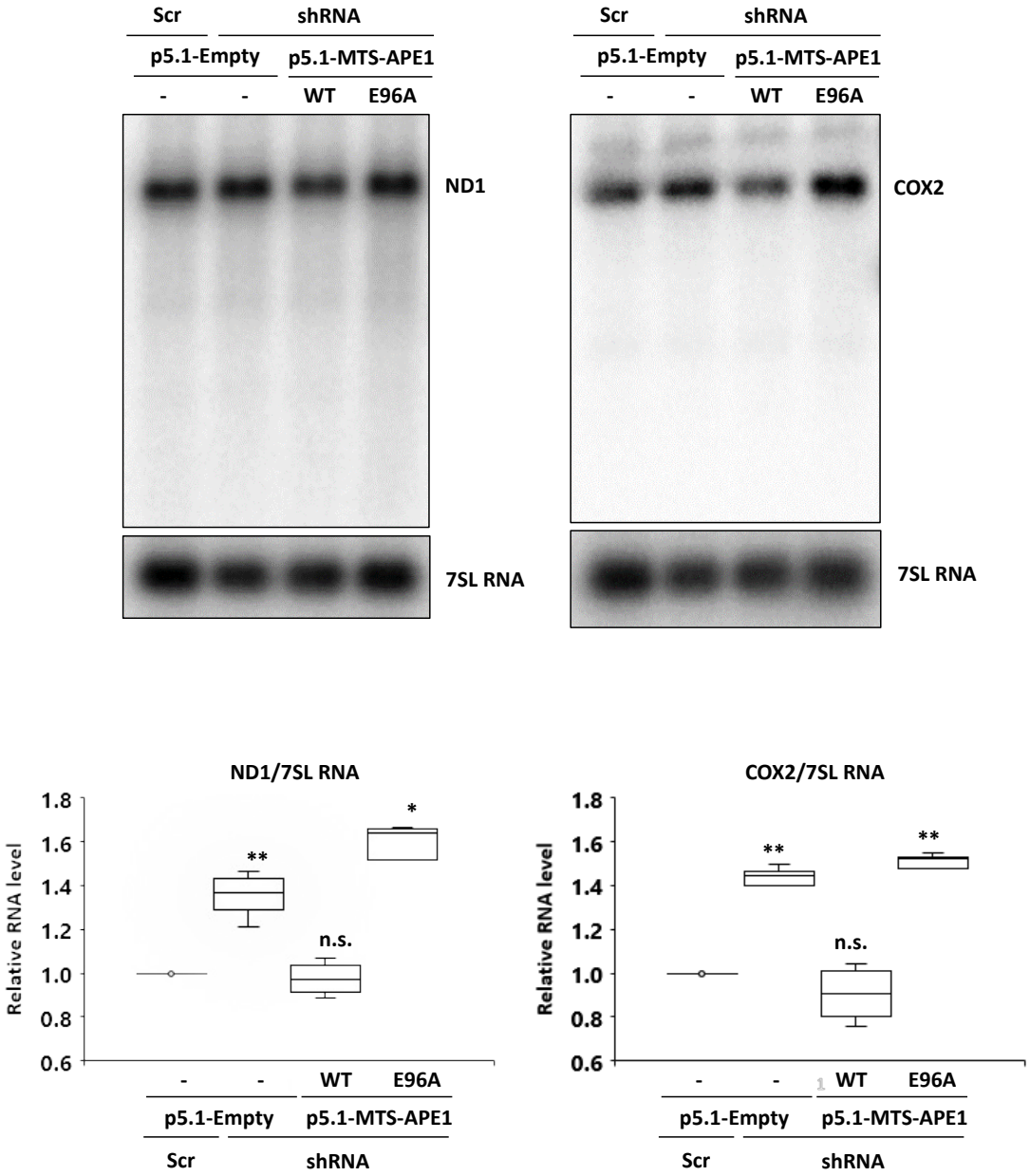

Figure 59. Northern blot analysis of RNA isolated from control (Scr) and APE1 shRNA clones. Clones were treated with doxycycline and transiently transfected with empty vector (p5.1-Empty) or FLAG-tagged expression plasmids codifying for siRNA-resistant APE1 forms MTS-APE1^{WT} and MTS-APE1^{E96A}. Mitochondrial encoded ND1 (*left*) and COX2 (*right*) mRNAs were detected with the help of strand-specific radiolabeled riboprobes. Nuclear encoded 7SL RNA was used as a loading control. **(*top*)** Representative autoradiograms are shown. **(*bottom*)** Box plots show quantitation and mean±SD of four biological replicates. Statistical significance was calculated respect to the control sample (Scr-Empty). (n.s.: not significant; *: $p<0.05$; **: $p<0.01$).

2.5 Loss of mitochondrial APE1 negatively affects mitochondrial translation and respiration

We proved that APE1 exerted endoribonuclease activity on mitochondrial AP-RNA and that damaged mRNA species were not efficiently removed in the absence of the protein. To deeply investigate this new function of APE1, we evaluated the downstream effects exerted by the accumulation of damaged mRNAs on the expression of mitochondrial encoded polypeptides. Western blot analyses were performed on Control (Scr), APE1 defective (shRNA), and knock-in ($APE1^{WT}$) clones using specific antibodies for Complex I nuclear (NDUFA1 and NDUFS1) and mitochondrial (ND5) encoded proteins, and Complex IV nuclear (COX6B) and mitochondrial (COX2) encoded proteins. As a positive control, cells were also treated with chloramphenicol (CHF) for 24 hours to selectively inhibit mitochondrial protein translation [360]. Although after APE1 silencing the amount of mRNA was higher in shRNA cells (Fig. 53, 54 and 58), we registered a significant reduction in terms of protein expression (Fig. 60). In details, COX2 levels were significantly lower both in shRNA cells and after CHF treatment, but the phenotype was reverted by the re-expression of $APE1^{WT}$. However, expression of nuclear encoded COX6B subunit was also affected by APE1 silencing and CHF treatment. Concerning the protein of Complex I: expression of ND5 was slightly but significantly reduced after the silencing of APE1. However, also nuclear encoded NDFUFA1 and NDUFS1 expression were found to be downregulated. Indeed, also the positive control treatment with CHF elicited a reduction of protein levels, which could be explained considering that the assembly and stability of Complex I depend on the interaction and stability of respiratory complexes III and IV that serve as an anchor at the membrane to recruit Complex I into the respiratory chain [361,362]. Therefore, to gain more knowledge on the effect of APE1 expression on the mitochondrial encoded polypeptides we analyzed the mitochondrial translation products. HeLa clones were treated with emetine to selectively block cytoplasmic translation, and then incubated with Met^{35S} for one hour to label newly synthetized mitochondrial polypeptides. Samples were separated on SDS-PAGE and protein expression profile was visualized by autoradiography (Fig. 61, *left*). Densitometry analysis was performed to measure the levels of ND1, ATP6, and ND6 proteins, and confirmed significantly impaired expression in APE1 shRNA that was rescued in $APE1^{WT}$ clone (Fig. 61, *right*). Altogether, our data have confirmed that APE1 exerts endoribonuclease activity on damaged mt-mRNAs contributing to the efficient functionality of mitochondrial translation processes.

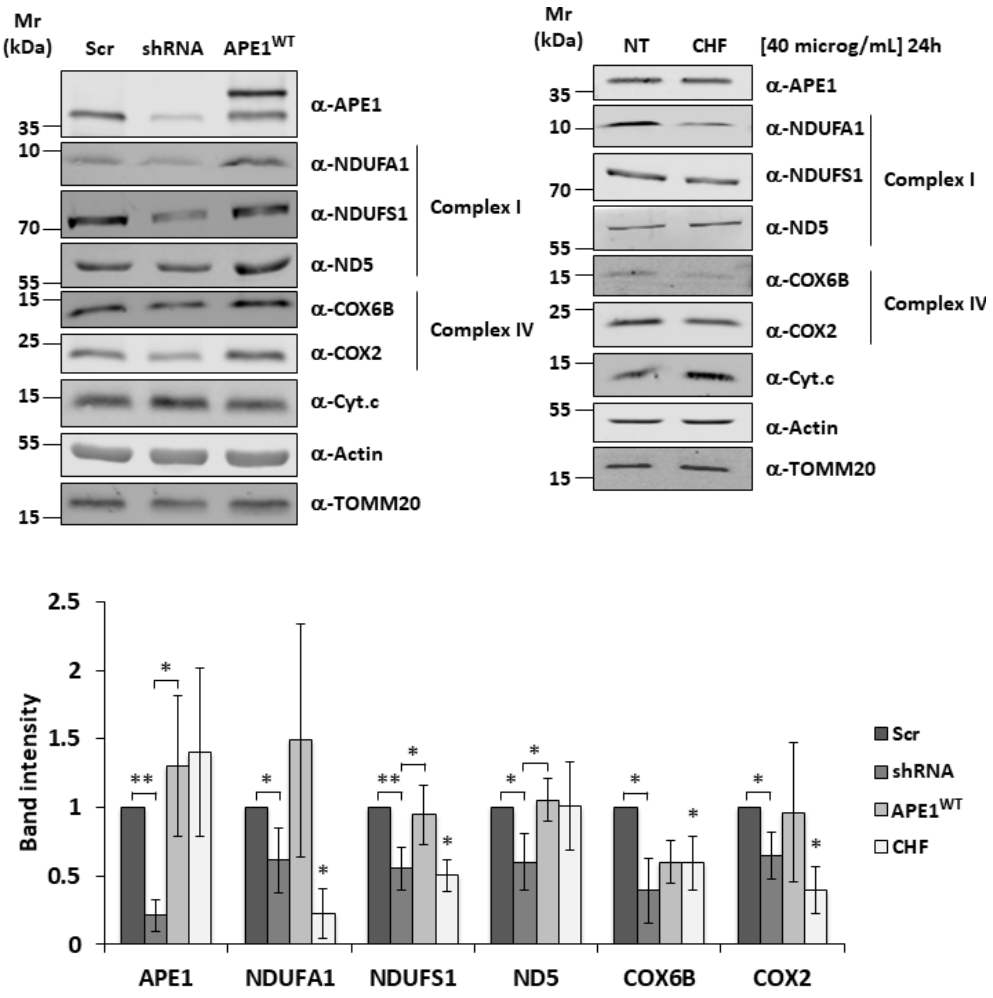

Figure 60. Western blot analysis of total cell extract of control (Scr), APE1 shRNA and knock-in (APE1^{WT}) clones. (*top*) Western blot analysis of clones treated with doxycycline for 9 days. Specific antibodies for Complex I (NDUFA1, NDUFS1, ND5) and Complex IV (COX6B, COX2) proteins were used. Anti-Actin and anti-TOMM20 were used as loading controls. As a positive control, the cells were treated with chloramphenicol (CHF) for 24 hours to inhibit mitochondrial translation. **(*bottom*)** Histogram reports densitometric analyses of each protein relative to the control sample. (*: $p<0.05$; **: $p<0.01$).

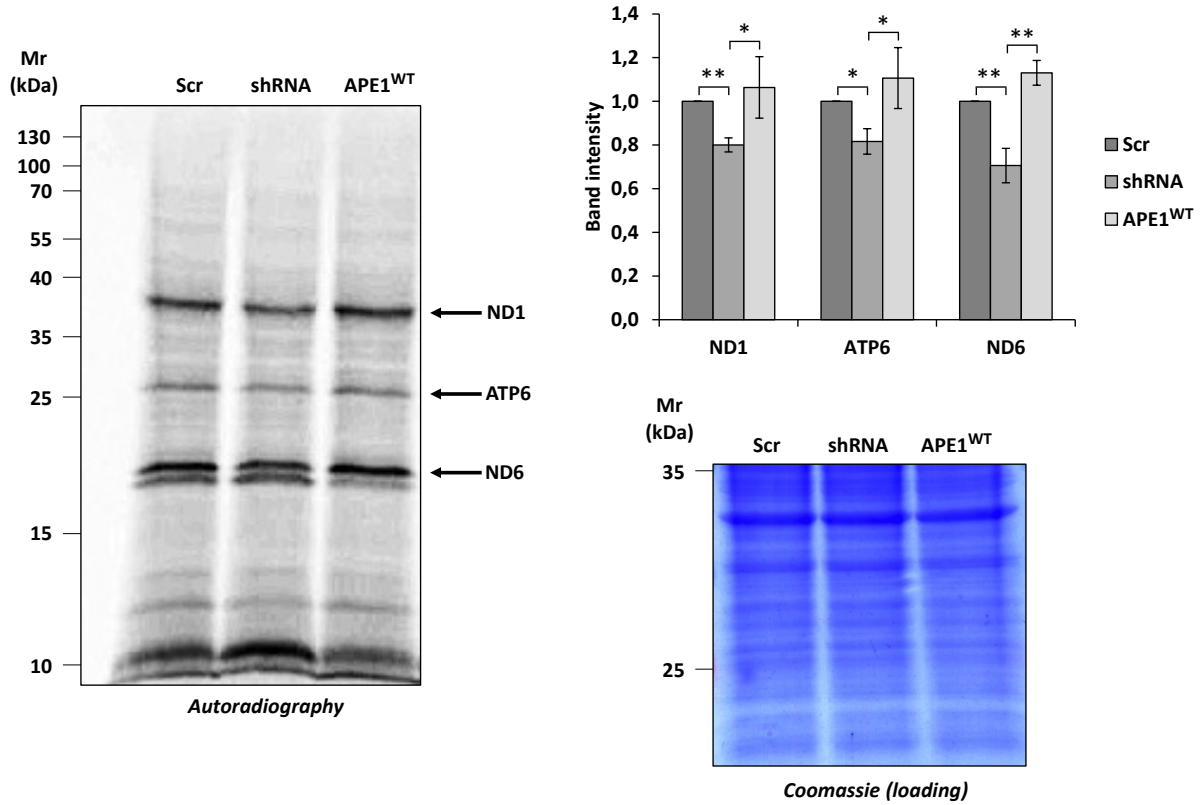

Figure 61. Representative autoradiography image of SDS-PAGE electrophoresis of mitochondria translation analysis. (*left*) Rapresentative image of SDS-PAGE electrophoresis of control (Scr), APE1 shRNA and knock-in (APE1^{WT}) clones after emetine/^{35}S treatment. **(*top-right*)** Bands corresponding to ND1, ATP6, and ND6 were quantified and data were reported in the histogram (*: p<0.05; **: p<0.01). **(*top-bottom*)** Comassie stained gel used ad loading control.

Considering that all 13 mitochondrial encoded polypeptides are components of the respiratory complexes I, III, IV and V, we evaluated the effect of APE1 loss of expression on mitochondrial respiration by examining the formation and stability of OXPHOS complexes and the respiratory parameters. BN-PAGE analyses highlighted the reduction in the stability of respiratory complexes I and III, while we did not observe any significant difference in Complex V (Fig. 62). Complex I is composed of seven mitochondrial encoded subunits (ND1, ND2, ND3, ND4, ND4L, ND5, ND6) that constitute its transmembrane domain. This explains how even the modest reductions in the expression levels of its subunits can affect its assembly and stability. This data was further supported by the measurement of Complex I activity, confirming that reduced complex stability determined a significantly lower activity in APE1 shRNA cells that was rescued in the knock in clone (Fig. 63). Complex III is a small complex composed of ten nuclear and only one mitochondrial encoded protein (CytB) but which is in the core of the complex and represents the central catalytic subunit of the complex. On the other hand, Complex V is a large complex composed of 29 proteins of 18 kinds, two of which (ATP6 and ATP8) are mitochondrial encoded. However, it has been demonstrated that although ATP6 mutation inhibits and destabilizes the ATP Synthase, it does not prevent the assembly and oligomerization of the complex [363]. To provide the last proof for the direct role of APE1 in mitochondrial respiration, we conducted Seahorse analyses to measure the respiratory parameters, and confirmed significantly reduced basal respiration (60±10%), maximum respiration (62±22%), and

ATP production (53±4%) in APE1 shRNA clone as well as demonstrated that all parameters were efficiently rescued by the re-expression of APE1^{WT} (Fig. 64).

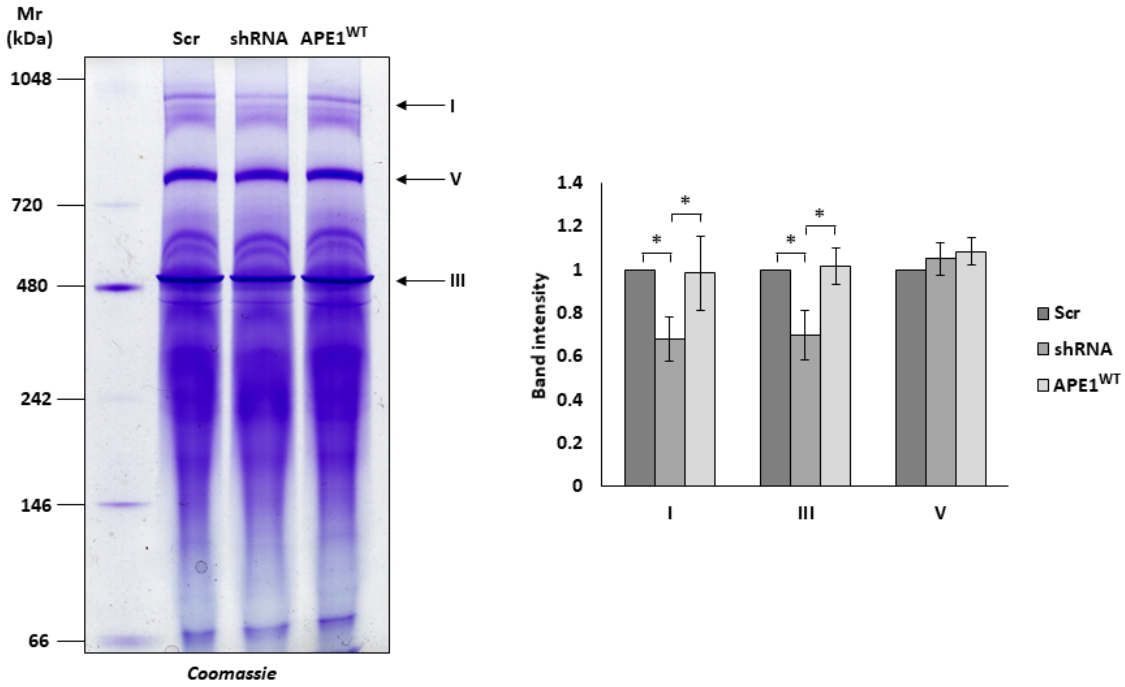

figure 62. Coomassie staining of mitochondrial respiratory complexes. (*left*) Image from Scr, shRNA and APE1^{WT} clones after BN-PAGE electrophoresis. **(*right*)** Bands corresponding to complexes I, III, and V were quantified and data relative to the control sample were reported in the histogram. (*: $p<0.05$).

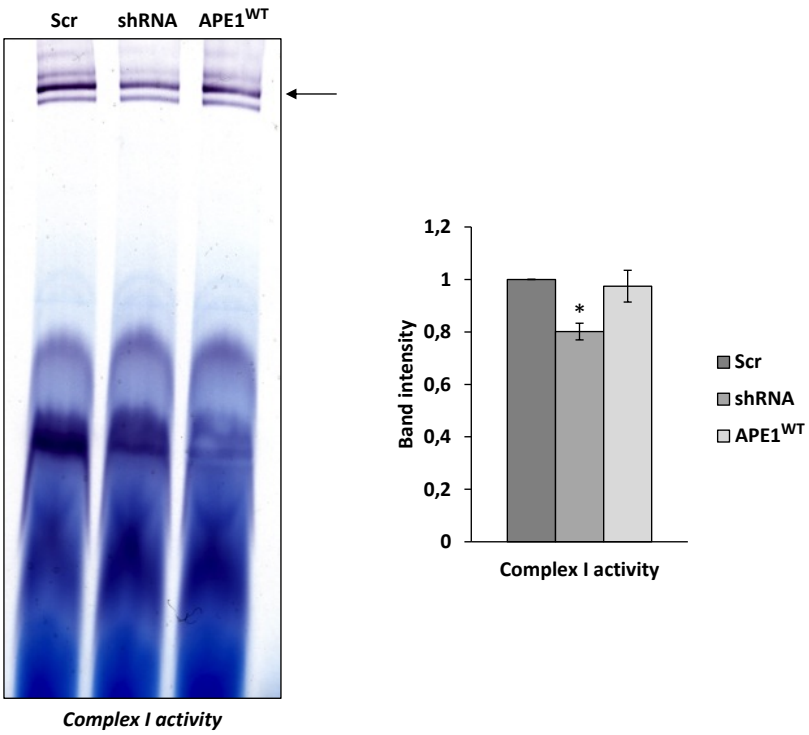

Figure 63. In-gel activity analysis of respiratory Complex I. **(*left*)** Image from in-gel activity of respiratory complex I. **(*right*)** Bands corresponding to the activity (arrow) were quantified and data relative to the control sample were reported in the histogram (*: $p<0.05$).

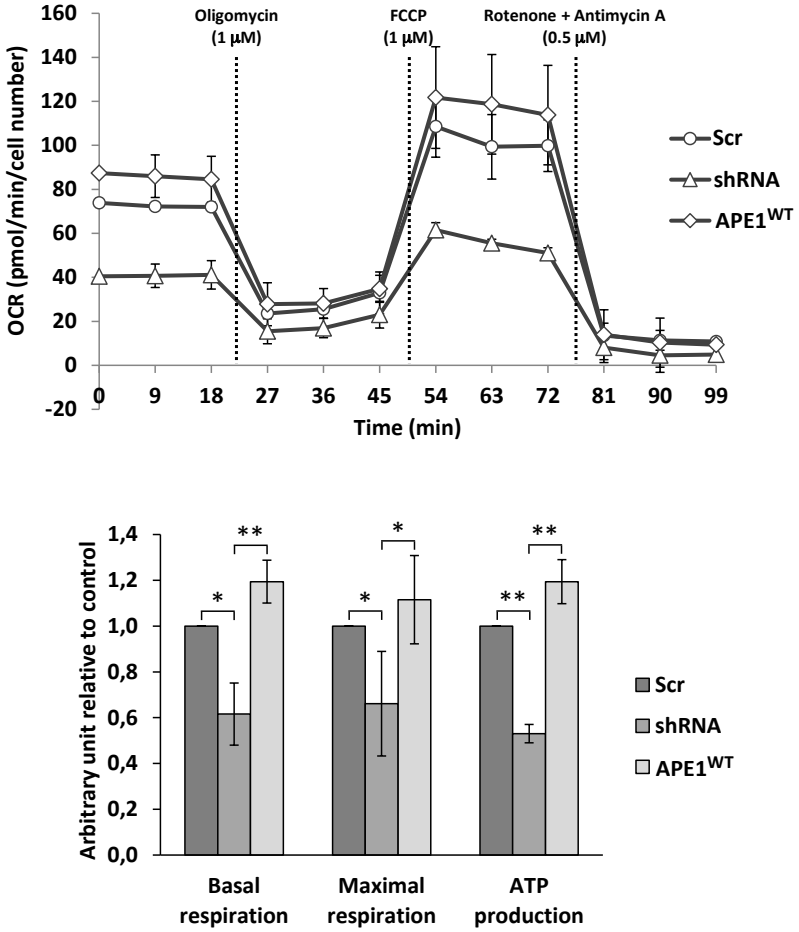

Figure 64. Oxygen consumption rate evaluation of control Scr, shRNA and APE1^{WT} clones. (*top*) Basal OCR was first evaluated, then cells were treated with the reported amounts of oligomycin, FCCP, rotenone and antimycin A, and OCR was measured three times after each injection. Diagram reports the OCRs of the clones relative to the Scr clone. **(*bottom*)** Histogram reports the basal respiration, maximal respiration, and ATP production capacity of clones extrapolated from the diagram. (*: $p<0.05$; **: $p<0.01$).

DISCUSSION AND CONCLUSIONS

In the first part of this study, we investigated the role played by the interaction between Mia40 and the DNA repair protein APE1 in controlling its trafficking into the mitochondrial compartment and the involvement of the protein transport pathway, MIA, in the maintenance of the mitochondrial genome. APE1 is a ubiquitously expressed protein, which mainly localizes within the nuclear compartment but is also present in the mitochondrial IMS and matrix. Indeed, APE1 is a key protein in repairing small non-helix distorting oxidative, alkylated and abasic lesions of both the nuclear and mitochondrial genomes. Data reported in literature, concerning APE1 trafficking, are still scanty and in some case contrasting. With this research work we fulfill currently lacking information and depict a new model involving the MIA pathway that explains how APE1 is translocated into the mitochondrial compartment. Several data reported in literature demonstrate that APE1 is present within the mitochondria of mammalian cells in its full length form [66,67,134], therefore excluding the hypothesis of the involvement of a proteolytic process, as previously hypothesized, to be responsible of the NLS removal and the re-directioning of APE1 into the mitochondrion [137]. Mitochondrial targeting signal of APE1's has been identified in the region spanning the residues 289–318 where Lys299 and Arg301 are the critical sites that, if mutated, completely abolish APE1 mitochondrial translocation under oxidative stress conditions [134]. Previous studies have also shown that APE1 translocates into the mitochondria mainly through the TOM-dependent pathway, but detailed mechanisms have not yet been proposed [134]. Our data demonstrate that after the passage through TOM channel, Mia40 is able to interact and bind APE1 by forming a disulfide bridge between APE1's Cys93 and Mia40's Cys55 residues. Through GST pull-down experiments we demonstrated that mutation of Cys93 completely abolish the interaction with Mia40. Moreover, while mutating Cys65 to serine, we observed an increased interaction between the two proteins. This could be explained taking into account that when Cys65 alone is mutated, Mia40 is able to bind APE1's Cys93 residue but cannot complete the reaction because of the lack of the second cysteine (Cys65), necessary for the disulfide bond formation. Therefore, the reaction is blocked explaining the increased interaction observed. Alternatively, the Cys65 mutant shows a higher affinity because this mutant has been demonstrated to adopt an unfolded structure, which exposes Cys93 residue therefore facilitating the interaction and the binding of Mia40 [364]. While the C-term DNA-repair domain of APE1 is highly conserved among different species, the N-term redox domain is unique to mammals and has been acquired during phylogenetic evolution [114]. Through its redox domain, APE1 exerts its activity by reducing key cysteine residues of a number of important transcription factors involved in both cell survival processes and apoptosis induction. In the N-term domain three cysteine residues (65, 93, and 99) are present. The current crystallographic structure was obtained in 1997 using a recombinant protein missing the first 35 N-terminal amino acids [100]. The Cys65 is absolutely required for redox activity on nuclear transcriptional factors but in this model it appears as a buried residue, and therefore APE1 should undergo a local or a more extensive remodelling process to expose the Cys65 to the surface for the interaction with TFs [365]. Cys99 is exposed on the surface of the protein but its substitution has no effect on redox activity. Cys93 is also a buried residue and before the determination of the crystal structure of APE1, it was proposed that Cys65 and 93 may form a disulfide bond [109]. Indeed, in the crystallographic structure of APE1, Cys65 and Cys93 are positioned on opposite sides of a β sheet with a distance > of 8 Å apart and therefore a substantial conformational change in the structure of the protein would be required for a disulfide bond formation between these residues [109]. Future studies are required to investigate APE1 structure and structural changes but it is likely that APE1 is a multifunctional dynamic protein that in vivo may adopt different structural conformations to fulfill its activities. In a previous work, we demonstrated that the majority of APE1 protein accumulates within the IMS [67]. Here we showed that Mia40 is involved in the transport of APE1 into the IMS. However, a portion of APE1 is further translocated through a still unidentified mechanism, to the matrix where the mtDNA resides.

Accumulation within the IMS could represent a storage site of the protein or, alternatively, APE1 could contribute to the redox homeostasis of the IMS within the glutathione (GSH)/glutathione disulfide (GSSG) and the reduced/oxidized thioredoxin systems. To assess the physiological relevance of the proposed import mechanism, we correlated the expression levels of Mia40 with the mitochondrial APE1 content and the stability of mtDNA. Experiments highlighted that loss of Mia40 expression in HeLa cells determined a significant reduction of mtAPE1 form that consequently leads to increased levels of mtDNA damage as a consequence of oxidative stress induction. Therefore, our data clearly support a direct involvement of Mia40 in controlling APE1 trafficking into the mitochondria and, consequently, in the stability of mtDNA. It has already been reported that APE1 is upregulated and mislocalized in many tumors, including ovarian cancer, lung cancer, breast cancer, hepatocellular carcinoma, and others [353,366–368]. In particular, a cytoplasmic relocalization of APE1 has been found to be associated with a higher aggressiveness of the tumor and a poor prognosis for the patient in HCC [353]. Because Mia40 was also found to be upregulated in some tumors [43], we decided to analyse APE1 and Mia40 expression levels in two HCC cell lines with different degree of differentiation. Higher expression levels of Mia40 in the HCC poorly differentiated JHH6 cell line positively correlate with augmented levels of mitochondrial APE1 and consequently were associated with an increased resistance to the treatment with an alkylating agent with respect to the well-differentiated Huh7 cell line. Also in this case, alteration in Mia40 expression and activity in JHH6 cells upon silencing, determined a reduction of mitochondrial APE1 content, which resulted in an increased cellular sensitivity to alkylating and oxidative stress. Alkylating antineoplastic agents are lipophilic and have positive charges and therefore tend to accumulate within the mitochondria and generate alkylation lesions on mtDNA with 10-fold higher ratio respect to nDNA [189]. APE1 translocates into mitochondria increasing mtDNA repair rate and therefore, in our model, increased expression of Mia40 could lead to the promotion of cell survival. In summary, our data strongly support the hypothesis for a redox-assisted mechanism dependent on Mia40 in controlling APE1 trafficking within mitochondria.

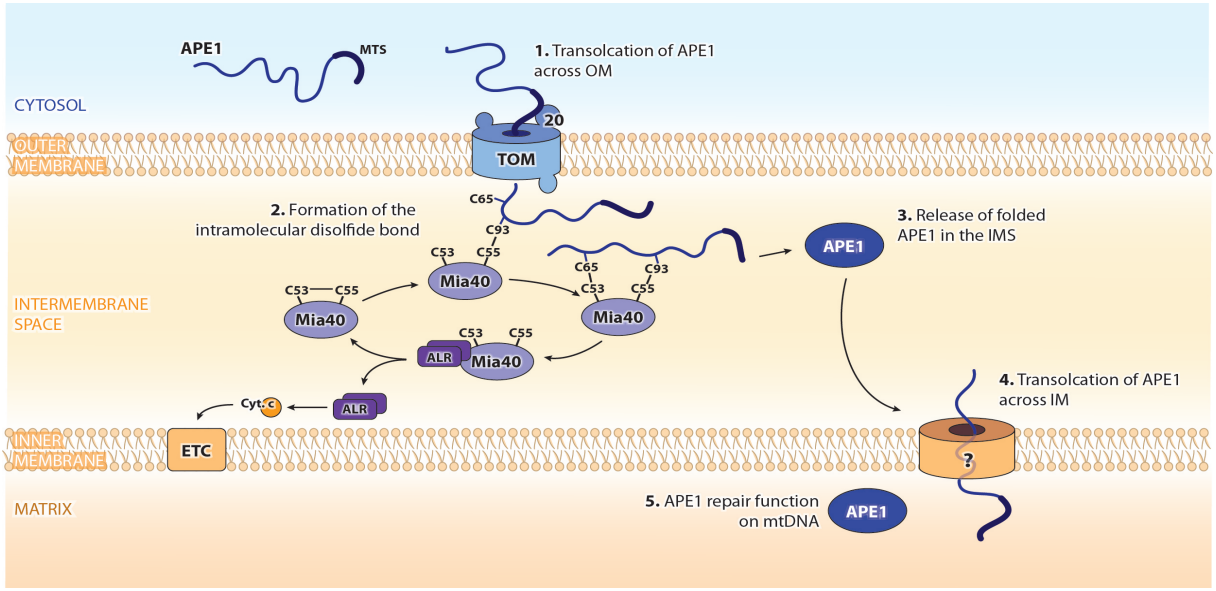

Figure 42. Ape1-Mia40 interaction model. After the passage through the TOM complex (1) Ape1 became substrate of Mia40 that catalize a disulfide bond between the Cys55 of Mia40 and Cys93 of APE1 (2). After the folding of APE1 and its release for Mia40 (3) the protein can interact with the translocase responsible for its passage in the matrix (4). One in the matrix compartment APE1 can exert its function on mtDNA (5).

Over the years, research on APE1 has been mainly associated with its role in the nuclear BER DNA repair pathway considering secondary for the cell fate the endonuclease activity of APE1 on the mitochondrial DNA. It is from the last decade that more research groups have directed their studies toward the biological relevance of APE1 extra-nuclear localization and also toward the characterization of uncanonical functions of this DNA repair enzyme, such as its RNA endoribonuclease activity [85,123,124,126]. Our research merges these two aspects offering a completely new point of view in the study of APE1, and provides for the first time a direct proof of the essential role of this protein in mitochondrial RNA biology.

In the second part of this thesis, with the idea of identifying the inner membrane protein complex responsible for the matrix internalization of APE1, we decided to perform an IP-MS analysis trying to identify the mitochodndrial interactome of APE1. The analysis of the data resulting from the experiment unveil that, in mitochondria, APE1 is mainly associated with ribosome components and RNA processing proteins. Next, we proved that APE1 not only interacts with RNA proteins but also binds RNA and that oxidative stress conditions enhance this binding. As for the DNA, also RNA can undergo oxidative damage forming 8-hydroxyguanosine (8-OHG) which could be released leaving AP sites [357] and measurements of mitochondrial mRNA AP sites confirmed significantly higher levels of AP-RNA in the absence of APE1. Next, we extended our investigation demonstrating a direct correlation between the levels of APE1 in mitochondria and the half-life of mRNAs. Considering that the majority of APE1 localizes within the nuclear compartment where it exerts endonuclease activity and regulates gene expression by stimulating the DNA-binding activity of several transcriptional factors, it was necessary to discriminate if our observations could be related to the biological activity of the nuclear rather than of the mitochondrial form of APE1. For this purpose, rescue experiments were performed on the background of APE1 knockout cells by re-expressing a recombinant form of the protein that was targeted only into the mitochondrial matrix. Data confirmed that mRNA's half-life was significantly longer in the absence of mitochondrial APE1 as a consequence of impaired degradation processes due to the loss of APE1 expression or re-expression of the endonuclease defective mutant E96A. Accumulation of non-functional mRNAs negatively affects mitochondrial translation processes and, as a final consequence, the assembly/stability of respiratory complexes and mitochondrial respiration. This study not only confirms and extends the emerging role of APE1 in RNA biology, but also reveals for the first time a new function of the mitochondrial form of this protein in mitochondria metabolism.

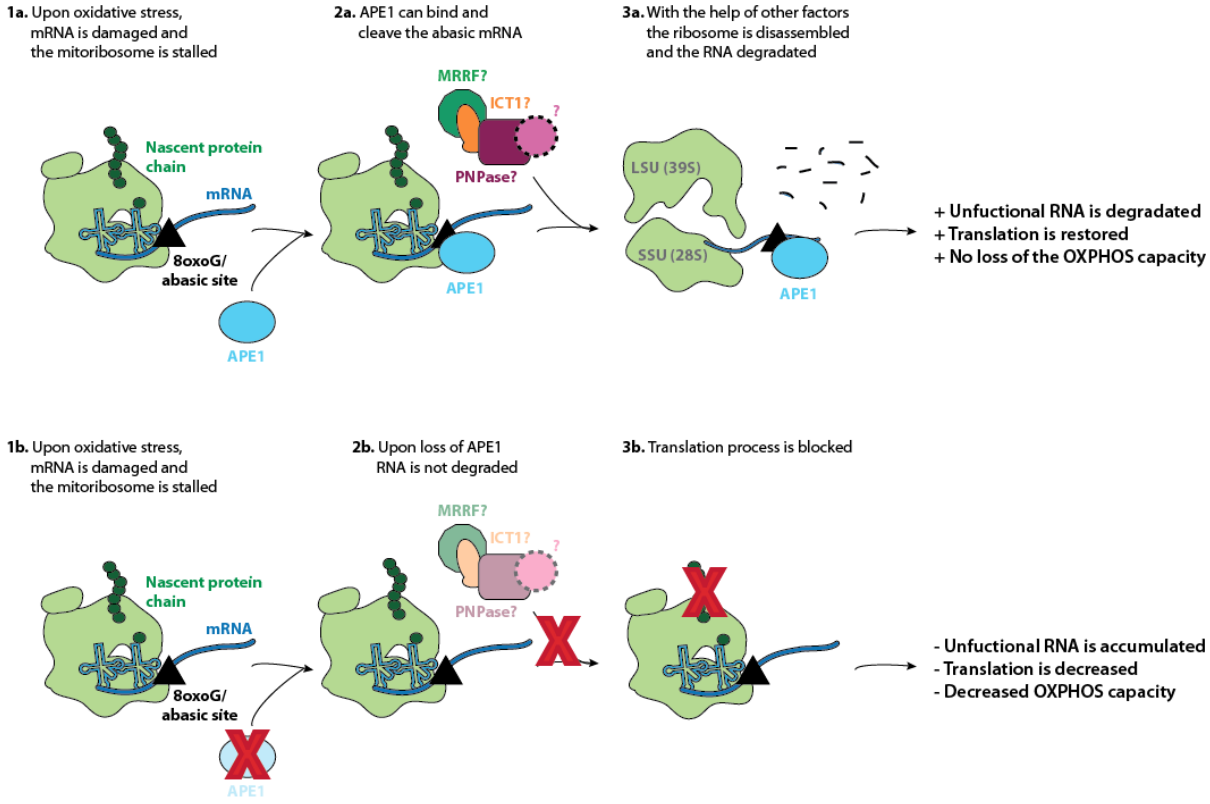

Figure 42. APE1 function on mt-mRNA metabolism and translation model. When APE1 is present in the mitochondrial matrix (*top*, 1a) it can bind to the abasic RNA present (2a) cleaving it and making it available for the degradation (3a). If APE1 is not present in the matrix (*bottom*, 1b), the damaged mRNA could not be cleaved (2b) leading to the stalling of the ribosome and shutting down the translation process (2c).

Therefore, in the light of this observation, all data regarding the extra-nuclear localization of APE1 in correlation with tumorigenesis and tumor resistance could be re-interpreted considering APE1 as not only a DNA repair protein but also as a key component of the mitochondrial RNA degradosome. Despite molecular details of APE1 enzymatic activity were presented in this work, the possible involvement of other factors in this complex biological process have still to be investigated. Our study provides a rationale for targeting the mitochondrial form of APE1 as a promising therapeutic tool in cancer therapy.

BIBLIOGRAPHY

1. De Grey, A. D. N. J. Incorporation of transmembrane hydroxide transport into the chemiosmotic theory. *Bioelectrochemistry Bioenerg.* **49,** 43–50 (1999).

2. Okuno, D., Iino, R. & Noji, H. Rotation and structure of FoF1-ATP synthase. *Journal of Biochemistry* **149,** 655–664 (2011).

3. Stock, D., Leslie, A. G. W. & Walker, J. E. Molecular Architcture of the Rotary Motor in ATP Synthase. *Science (80-.).* **286,** 1700–1705 (1999).

4. Muller, F. L., Liu, Y. & Van Remmen, H. Complex III releases superoxide to both sides of the inner mitochondrial membrane. *J. Biol. Chem.* **279,** 49064–49073 (2004).

5. Murphy, M. P. How mitochondria produce reactive oxygen species. *Biochem. J.* **417,** 1–13 (2009).

6. Hide, R. Jupiter's Great Red Spot revisited. *Phys. Earth Planet. Inter.* **6,** 99 (1972).

7. Neupert, W. & Herrmann, J. M. Translocation of Proteins into Mitochondria Translocase: a membrane- embedded protein complex that mediates translocation of polypeptides from one side of the membrane to the other side. *Annu. Rev. Biochem* **76,** 723–49 (2007).

8. Gabaldón, T. & Huynen, M. A. Shaping the mitochondrial proteome. in *Biochimica et Biophysica Acta - Bioenergetics* **1659,** 212–220 (2004).

9. Pagliarini, D. J. *et al.* A Mitochondrial Protein Compendium Elucidates Complex I Disease Biology. *Cell* **134,** 112–123 (2008).

10. Sickmann, A. *et al.* The proteome of Saccharomyces cerevisiae mitochondria. *Proc. Natl. Acad. Sci.* **100,** 13207–13212 (2003).

11. Forner, F., Foster, L. J., Campanaro, S., Valle, G. & Mann, M. Quantitative Proteomic Comparison of Rat Mitochondria from Muscle, Heart, and Liver. *Mol. Cell. Proteomics* **5,** 608–619 (2006).

12. Schmidt, O., Pfanner, N. & Meisinger, C. Mitochondrial protein import: From proteomics to functional mechanisms. *Nature Reviews Molecular Cell Biology* **11,** 655–667 (2010).

13. Chacinska, A., Koehler, C. & Milenkovic, D. Importing mitochondrial proteins: machineries and mechanisms. *Cell* **138,** 628–644 (2009).

14. Riemer, J., Fischer, M. & Herrmann, J. M. Oxidation-driven protein import into mitochondria: Insights and blind spots. *Biochimica et Biophysica Acta - Biomembranes* **1808,** 981–989 (2011).

15. Riemer, J., Bulleid, N. & Herrmann, J. M. Disulfide Formation in the ER and Mitochondria: Two Solutions to a Common Process. *Science* **324,** 1284–1287 (2009).

16. Banci, L. *et al.* An intrinsically disordered domain has a dual function coupled to compartment-dependent redox control. *J. Mol. Biol.* **425,** 594–608 (2013).

17. Durigon, R., Wang, Q., Ceh Pavia, E., Grant, C. M. & Lu, H. Cytosolic thioredoxin system facilitates the import of mitochondrial small Tim proteins. *EMBO Rep.* **13,**

916–922 (2012).

18. Milenkovic, D. *et al.* Identification of the signal directing Tim9 and Tim10 into the intermembrane space of mitochondria. *Mol. Biol. Cell* **20,** 2530–9 (2009).

19. Sideris, D. P. *et al.* A novel intermembrane space-targeting signal docks cysteines onto Mia40 during mitochondrial oxidative folding. *J. Cell Biol.* **187,** 1007–1022 (2009).

20. Mesecke, N. *et al.* A disulfide relay system in the intermembrane space of mitochondria that mediates protein import. *Cell* **121,** 1059–1069 (2005).

21. Bien, M. *et al.* Mitochondrial Disulfide Bond Formation Is Driven by Intersubunit Electron Transfer in Erv1 and Proofread by Glutathione. *Mol. Cell* **37,** 516–528 (2010).

22. Banci, L. *et al.* Molecular chaperone function of Mia40 triggers consecutive induced folding steps of the substrate in mitochondrial protein import. *Proc. Natl. Acad. Sci. U. S. A.* **107,** 20190–5 (2010).

23. Allen, S., Balabanidou, V., Sideris, D. P., Lisowsky, T. & Tokatlidis, K. Erv1 mediates the Mia40-dependent protein import pathway and provides a functional link to the respiratory chain by shuttling electrons to cytochrome c. *J. Mol. Biol.* **353,** 937–944 (2005).

24. Li, Y. *et al.* Identification of hepatopoietin dimerization, its interacting regions and alternative splicing of its transcription. *Eur. J. Biochem.* **269,** 3888–3893 (2002).

25. Gatzidou, E., Kouraklis, G. & Theocharis, S. Insights on augmenter of liver regeneration cloning and function. *World Journal of Gastroenterology* **12,** 4951–4958 (2006).

26. Polimeno, L. *et al.* Expression and localization of augmenter of liver regeneration in human muscle tissue. *Int. J. Exp. Pathol.* **90,** 423–30 (2009).

27. Lee, J. E., Hofhaus, G. & Lisowsky, T. Erv1p from Saccharomyces cerevisiae is a FAD-linked sulfhydryl oxidase. *FEBS Lett.* **477,** 62–66 (2000).

28. Daithankar, V. N., Farrell, S. R. & Thorpe, C. Augmenter of liver regeneration: Substrate specificity of a flavin-dependent oxidoreductase from the mitochondrial intermembrane space. *Biochemistry* **48,** 4828–4837 (2009).

29. Banci, L. *et al.* Molecular recognition and substrate mimicry drive the electron-transfer process between MIA40 and ALR. *Proc. Natl. Acad. Sci. U. S. A.* **108,** 4811–6 (2011).

30. Banci, L. *et al.* An electron-transfer path through an extended disulfide relay system: The case of the redox protein ALR. *J. Am. Chem. Soc.* **134,** 1442–1445 (2012).

31. Farrell, S. R. & Thorpe, C. Augmenter of liver regeneration: A flavin-dependent sulfhydryl oxidase with cytochrome c reductase activity. *Biochemistry* **44,** 1532–1541 (2005).

32. Böttinger, L. *et al.* In vivo evidence for cooperation of Mia40 and Erv1 in the oxidation of mitochondrial proteins. *Mol. Biol. Cell* **23,** 3957–69 (2012).

33. Kay, C. W. M., Elsässer, C., Bittl, R., Farrell, S. R. & Thorpe, C. Determination of the distance between the two neutral flavin radicals in augmenter of liver regeneration by pulsed ELDOR. *J. Am. Chem. Soc.* **128,** 76–77 (2006).

34. Bihlmaier, K. *et al.* The disulfide relay system of mitochondria is connected to the respiratory chain. *J. Cell Biol.* **179,** 389–395 (2007).

35. Kojer, K. *et al.* Glutathione redox potential in the mitochondrial intermembrane space is linked to the cytosol and impacts the Mia40 redox state. *EMBO J.* **31,** 3169–82 (2012).

36. Curran, S. P. *et al.* The role of Hot13p and redox chemistry in the mitochondrial TIM22 import pathway. *J. Biol. Chem.* **279,** 43744–43751 (2004).

37. Mesecke, N. *et al.* The zinc-binding protein Hot13 promotes oxidation of the mitochondrial import receptor Mia40. *{EMBO} Rep.* **9,** 1107–1113 (2008).

38. Chacinska, A. *et al.* Essential role of Mia40 in import and assembly of mitochondrial intermembrane space proteins. *EMBO J.* **23,** 3735–3746 (2004).

39. Naoé, M. *et al.* Identification of Tim40 that mediates protein sorting to the mitochondrial intermembrane space. *J. Biol. Chem.* **279,** 47815–47821 (2004).

40. Banci, L. *et al.* MIA40 is an oxidoreductase that catalyzes oxidative protein folding in mitochondria. *Nat. Struct. Mol. Biol.* **16,** 198–206 (2009).

41. Kawano, S. *et al.* Structural basis of yeast Tim40/Mia40 as an oxidative translocator in the mitochondrial intermembrane space. *Proc. Natl. Acad. Sci. U. S. A.* **106,** 14403–7 (2009).

42. Hofmann, S. *et al.* Functional and mutational characterization of human MIA40 acting during import into the mitochondrial intermembrane space. *J. Mol. Biol.* **353,** 517–528 (2005).

43. Yang, J. *et al.* Human CHCHD4 mitochondrial proteins regulate cellular oxygen consumption rate and metabolism and provide a critical role in hypoxia signaling and tumor progression. *J. Clin. Invest.* **122,** 600–611 (2012).

44. Sztolsztener, M. E., Brewinska, A., Guiard, B. & Chacinska, A. Disulfide Bond Formation: Sulfhydryl Oxidase ALR Controls Mitochondrial Biogenesis of Human MIA40. *Traffic* **14,** 309–320 (2013).

45. Milenkovic, D. *et al.* Biogenesis of the essential Tim9-Tim10 chaperone complex of mitochondria: Site-specific recognition of cysteine residues by the intermembrane space receptor Mia40. *J. Biol. Chem.* **282,** 22472–22480 (2007).

46. Sideris, D. P. & Tokatlidis, K. Oxidative folding of small Tims is mediated by site-specific docking onto Mia40 in the mitochondrial intermembrane space. *Mol. Microbiol.* **65,** 1360–1373 (2007).

47. Grumbt, B., Stroobant, V., Terziyska, N., Israel, L. & Hell, K. Functional characterization of Mia40p, the central component of the disulfide relay system of the mitochondrial intermembrane space. *J. Biol. Chem.* **282,** 37461–37470 (2007).

48. Banci, L. *et al.* Mitochondrial copper(I) transfer from Cox17 to Sco1 is coupled to electron transfer. *Proc. Natl. Acad. Sci.* **105,** 6803–6808 (2008).

49. Fischer, M. *et al.* Protein import and oxidative folding in the mitochondrial intermembrane space of intact mammalian cells. *Mol. Biol. Cell* **24,** 2160–70 (2013).

50. Longen, S. *et al.* Systematic Analysis of the Twin Cx9C Protein Family. *J. Mol. Biol.* **393,** 356–368 (2009).

51. Cavallaro, G. Genome-wide analysis of eukaryotic twin CX9C proteins. *Mol. Biosyst.* **6,** 2459–2470 (2010).

52. Gabriel, K. *et al.* Novel Mitochondrial Intermembrane Space Proteins as Substrates of the MIA Import Pathway. *J. Mol. Biol.* **365,** 612–620 (2007).

53. Tamura, Y., Endo, T., Iijima, M. & Sesaki, H. Ups1p and Ups2p antagonistically regulate cardiolipin metabolism in mitochondria. *J. Cell Biol.* **185,** 1029–1045 (2009).

54. Banci, L. *et al.* Solution structure of Cox11, a novel type of β-immunoglobulin-like fold involved in CuB site formation of cytochrome c oxidase. *J. Biol. Chem.* **279,** 34833–34839 (2004).

55. Sturtz, L. A., Diekert, K., Jensen, L. T., Lill, R. & Culotta, V. C. A fraction of yeast Cu,Zn-superoxide dismutase and its metallochaperone, CCS, localize to the intermembrane space of mitochondria. A physiological role for SOD1 in guarding against mitochondrial oxidative damage. *J. Biol. Chem.* **276,** 38084–38089 (2001).

56. Lamb, A. L., Torres, A. S., O'Halloran, T. V & Rosenzweig, A. C. Heterodimeric structure of superoxide dismutase in complex with its metallochaperone. *Nat. Struct. Biol.* **8,** 751–755 (2001).

57. Reddehase, S., Grumbt, B., Neupert, W. & Hell, K. The Disulfide Relay System of Mitochondria Is Required for the Biogenesis of Mitochondrial Ccs1 and Sod1. *J. Mol. Biol.* **385,** 331–338 (2009).

58. Kloppel, C. *et al.* Mia40-dependent oxidation of cysteines in domain I of Ccs1 controls its distribution between mitochondria and the cytosol. *Mol. Biol. Cell* **22,** 3749–3757 (2011).

59. Terziyska, N. *et al.* The sulfhydryl oxidase Erv1 is a substrate of the Mia40-dependent protein translocation pathway. *FEBS Lett.* **581,** 1098–1102 (2007).

60. Graham, L. A. & Trumpower, B. L. Mutational analysis of the mitochondrial Rieske iron-sulfur protein of Saccharomyces cerevisiae. III. Import, protease processing, and assembly into the cytochrome bc1complex of iron-sulfur protein lacking the iron-sulfur cluster. *J. Biol. Chem.* **266,** 22485–22492 (1991).

61. Merbitz-Zahradnik, T., Zwicker, K., Nett, J. H., Link, T. A. & Trumpower, B. L. Elimination of the Disulfide Bridge in the Rieske Iron-Sulfur Protein Allows Assembly of the [2Fe-2S] Cluster into the Rieske Protein but Damages the Ubiquinol Oxidation Site in the Cytochrome bc1 Complex. *Biochemistry* **42,** 13637–13645 (2003).

62. Wrobel, L., Trojanowska, A., Sztolsztener, M. E. & Chacinska, A. Mitochondrial protein import: Mia40 facilitates Tim22 translocation into the inner membrane of mitochondria. *Mol. Biol. Cell* **24,** 543–554 (2013).

63. Weckbecker, D., Longen, S., Riemer, J. & Herrmann, J. M. Atp23 biogenesis reveals a chaperone-like folding activity of Mia40 in the IMS of mitochondria. *EMBO J.* **31,** 4348–4358 (2012).

64. Longen, S., Woellhaf, M., Petrungaro, C., Riemer, J. & Herrmann, J. The Disulfide

Relay of the Intermembrane Space Oxidizes the Ribosomal Subunit Mrp10 on Its Transit into the Mitochondrial Matrix. *Dev. Cell* **28,** 30–42 (2014).

65. Zhuang, J. *et al.* Mitochondrial disulfide relay mediates translocation of p53 and partitions its subcellular activity. *Proc. Natl. Acad. Sci. U. S. A.* **110,** 17356–61 (2013).

66. Tell, G. *et al.* Mitochondrial localization of APE/Ref-1 in thyroid cells. *Mutat. Res. - DNA Repair* **485,** 143–152 (2001).

67. Vascotto, C. *et al.* Knock-in reconstitution studies reveal an unexpected role of Cys-65 in regulating APE1/Ref-1 subcellular trafficking and function. *Mol. Biol. Cell* **22,** 3887–901 (2011).

68. Koehler, C. M., Leuenberger, D., Merchant, S., Renold, A. & Junne, T. Human deafness dystonia syndrome is a mitochondrial disease. *Cell Biol.* **96,** 2141–2146 (1999).

69. Tranebjaerg, L., Jensen, P. K. & van Ghelue, M. X-linked recessive deafness-dystonia syndrome (Mohr-Tranebjaerg syndrome). *Adv. Otorhinolaryngol.* **56,** 176–80 (2000).

70. Roesch, K., Curran, S. P., Tranebjaerg, L. & Koehler, C. M. Human deafness dystonia syndrome is caused by a defect in assembly of the DDP1/TIMM8a-TIMM13 complex. *Hum. Mol. Genet.* **11,** 477–486 (2002).

71. Di Fonzo, A. *et al.* The Mitochondrial Disulfide Relay System Protein GFER Is Mutated in Autosomal-Recessive Myopathy with Cataract and Combined Respiratory-Chain Deficiency. *Am. J. Hum. Genet.* **84,** 594–604 (2009).

72. Daithankar, V. N., Schaefer, S. A., Dong, M., Bahnson, B. J. & Thorpe, C. Structure of the human sulfhydryl oxidase augmenter of liver regeneration and characterization of a human mutation causing an autosomal recessive myopathy. *Biochemistry* **49,** 6737–6745 (2010).

73. Napoli, E. *et al.* Defective mitochondrial disulfide relay system, altered mitochondrial morphology and function in Huntington's disease. *Hum. Mol. Genet.* **22,** 989–1004 (2013).

74. Varabyova, A. *et al.* Mia40 and MINOS act in parallel with Ccs1 in the biogenesis of mitochondrial Sod1. in *FEBS Journal* **280,** 4943–4959 (2013).

75. Hanahan, D. & Weinberg, R. A. Hallmarks of Cancer: The Next Generation. *Cell* **144,** 646–674 (2011).

76. Matoba, S. *et al.* p53 regulates mitochondrial respiration. *Science (80-.).* **312,** 1650–1653 (2006).

77. Chandel, N. & McClintock, D. Reactive Oxygen Species Generated at Mitochondrial Complex III Stabilize Hypoxia-inducible Factor-1α during Hypoxia A MECHANISM OF O2 SENSING. *J. Biol. ...* **275,** 25130–25138 (2000).

78. Suh, J. H., Heath, S. H. & Hagen, T. M. Two subpopulations of mitochondria in the aging rat heart display heterogenous levels of oxidative stress. *Free Radic. Biol. Med.* **35,** 1064–1072 (2003).

79. Sciacovelli, M. *et al.* The mitochondrial chaperone TRAP1 promotes neoplastic growth

by inhibiting succinate dehydrogenase. *Cell Metab.* **17,** 988–999 (2013).

80. Fung, H. & Demple, B. A vital role for Ape1/Ref1 protein in repairing spontaneous DNA damage in human cells. *Mol. Cell* **17,** 463–470 (2005).

81. Tell, G., Quadrifoglio, F., Tiribelli, C. & Kelley, M. R. The Many Functions of APE1/Ref-1: Not Only a DNA Repair Enzyme. *Antioxid. Redox Signal.* **11,** 601–619 (2009).

82. Tell, G., Damante, G., Caldwell, D. & Kelley, M. R. The Intracellular Localization of APE1/Ref-1: More than a Passive Phenomenon? *Antioxid. Redox Signal.* **7,** 367–384 (2005).

83. Xanthoudakis, S., Miao, G. G. & Curran, T. The redox and DNA-repair activities of Ref-1 are encoded by nonoverlapping domains. *Proc. Natl. Acad. Sci.* **91,** 23–27 (1994).

84. Malfatti, M. C. *et al.* Abasic and oxidized ribonucleotides embedded in DNA are processed by human APE1 and not by RNase H2. *Nucleic Acids Res.* **45,** 11193–11212 (2017).

85. Antoniali, G. *et al.* Mammalian APE1 controls miRNA processing and its interactome is linked to cancer RNA metabolism. *Nat. Commun.* **8,** (2017).

86. Vascotto, C. *et al.* APE1/Ref-1 Interacts with NPM1 within Nucleoli and Plays a Role in the rRNA Quality Control Process. *Mol. Cell. Biol.* **29,** 1834–1854 (2009).

87. Berquist, B. R., McNeill, D. R. & Wilson, D. M. Characterization of Abasic Endonuclease Activity of Human Ape1 on Alternative Substrates, as Well as Effects of ATP and Sequence Context on AP Site Incision. *J. Mol. Biol.* **379,** 17–27 (2008).

88. Okazaki, T. *et al.* A redox factor protein, ref1, is involved in negative gene regulation by extracellular calcium. *J. Biol. Chem.* **269,** 27855–27862 (1994).

89. Fantini, D. *et al.* Critical lysine residues within the overlooked N-terminal domain of human APE1 regulate its biological functions. *Nucleic Acids Res.* **38,** 8239–8256 (2010).

90. Busso, C., Iwakuma, T. & Izumi, T. Ubiquitination of mammalian AP endonuclease (APE1) regulated by the p53–MDM2 signaling pathway. *Oncogene* **28,** 1616–1625 (2009).

91. Robson, C. N. *et al.* Structure of the human DNA repair gene HAP1 and its localisation to chromosome 14q 11.2-12. *Nucleic Acids Res.* **20,** 4417–4421 (1992).

92. Li, M. & Wilson, D. M. Human Apurinic/Apyrimidinic Endonuclease 1. *Antioxid. Redox Signal.* **20,** 678–707 (2014).

93. Evans, A. R., Limp-Foster, M. & Kelley, M. R. Going APE over ref-1. *Mutation Research - DNA Repair* **461,** 83–108 (2000).

94. Fung, H., Bennett, R. A. O. & Demple, B. Key Role of a Downstream Specificity Protein 1 Site in Cell Cycle-regulated Transcription of the AP Endonuclease Gene APE1/APEX in NIH3T3 Cells. *J. Biol. Chem.* **276,** 42011–42017 (2001).

95. Zaky, A. *et al.* Regulation of the human AP-endonuclease (APE1/Ref-1) expression by the tumor suppressor p53 in response to DNA damage. *Nucleic Acids Res.* **36,** 1555–

1566 (2008).

96. Izumi, T., Henner, W. D. & Mitra, S. Negative regulation of the major human AP-endonuclease, a multifunctional protein. *Biochemistry* **35,** 14679–14683 (1996).

97. Asai, T., Kambe, F., Kikumori, T. & Seo, H. Increase in Ref-l mRNA and protein by thyrotropin in rat thyroid FRTL-5 cells. *Biochem. Biophys. Res. Commun.* **236,** 71–74 (1997).

98. Ramana, C. V, Boldogh, I., Izumi, T. & Mitra, S. Activation of apurinic/apyrimidinic endonuclease in human cells by reactive oxygen species and its correlation with their adaptive response to genotoxicity of free radicals. *Proc. Natl. Acad. Sci. U. S. A.* **95,** 5061–5066 (1998).

99. Dlakić, M. Functionally unrelated signalling proteins contain a fold similar to Mg2+-dependent endonucleases. *Trends in Biochemical Sciences* **25,** 272–273 (2000).

100. Gorman, M. a. *et al.* The crystal structure of the human DNA repair endonuclease HAP1 suggests the recognition of extra-helical deoxyribose at DNA abasic sites. *EMBO J.* **16,** 6548–6558 (1997).

101. Beernink, P. T. *et al.* Two divalent metal ions in the active site of a new crystal form of human apurinic/apyrimidinic endonuclease, Ape1: Implications for the catalytic mechanism. *J. Mol. Biol.* **307,** 1023–1034 (2001).

102. Vascotto, C. *et al.* Genome-Wide analysis and proteomic studies reveal APE1/Ref-1 multifunctional role in mammalian cells. *Proteomics* **9,** 1058–1074 (2009).

103. Miroshnikova, A. D., Kuznetsova, A. A., Vorobjev, Y. N., Kuznetsov, N. A. & Fedorova, O. S. Effects of mono- and divalent metal ions on DNA binding and catalysis of human apurinic/apyrimidinic endonuclease 1. *Mol. Biosyst.* **12,** 1527–1539 (2016).

104. Jackson, E. B., Theriot, C. A., Chattopadhyay, R., Mitra, S. & Izumi, T. Analysis of nuclear transport signals in the human apurinic/apyrimidinic endonuclease (APE1/Ref1). *Nucleic Acids Res.* **33,** 3303–3312 (2005).

105. Lirussi, L. *et al.* Nucleolar accumulation of APE1 depends on charged lysine residues that undergo acetylation upon genotoxic stress and modulate its BER activity in cells. *Mol. Biol. Cell* **23,** 4079–4096 (2012).

106. Bhakat, K., Mantha, A. & Mitra, S. Transcriptional regulatory functions of mammalian AP-endonuclease (APE1/Ref-1), an essential multifunctional protein. *Antioxidants redox ...* **11,** 621–638 (2009).

107. Xanthoudakis, S. & Curran, T. Identification and characterization of Ref-1, a nuclear protein that facilitates AP-1 DNA-binding activity. *EMBO J.* **11,** 653–665 (1992).

108. Jayaraman, L. *et al.* Identification of redox/repair protein Ref-1 as a potent activator of p53. *Genes Dev.* **11,** 558–570 (1997).

109. Walker, L. J., Robson, C. N., Black, E., Gillespie, D. & Hickson, I. D. Identification of residues in the human DNA repair enzyme HAP1 (Ref-1) that are essential for redox regulation of Jun DNA binding. *Mol. Cell. Biol.* **13,** 5370–6 (1993).

110. Huang, L. E., Arany, Z., Livingston, D. M. & Franklin Bunn, H. Activation of hypoxia-inducible transcription factor depends primarily upon redox-sensitive stabilization of its α subunit. *J. Biol. Chem.* **271,** 32253–32259 (1996).

111. Nishi, T. *et al.* Spatial redox regulation of a critical cysteine residue of NF-kappa B in vivo. *J. Biol. Chem.* **277,** 44548–44556 (2002).

112. R. Kelley, M., M. Georgiadis, M. & L. Fishel, M. APE1/Ref-1Role in Redox Signaling: Translational Applications of Targeting the Redox Function of the DNA Repair/Redox Protein APE1/Ref-1. *Curr. Mol. Pharmacol.* **5,** 36–53 (2012).

113. Luo, M. *et al.* Characterization of the redox activity and disulfide bond formation in apurinic/apyrimidinic endonuclease. *Biochemistry* **51,** 695–705 (2012).

114. Georgiadis, M. M. *et al.* Evolution of the redox function in mammalian apurinic/apyrimidinic endonuclease. *Mutat. Res. - Fundam. Mol. Mech. Mutagen.* **643,** 54–63 (2008).

115. Hegde, M. L., Hazra, T. K. & Mitra, S. Early steps in the DNA base excision/single-strand interruption repair pathway in mammalian cells. *Cell Research* **18,** 27–47 (2008).

116. Fortini, P., Parlanti, E., Sidorkina, O. M., Laval, J. & Dogliotti, E. The type of DNA glycosylase determines the base excision repair pathway in mammalian cells. *J. Biol. Chem.* **274,** 15230–15236 (1999).

117. Chou, K. M. & Cheng, Y. C. The exonuclease activity of human apurinic/apyrimidinic endonuclease (APE1). Biochemical properties and inhibition by the natural dinucleotide Gp4G. *J. Biol. Chem.* **278,** 18289–18296 (2003).

118. Barzilay, G., Walker, L. J., Robson, C. N. & Hickson, I. D. Site-directed mutagenesis of the human DNA repair enzyme HAP1: Identification of residues important for AP endonuclease and RNase H activity. *Nucleic Acids Res.* **23,** 1544–1550 (1995).

119. Masuda, Y., Bennett, R. A. O. & Demple, B. Rapid dissociation of human apurinic endonuclease (Ape1) from incised DNA induced by magnesium. *J. Biol. Chem.* **273,** 30360–30365 (1998).

120. Masuda, Y., Bennett, R. A. O. & Demple, B. Dynamics of the interaction of human apurinic endonuclease (Ape1) with its substrate and product. *J. Biol. Chem.* **273,** 30352–30359 (1998).

121. Vohhodina, J., Harkin, D. P. & Savage, K. I. Dual roles of DNA repair enzymes in RNA biology/post-transcriptional control. *Wiley Interdisciplinary Reviews: RNA* **7,** 604–619 (2016).

122. Barzilay, G., Walker, L. J., Robson, C. N. & Hickson, I. D. Site-directed mutagenesis of the human DNA repair enzyme HAP1: Identification of residues important for AP endonuclease and RNase H activity. *Nucleic Acids Res.* **23,** 1544–1550 (1995).

123. Berquist, B. R., McNeill, D. R. & Wilson, D. M. Characterization of Abasic Endonuclease Activity of Human Ape1 on Alternative Substrates, as Well as Effects of ATP and Sequence Context on AP Site Incision. *J. Mol. Biol.* **379,** 17–27 (2008).

124. Barnes, T. *et al.* Identification of Apurinic/apyrimidinic endonuclease 1 (APE1) as the endoribonuclease that cleaves c-myc mRNA. *Nucleic Acids Res.* **37,** 3946–3958 (2009).

125. Vascotto, C. *et al.* APE1/Ref-1 interacts with NPM1 within nucleoli and plays a role in the rRNA quality control process. *Mol. Cell. Biol.* **29,** (2009).

126. Frehlick, L. J., Eirín-López, J. M. & Ausió, J. New insights into the nucleophosmin/nucleoplasmin family of nuclear chaperones. *BioEssays* **29,** 49–59 (2007).

127. Bhakat, K., Izumi, T. & Yang, S. Role of acetylated human AP-endonuclease (APE1/Ref-1) in regulation of the parathyroid hormone gene. *EMBO ...* **22,** 6299–6309 (2003).

128. Izumi, T. *et al.* MDM2 is a novel E3 ligase for HIV-1 Vif. *Retrovirology* **6,** 1 (2009).

129. Qu, J., Liu, G. H., Huang, B. & Chen, C. Nitric oxide controls nuclear export of APE1/Ref-1 through S-nitrosation of Cysteines 93 and 310. *Nucleic Acids Res.* **35,** 2522–2532 (2007).

130. Takao, M., Aburatani, H., Kobayashi, K. & Yasui, A. Mitochondrial targeting of human DNA glycosylases for repair of oxidative DNA damage. *Nucleic Acids Res* **26,** 2917–2922 (1998).

131. Jackson, E. B., Theriot, C. a., Chattopadhyay, R., Mitra, S. & Izumi, T. Analysis of nuclear transport signals in the human apurinic/apyrimidinic endonuclease (APE1/Ref1). *Nucleic Acids Res.* **33,** 3303–3312 (2005).

132. Tell, G. *et al.* TSH controls Ref-1 nuclear translocation in thyroid cells. in *Journal of Molecular Endocrinology* **24,** 383–390 (2000).

133. Torres-Gonzalez, M., Gawlowski, T., Kocalis, H., Scott, B. T. & Dillmann, W. H. Mitochondrial 8-oxoguanine glycosylase decreases mitochondrial fragmentation and improves mitochondrial function in H9C2 cells under oxidative stress conditions. *AJP Cell Physiol.* **306,** C221–C229 (2014).

134. Li, M. *et al.* Identification and characterization of mitochondrial targeting sequence of human apurinic/apyrimidinic endonuclease 1. *J. Biol. Chem.* **285,** 14871–81 (2010).

135. Pinz, K. G. & Bogenhagen, D. F. Efficient repair of abasic sites in DNA by mitochondrial enzymes. *Mol. Cell. Biol.* **18,** 1257–1265 (1998).

136. Szczesny, B., Tann, A. W., Longley, M. J., Copeland, W. C. & Mitra, S. Long patch base excision repair in mammalian mitochondrial genomes. *J. Biol. Chem.* **283,** 26349–26356 (2008).

137. Chattopadhyay, R. *et al.* Identification and characterization of mitochondrial abasic (AP)-endonuclease in mammalian cells. *Nucleic Acids Res.* **34,** 2067–2076 (2006).

138. Koehler, C. M. & Tienson, H. L. Redox regulation of protein folding in the mitochondrial intermembrane space. *Biochim. Biophys. Acta* **1793,** 139–145 (2009).

139. Xanthoudakis, S., Smeyne, R. J., Wallace, J. D. & Curran, T. The redox/DNA repair protein, Ref-1, is essential for early embryonic development in mice. *Proc Natl Acad Sci U S A* **93,** 8919–8923 (1996).

140. Izumi, T. *et al.* Two essential but distinct functions of the mammalian abasic endonuclease. *Proc. Natl. Acad. Sci.* **102,** 5739–5743 (2005).

141. Kisby, G. E., Milne, J. & Sweatt, C. Evidence of reduced DNA repair in amyotrophic lateral sclerosis brain tissue. *Neuroreport* **8,** 1337–1340 (1997).

142. Andersen, P. M. The genetics of amyotrophic lateral sclerosis (ALS). *Suppl. Clin. Neurophysiol.* **57,** 211–27 (2004).

143. Abbotts, R. & Madhusudan, S. Human AP endonuclease 1 (APE1): from mechanistic insights to druggable target in cancer. *Cancer Treat. Rev.* **36,** 425–35 (2010).

144. Silber, J. R. *et al.* The Apurinic / Apyrimidinic Endonuclease Activity of Ape1 / Ref-1 Contributes to Human Glioma Cell Resistance to Alkylating Agents and Is Elevated by Oxidative Stress The Apurinic / Apyrimidinic Endonuclease Activity of Ape1 / Ref-1 Contributes to Human G. 3008–3018 (2002).

145. Angkeow, P., Deshpande, S. & Qi, B. Redox factor-1: an extra-nuclear role in the regulation of endothelial oxidative stress and apoptosis. *Cell death …* **107,** 20190–20195 (2002).

146. Bobola, M. S. *et al.* Apurinic/apyrimidinic endonuclease activity is associated with response to radiation and chemotherapy in medulloblastoma and primitive neuroectodermal tumors. *Clin. Cancer Res.* **11,** 7405–7414 (2005).

147. Rai, G. *et al.* Synthesis, biological evaluation, and structure-activity relationships of a novel class of apurinic/apyrimidinic endonuclease 1 inhibitors. *J. Med. Chem.* **55,** 3101–3112 (2012).

148. De Vries, R. DNA condensation in bacteria: Interplay between macromolecular crowding and nucleoid proteins. *Biochimie* **92,** 1715–1721 (2010).

149. NASS, M. M. & NASS, S. INTRAMITOCHONDRIAL FIBERS WITH DNA CHARACTERISTICS. I. FIXATION AND. *J. Cell Biol.* **19,** 593–611 (1963).

150. Anderson, S. *et al.* Sequence and organization of the human mitochondrial genome. *Nature* **290,** 457–465 (1981).

151. Kvist, L. Paternal Leakage of Mitochondrial DNA in the Great Tit (Parus major). *Mol. Biol. Evol.* **20,** 243–247 (2003).

152. Kasamatsu, H. & Vinograd, J. Replication of Circular DNA in Eukaryotic Cells. *Annu. Rev. Biochem.* **43,** 695–719 (1974).

153. Ojala, D., Montoya, J. & Attardi, G. TRNA punctuation model of RNA processing in human mitochondria. *Nature* **290,** 470–474 (1981).

154. Satoh, M. & Kuroiwa, T. Organization of multiple nucleoids and DNA molecules in mitochondria of a human cell. *Exp. Cell Res.* **196,** 137–140 (1991).

155. Bereiter-Hahn, J. & Vöth, M. Distribution and dynamics of mitochondrial nucleoids in animal cells in culture. *Exp. Biol. Online* **1,** 1–17 (1997).

156. Margineantu, D. H. *et al.* Cell cycle dependent morphology changes and associated mitochondrial DNA redistribution in mitochondria of human cell lines. *Mitochondrion* **1,** 425–435 (2002).

157. Iborra, F. J. *et al.* The functional organization of mitochondrial genomes in human cells. *BMC Biol.* **2,** 9 (2004).

158. Legros, F. Organization and dynamics of human mitochondrial DNA. *J. Cell Sci.* **117,** 2653–2662 (2004).

159. Nass, M. M. K. Mitochondrial DNA: Advances, Problems, and Goals. *Science (80-.).* **165,** 25–35 (1969).

160. Hensen, F., Cansiz, S., Gerhold, J. M. & Spelbrink, J. N. To be or not to be a nucleoid protein: A comparison of mass-spectrometry based approaches in the identification of potential mtDNA-nucleoid associated proteins. *Biochimie* **100,** 219–226 (2014).

161. Bogenhagen, D. F., Rousseau, D. & Burke, S. The layered structure of human mitochondrial DNA nucleoids. *J. Biol. Chem.* **283,** 3665–3675 (2008).

162. Spelbrink, J. N. Functional organization of mammalian mitochondrial DNA in nucleoids: History, recent developments, and future challenges. *IUBMB Life* **62,** 19–32 (2010).

163. Kloc, M., Chan, A. P., Etkin, L. D. & Bilinski, S. Mitochondrial ribosomal RNA in the germinal granules in Xenopus embryos revisited. *Differentiation* **67,** 80–83 (2001).

164. Gilkerson, R. *et al.* The mitochondrial nucleoid: integrating mitochondrial DNA into cellular homeostasis. *Cold Spring Harbor perspectives in biology* **5,** a011080 (2013).

165. Spelbrink, J. N. *et al.* Human mitochondrial DNA deletions associated with mutations in the gene encoding Twinkle, a phage T7 gene 4-like protein localized in mitochondria. *Nat. Genet.* **28,** 223–231 (2001).

166. Barat, M., Rickwood, D., Dufresne, C. & Mounolou, J. C. Characterization of DNA-protein complexes from the mitochondria of Xenopus laevis oocytes. *Exp. Cell Res.* **157,** 207–217 (1985).

167. Van Tuyle, G. & Pavco, P. Characterization of a rat liver mitochondrial DNA-protein complex. Replicative intermediates are {…}. *J. Biol. Chem.* **256,** 12772–9 (1981).

168. Mignotte, B., Barat, M. & Mounolou, J.-C. Characterization of a mitochondrial protein binding to single-stranded DNA. *Nucleic Acids Res* **13,** 1703–1716 (1985).

169. Hoke, G. D., Pavco, P. A., Ledwith, B. J. & Van Tuyle, G. C. Structural and functional studies of the rat mitochondrial single strand DNA binding protein P16. *Arch. Biochem. Biophys.* **282,** 116–124 (1990).

170. Ghrir, R., Lecaer, J. P., Dufresne, C. & Gueride, M. Primary structure of the two variants of Xenopus laevis mtSSB, a mitochondrial DNA binding protein. *Arch. Biochem. Biophys.* **291,** 395–400 (1991).

171. CURTH, U. *et al.* Single-stranded-DNA-binding proteins from human mitochondria and Escherichia coli have analogous physicochemical properties. *Eur. J. Biochem.* **221,** 435–443 (1994).

172. Maier, D. *et al.* Mitochondrial single-stranded DNA-binding protein is required for mitochondrial DNA replication and development in Drosophila melanogaster. *Mol Biol Cell* **12,** 821–830 (2001).

173. Garrido, N. *et al.* Composition and Dynamics of Human Mitochondrial Nucleoids. *Mol. Biol. Cell* **14,** 1583–1896 (2003).

174. Bogenhagen, D. F., Wang, Y., Shen, E. L. & Kobayashi, R. Protein Components of Mitochondrial DNA Nucleoids in Higher Eukaryotes. *Mol. Cell. Proteomics* **2,** 1205–1216 (2003).

175. Parisi, M. A. & Clayton, D. A. Similarity of human mitochondrial transcription factor 1 to high mobility group proteins. *Science* **252,** 965–969 (1991).

176. Fisher, R. P. & Clayton, D. A. Purification and characterization of human mitochondrial transcription factor 1. *Mol. Cell. Biol.* **8,** 3496–3509 (1988).

177. Sato, H., Tachifuji, A., Tamura, M. & Miyakawa, I. Identification of the YMN-1 antigen protein and biochemical analyses of protein components in the mitochondrial nucleoid fraction of the yeast Saccharomyces cerevisiae. *Protoplasma* **219,** 51–58 (2002).

178. Kaufman, B. A. *et al.* The Mitochondrial Transcription Factor TFAM Coordinates the Assembly of Multiple DNA Molecules into Nucleoid-like Structures. *Mol. Biol. Cell* **18,** 3225–3236 (2007).

179. Ghivizzani, S. C., Madsen, C. S., Nelen, M. R., Ammini, C. V & Hauswirth, W. W. In organello footprint analysis of human mitochondrial DNA: human mitochondrial transcription factor A interactions at the origin of replication. *Mol. Cell. Biol.* **14,** 7717–7730 (1994).

180. Maniura-Weber, K., Goffart, S., Garstka, H. L., Montoya, J. & Wiesner, R. J. Transient overexpression of mitochondrial transcription factor A (TFAM) is sufficient to stimulate mitochondrial DNA transcription, but not sufficient to increase mtDNA copy number in cultured cells. *Nucleic Acids Res.* **32,** 6015–6027 (2004).

181. Takamatsu, C. *et al.* Regulation of mitochondrial D-loops by transcription factor A and single-stranded DNA-binding protein. *EMBO Rep.* **3,** 451–456 (2002).

182. Alam, T. I. *et al.* Human mitochondrial DNA is packaged with TFAM. *Nucleic Acids Research* **31,** 1640–1645 (2003).

183. Ekstrand, M. I. *et al.* Mitochondrial transcription factor A regulates mtDNA copy number in mammals. *Hum. Mol. Genet.* **13,** 935–944 (2004).

184. Antoshechkin, I. & Bogenhagen, D. F. Distinct roles for two purified factors in transcription of Xenopus mitochondrial DNA. *Mol. Cell. Biol* **15,** 7032–7042 (1995).

185. Van Tuyle, G. C. & Pavco, P. A. The rat liver mitochondrial DNA-protein complex: Displaced single strands of replicative intermediates are protein coated. *J. Cell Biol.* **100,** 251–257 (1985).

186. Shen, E. L. & Bogenhagen, D. F. Developmentally-regulated packaging of mitochondrial DNA by the HMG-box protein mtTFA during Xenopus oogenesis. *Nucleic Acids Res.* **29,** 2822–2828 (2001).

187. Pohjoismäki, J. L. O. *et al.* Alterations to the expression level of mitochondrial transcription factor A, TFAM, modify the mode of mitochondrial DNA replication in cultured human cells. *Nucleic Acids Res.* **34,** 5815–5828 (2006).

188. Ames, B. N., Shigenaga, M. K. & Gold, L. S. DNA lesions, inducible DNA repair, and cell division: Three key factors in mutagenesis and carcinogenesis. in *Environmental*

Health Perspectives **101,** 35–44 (1993).

189. Bandy, B. & Davison, A. J. Mitochondrial mutations may increase oxidative stress: Implications for carcinogenesis and aging? *Free Radic. Biol. Med.* **8,** 523–539 (1990).

190. Singer, T. P. & Ramsay, R. R. Mechanism of the neurotoxicity of MPTP. An update. *FEBS Lett.* **274,** 1–8 (1990).

191. Cooke, M. S., Evans, M. D., Dizdaroglu, M. & Lunec, J. Oxidative DNA damage: mechanisms, mutation, and disease. *Faseb J* **17,** 1195–214 (2003).

192. Richter, C., Park, J. W. & Ames, B. N. Normal oxidative damage to mitochondrial and nuclear DNA is extensive. *Proc. Natl. Acad. Sci. U. S. A.* **85,** 6465–7 (1988).

193. Yakes, F. M. & Van Houten, B. Mitochondrial DNA damage is more extensive and persists longer than nuclear DNA damage in human cells following oxidative stress. *Proc. Natl. Acad. Sci. U. S. A.* **94,** 514–9 (1997).

194. Clayton, D. a, Doda, J. N. & Friedberg, E. C. The absence of a pyrimidine dimer repair mechanism in mammalian mitochondria. *Proc. Natl. Acad. Sci. U. S. A.* **71,** 2777–2781 (1974).

195. Tomkinson, A. E., Thomas Bonk, R., Kim, J., Bartfeld, N. & Linn, S. Mammalian mitochondrial endonuclease activities specific for ultraviolet-irradiated DNA. *Nucleic Acids Res.* **18,** 929–935 (1990).

196. Driggers, W. J., LeDoux, S. P. & Wilson, G. L. Repair of oxidative damage within the mitochondrial DNA of RINr 38 cells. *J. Biol. Chem.* **268,** 22042–22045 (1993).

197. Croteau, D. L. & Bohr, V. a. Repair of Oxidative Damage to Nuclear and Mitochondrial DNA in Mammalian Cells. *J. Biol. Chem.* **272,** 25409–25412 (1997).

198. Stierum, R. H., Dianov, G. L. & Bohr, V. a. Single-nucleotide patch base excision repair of uracil in DNA by mitochondrial protein extracts. *Nucleic Acids Res.* **27,** 3712–3719 (1999).

199. Kang, D. *et al.* Intracellular localization of 8-Oxo-dGTPase in human cells, with special reference to the role of the enzyme in mitochondria. *J. Biol. Chem.* **270,** 14659–14665 (1995).

200. Dome??a, J. D. & Mosbaugh, D. W. Purification of Nuclear and Mitochondrial Uracil-DNA Glycosylase from Rat Liver. Identification of Two Distinct Subcellular Forms. *Biochemistry* **24,** 7320–7328 (1985).

201. Tomkinson, a. E., Bonk, R. T. & Linn, S. Mitochondrial endonuclease activities specific for apurinic/apyrimidinic sites in DNA from mouse cells. *J. Biol. Chem.* **263,** 12532–12537 (1988).

202. Lakshmipathy, U. & Campbell, C. The human DNA ligase III gene encodes nuclear and mitochondrial proteins. *Mol. Cell. Biol.* **19,** 3869–76 (1999).

203. Sykora, P., Wilson, D. M. & Bohr, V. A. Repair of persistent strand breaks in the mitochondrial genome. *Mech. Ageing Dev.* **133,** 169–175 (2012).

204. Mason, P. A., Matheson, E. C., Hall, A. G. & Lightowlers, R. N. Mismatch repair activity in mammalian mitochondria. *Nucleic Acids Research* **31,** 1052–1058 (2003).

205. Thyagarajan, B., Padua, R. a. & Campbell, C. Mammalian mitochondria possess homologous DNA recombination activity. *J. Biol. Chem.* **271,** 27536–27543 (1996).

206. Coffey, G., Lakshmipathy, U. & Campbell, C. Mammalian mitochondrial extracts possess DNA end-binding activity. *Nucleic Acids Res.* **27,** 3348–3354 (1999).

207. Mai, N., Chrzanowska-Lightowlers, Z. M. A. & Lightowlers, R. N. The process of mammalian mitochondrial protein synthesis. *Cell Tissue Res.* 1–16 (2016). doi:10.1007/s00441-016-2456-0

208. Pearce, S. F. *et al.* Regulation of Mammalian Mitochondrial Gene Expression: Recent Advances. *Trends Biochem. Sci.* **9,** 323–337 (2017).

209. Antonicka, H., Sasarman, F., Nishimura, T., Paupe, V. & Shoubridge, E. A. The mitochondrial RNA-binding protein GRSF1 localizes to RNA granules and is required for posttranscriptional mitochondrial gene expression. *Cell Metab.* **17,** 386–398 (2013).

210. Jourdain, A. A. *et al.* GRSF1 regulates RNA processing in mitochondrial RNA granules. *Cell Metab.* **17,** 399–410 (2013).

211. Antonicka, H. & Shoubridge, E. A. Mitochondrial RNA Granules Are Centers for Posttranscriptional RNA Processing and Ribosome Biogenesis. *Cell Rep.* **10,** 920–932 (2015).

212. Borowski, L. S., Dziembowski, A., Hejnowicz, M. S., Stepien, P. P. & Szczesny, R. J. Human mitochondrial RNA decay mediated by PNPase-hSuv3 complex takes place in distinct foci. *Nucleic Acids Res.* **41,** 1223–1240 (2013).

213. Tu, Y. T. & Barrientos, A. The Human Mitochondrial DEAD-Box Protein DDX28 Resides in RNA Granules and Functions in Mitoribosome Assembly. *Cell Rep.* **10,** 854–864 (2015).

214. Barrientos, A. Mitochondriolus: assembling mitoribosomes. *Oncotarget* **6,** 16800–16801 (2015).

215. He, J. *et al.* Human C4orf14 interacts with the mitochondrial nucleoid and is involved in the biogenesis of the small mitochondrial ribosomal subunit. *Nucleic Acids Res.* **40,** 6097–6108 (2012).

216. He, J. *et al.* Mitochondrial nucleoid interacting proteins support mitochondrial protein synthesis. *Nucleic Acids Res.* **40,** 6109–6121 (2012).

217. Bogenhagen, D. F., Martin, D. W. & Koller, A. Initial steps in RNA processing and ribosome assembly occur at mitochondrial DNA nucleoids. *Cell Metab.* **19,** 618–629 (2014).

218. Rackham, O. *et al.* Hierarchical RNA Processing Is Required for Mitochondrial Ribosome Assembly. *Cell Rep.* **16,** 1874–1890 (2016).

219. Jourdain, A. A., Boehm, E., Maundrell, K. & Martinou, J. C. Mitochondrial RNA granules: Compartmentalizing mitochondrial gene expression. *J. Cell Biol.* **212,** 611–614 (2016).

220. Szczesny, R. J. *et al.* Human mitochondrial RNA turnover caught in flagranti: Involvement of hSuv3p helicase in RNA surveillance. *Nucleic Acids Res.* **38,** 279–298

(2009).

221. Montoya, J., Christianson, T., Levens, D., Rabinowitz, M. & Attardi, G. Identification of initiation sites for heavy-strand and light-strand transcription in human mitochondrial DNA. *Proc. Natl. Acad. Sci. U. S. A.* **79,** 7195–7199 (1982).

222. Montoya, J., Gaines, G. L. & Attardi, G. The pattern of transcription of the human mitochondrial rRNA genes reveals two overlapping transcription units. *Cell* **34,** 151–159 (1983).

223. Christianson, T. W. & Clayton, D. A. A tridecamer DNA sequence supports human mitochondrial RNA 3'-end formation in vitro. *Mol. Cell. Biol.* **8,** 4502–9 (1988).

224. Kruse, B., Narasimhan, N. & Attardi, G. Termination of transcription in human mitochondria: Identification and purification of a DNA binding protein factor that promotes termination. *Cell* **58,** 391–397 (1989).

225. Fernandez-Silva, P., Martinez-Azorin, F., Micol, V. & Attardi, G. The human mitochondrial transcription termination factor (mTERF) is a multizipper protein but binds to DNA as a monomer, with evidence pointing to intramolecular leucine zipper interactions. *EMBO J.* **16,** 1066–1079 (1997).

226. Terzioglu, M. *et al.* MTERF1 Binds mtDNA to prevent transcriptional interference at the light-strand promoter but is dispensable for rRNA gene transcription regulation. *Cell Metab.* **17,** 618–626 (2013).

227. Wanrooij, P. H., Uhler, J. P., Simonsson, T., Falkenberg, M. & Gustafsson, C. M. G-quadruplex structures in RNA stimulate mitochondrial transcription termination and primer formation. *Proc. Natl. Acad. Sci.* **107,** 16072–16077 (2010).

228. Nicholls, T. J. & Minczuk, M. In D-loop: 40 years of mitochondrial 7S DNA. *Exp. Gerontol.* **56,** 175–181 (2014).

229. Masters, B. S., Stohl, L. L. & Clayton, D. A. Yeast mitochondrial RNA polymerase is homologous to those encoded by bacteriophages T3 and T7. *Cell* **51,** 89–99 (1987).

230. Tiranti, V. *et al.* Identification of the gene encoding the human mitochondrial RNA polymerase (h-mtRPOL) by cyberscreening of the Expressed Sequence Tags database. *Hum. Mol. Genet.* **6,** 615–25 (1997).

231. Falkenberg, M. *et al.* Mitochondrial transcription factors B1 and B2 activate transcription of human mtDNA. *Nat. Genet.* **31,** 289–294 (2002).

232. Cotney, J., Wang, Z. & Shadel, G. S. Relative abundance of the human mitochondrial transcription system and distinct roles for h-mtTFB1 and h-mtTFB2 in mitochondrial biogenesis and gene expression. *Nucleic Acids Res.* **35,** 4042–4054 (2007).

233. Shutt, T. E. & Gray, M. W. Homologs of mitochondrial transcription factor B, sparsely distributed within the eukaryotic radiation, are likely derived from the dimethyladenosine methyltransferase of the mitochondrial endosymbiont. *Mol. Biol. Evol.* **23,** 1169–1179 (2006).

234. Litonin, D. *et al.* Human mitochondrial transcription revisited: Only TFAM and TFB2M are required for transcription of the mitochondrial genes in vitro. *J. Biol. Chem.* **285,** 18129–18133 (2010).

235. Shi, Y. *et al.* Mammalian transcription factor A is a core component of the mitochondrial transcription machinery. *Proc. Natl. Acad. Sci.* **109,** 16510–16515 (2012).

236. Minczuk, M. *et al.* TEFM (c17orf42) is necessary for transcription of human mtDNA. *Nucleic Acids Res.* **39,** 4284–4299 (2011).

237. Agaronyan, K., Morozov, Y. I., Anikin, M. & Temiakov, D. Replication-transcription switch in human mitochondria. *Science (80-.).* **347,** 548–551 (2015).

238. Posse, V., Shahzad, S., Falkenberg, M., Hällberg, B. M. & Gustafsson, C. M. TEFM is a potent stimulator of mitochondrial transcription elongation in vitro. *Nucleic Acids Res.* **43,** 2615–2624 (2015).

239. Van Haute, L. *et al.* Mitochondrial transcript maturation and its disorders. *J. Inherit. Metab. Dis.* **38,** 655–680 (2015).

240. Xu, F. *et al.* Disruption of a mitochondrial RNA-binding protein gene results in decreased cytochrome b expression and a marked reduction in ubiquinol-cytochrome c reductase activity in mouse heart mitochondria. *Biochem. J.* **416,** 15–26 (2008).

241. Antonicka, H., Sasarman, F., Nishimura, T., Paupe, V. & Shoubridge, E. A. The mitochondrial RNA-binding protein GRSF1 localizes to RNA granules and is required for posttranscriptional mitochondrial gene expression. *Cell Metab.* **17,** 386–398 (2013).

242. Lee, K. W., Okot-Kotber, C., La Comb, J. F. & Bogenhagen, D. F. Mitochondrial ribosomal RNA (rRNA) methyltransferase family members are positioned to modify nascent rRNA in foci near the mitochondrial DNA nucleoid. *J. Biol. Chem.* **288,** 31386–31399 (2013).

243. Holzmann, J. *et al.* RNase P without RNA: Identification and Functional Reconstitution of the Human Mitochondrial tRNA Processing Enzyme. *Cell* **135,** 462–474 (2008).

244. Yang, S. Y., He, X. Y. & Schulz, H. Multiple functions of type 10 17β-hydroxysteroid dehydrogenase. *Trends in Endocrinology and Metabolism* **16,** 167–175 (2005).

245. Vilardo, E. *et al.* A subcomplex of human mitochondrial RNase P is a bifunctional methyltransferase-extensive moonlighting in mitochondrial tRNA biogenesis. *Nucleic Acids Res.* **40,** 11583–11593 (2012).

246. Rossmanith, W. & Holzmann, J. Processing mitochondrial (t)RNAs: New enzyme, old job. *Cell Cycle* **8,** 1650–1653 (2009).

247. Lopez Sanchez, M. I. G. *et al.* RNA processing in human mitochondria. *Cell Cycle* **10,** 2904–2916 (2011).

248. Rossmanith, W. Localization of human RNase Z isoforms: Dual nuclear/mitochondrial targeting of the ELAC2 gene product by alternative translation initiation. *PLoS One* **6,** e19152 (2011).

249. Brzezniak, L. K., Bijata, M., Szczesny, R. J. & Stepien, P. P. Involvement of human ELAC2 gene product in 3' end processing of mitochondrial tRNAs. *RNA Biol.* **8,** 616–626 (2011).

250. Rackham, O. *et al.* Pentatricopeptide repeat domain protein 1 lowers the levels of mitochondrial leucine tRNAs in cells. *Nucleic Acids Res.* **37,** 5859–5867 (2009).

251. Hällberg, B. M. & Larsson, N. G. Making proteins in the powerhouse. *Cell Metab.* **20,** 226–240 (2014).

252. Johansson, M. J. O., Esberg, A., Huang, B., Bjork, G. R. & Bystrom, A. S. Eukaryotic Wobble Uridine Modifications Promote a Functionally Redundant Decoding System. *Mol. Cell. Biol.* **28,** 3301–3312 (2008).

253. Villarroya, M. *et al.* Characterization of Human GTPBP3, a GTP-Binding Protein Involved in Mitochondrial tRNA Modification. *Mol. Cell. Biol.* **28,** 7514–7531 (2008).

254. Li, X. & Guan, M.-X. A human mitochondrial GTP binding protein related to tRNA modification may modulate phenotypic expression of the deafness-associated mitochondrial 12S rRNA mutation. *Mol. Cell. Biol.* **22,** 7701–11 (2002).

255. Yan, Q. *et al.* Human TRMU encoding the mitochondrial 5-methylaminomethyl-2-thiouridylate- methyltransferase is a putative nuclear modifier gene for the phenotypic expression of the deafness-associated 12S rRNA mutations. *Biochem. Biophys. Res. Commun.* **342,** 1130–1136 (2006).

256. Yarham, J. W. *et al.* Defective i6A37 Modification of Mitochondrial and Cytosolic tRNAs Results from Pathogenic Mutations in TRIT1 and Its Substrate tRNA. *PLoS Genet.* **10,** e1004424 (2014).

257. Brulé, H., Elliott, M., Redlak, M., Zehner, Z. E. & Holmes, W. M. Isolation and characterization of the human tRNA-(N1G37) methyltransferase (TRM5) and comparison to the Escherichia coli TrmD protein. *Biochemistry* **43,** 9243–9255 (2004).

258. Reiter, V. *et al.* The CDK5 repressor CDK5RAP1 is a methylthiotransferase acting on nuclear and mitochondrial RNA. *Nucleic Acids Res.* **40,** 6235–6240 (2012).

259. Nagaike, T. *et al.* Identification and Characterization of Mammalian Mitochondrial tRNA nucleotidyltransferases. *J. Biol. Chem.* **276,** 40041–40049 (2001).

260. Brown, A. *et al.* Structure of the large ribosomal subunit from human mitochondria. *Science (80-.).* **346,** 718–722 (2014).

261. Greber, B. J. *et al.* The complete structure of the 55. *Nature* **348,** 303–308 (2014).

262. Kaushal, P. S. *et al.* Cryo-EM structure of the small subunit of the mammalian mitochondrial ribosome. *Proc. Natl. Acad. Sci.* **111,** 7284–7289 (2014).

263. Amunts, A., Brown, A., Toots, J., Scheres, S. H. W. & Ramakrishnan, V. The structure of the human mitochondrial ribosome. *Science (80-.).* **348,** 95–98 (2015).

264. Decatur, W. A. & Fournier, M. J. rRNA modifications and ribosome function. *Trends in Biochemical Sciences* **27,** 344–351 (2002).

265. Piekna-Przybylska, D. D., Decatur, W. A. & Fournier, M. J. The 3D rRNA modification maps database: With interactive tools for ribosome analysis. *Nucleic Acids Res.* **36,** D178-83 (2008).

266. Baer, R. J. & Dubin, D. T. Methylated regions of hamster mitochondrial ribosomal RNA: Structural and functional correlates. *Nucleic Acids Res.* **9,** 323–337 (1981).

267. Seidel-Rogol, B. L., McCulloch, V. & Shadel, G. S. Human mitochondrial transcription factor B1 methylates ribosomal RNA at a conserved stem-loop. *Nat. Genet.* **33,** 23–24 (2003).

268. Metodiev, M. D. *et al.* Methylation of 12S rRNA Is Necessary for In Vivo Stability of the Small Subunit of the Mammalian Mitochondrial Ribosome. *Cell Metab.* **9,** 386–397 (2009).

269. Xu, Z., O'Farrell, H. C., Rife, J. P. & Culver, G. M. A conserved rRNA methyltransferase regulates ribosome biogenesis. *Nat. Struct. Mol. Biol.* **15,** 534–536 (2008).

270. Cámara, Y. *et al.* MTERF4 regulates translation by targeting the methyltransferase NSUN4 to the mammalian mitochondrial ribosome. *Cell Metab.* **13,** 527–539 (2011).

271. Yakubovskaya, E. *et al.* Structure of the essential MTERF4:NSUN4 protein complex reveals how an MTERF protein collaborates to facilitate rRNA modification. *Structure* **20,** 1940–1947 (2012).

272. Dubin, D. T. & Taylor, R. H. Modification of mitochondrial ribosomal RNA from hamster cells: the presence of GmG and late-methylated UmGmU in the large subunit (17S) RNA. *J. Mol. Biol.* **121,** 523–40 (1978).

273. Ofengand, J. & Bakin, A. Mapping to nucleotide resolution of pseudouridine residues in large subunit ribosomal RNAs from representative eukaryotes, prokaryotes, archaebacteria, mitochondria and chloroplasts. *J. Mol. Biol.* **266,** 246–268 (1997).

274. Lee, K. W. & Bogenhagen, D. F. Assignment of 2???-O-methyltransferases to modification sites on the mammalian mitochondrial large subunit 16 S ribosomal RNA (rRNA). *J. Biol. Chem.* **289,** 24936–24942 (2014).

275. Rorbach, J. *et al.* MRM2 and MRM3 are involved in biogenesis of the large subunit of the mitochondrial ribosome. *Mol. Biol. Cell* **25,** 2542–2555 (2014).

276. Sirum-Connolly, K. & Mason, T. L. Functional requirement of a site-specific ribose methylation in ribosomal RNA. *Science (80-.).* **262,** 1886–1889 (1993).

277. Temperley, R. J., Wydro, M., Lightowlers, R. N. & Chrzanowska-Lightowlers, Z. M. Human mitochondrial mRNAs-like members of all families, similar but different. *Biochimica et Biophysica Acta - Bioenergetics* **1797,** 1081–1085 (2010).

278. Tomecki, R., Dmochowska, A., Gewartowski, K., Dziembowski, A. & Stepien, P. P. Identification of a novel human nuclear-encoded mitochondrial poly(A) polymerase. *Nucleic Acids Res.* **32,** 6001–6014 (2004).

279. Nagaike, T., Suzuki, T., Katoh, T. & Ueda, T. Human mitochondrial mRNAs are stabilized with polyadenylation regulated by mitochondria-specific poly(A) polymerase and polynucleotide phosphorylase. *J. Biol. Chem.* **280,** 19721–19727 (2005).

280. Bai, Y., Srivastava, S. K., Chang, J. H., Manley, J. L. & Tong, L. Structural Basis for Dimerization and Activity of Human PAPD1, a Noncanonical Poly(A) Polymerase. *Mol. Cell* **41,** 311–320 (2011).

281. Wilson, W. C. *et al.* A human mitochondrial poly(A) polymerase mutation reveals the complexities of post-transcriptional mitochondrial gene expression. *Hum. Mol. Genet.*

23, 6345–6355 (2014).

282. Rorbach, J., Bobrowicz, A., Pearce, S. & Minczuk, M. in *Methods in Molecular Biology* **1125,** 211–227 (2014).

283. Rorbach, J., Nicholls, T. J. J. & Minczuk, M. PDE12 removes mitochondrial RNA poly(A) tails and controls translation in human mitochondria. *Nucleic Acids Res.* **39,** 7750–7763 (2011).

284. Wydro, M., Bobrowicz, A., Temperley, R. J., Lightowlers, R. N. & Chrzanowska-Lightowlers, Z. M. Targeting of the cytosolic poly(A) binding protein PABPC1 to mitochondria causes mitochondrial translation inhibition. *Nucleic Acids Res.* **38,** 3732–3742 (2010).

285. Rorbach, J. & Minczuk, M. The post-transcriptional life of mammalian mitochondrial RNA. *Biochem. J.* **444,** 357–373 (2012).

286. Poulsen, J. B. *et al.* Human 2′-phosphodiesterase localizes to the mitochondrial matrix with a putative function in mitochondrial RNA turnover. *Nucleic Acids Res.* **39,** 3754–3770 (2011).

287. Sterky, F. H., Ruzzenente, B., Gustafsson, C. M., Samuelsson, T. & Larsson, N. G. LRPPRC is a mitochondrial matrix protein that is conserved in metazoans. *Biochem. Biophys. Res. Commun.* **398,** 759–764 (2010).

288. Gohil, V. M. *et al.* Mitochondrial and nuclear genomic responses to loss of LRPPRC expression. *J. Biol. Chem.* **285,** 13742–13747 (2010).

289. Sasarman, F., Brunel-Guitton, C., Antonicka, H., Wai, T. & Shoubridge, E. A. LRPPRC and SLIRP Interact in a Ribonucleoprotein Complex That Regulates Posttranscriptional Gene Expression in Mitochondria. *Mol. Biol. Cell* **21,** 1315–1323 (2010).

290. Sondheimer, N., Fang, J.-K., Polyak, E., Falk, M. J. & Avadhani, N. G. Leucine-Rich Pentatricopeptide-Repeat Containing Protein Regulates Mitochondrial Transcription. *Biochemistry* **49,** 7467–7473 (2010).

291. Ruzzenente, B. *et al.* LRPPRC is necessary for polyadenylation and coordination of translation of mitochondrial mRNAs. *EMBO J.* **31,** 443–456 (2012).

292. Mourier, A., Ruzzenente, B., Brandt, T., Kühlbrandt, W. & Larsson, N. G. Loss of LRPPRC causes ATP synthase deficiency. *Hum. Mol. Genet.* **23,** 2580–2592 (2014).

293. Chujo, T. *et al.* LRPPRC/SLIRP suppresses PNPase-mediated mRNA decay and promotes polyadenylation in human mitochondria. *Nucleic Acids Res.* **40,** 8033–8047 (2012).

294. Baughman, J. M. *et al.* A computational screen for regulators of oxidative phosphorylation implicates SLIRP in mitochondrial RNA homeostasis. *PLoS Genet.* **5,** (2009).

295. Minczuk, M., Lilpop, J., Boros, J. & Stepien, P. P. The 5′ region of the human hSUV3 gene encoding mitochondrial DNA and RNA helicase: Promoter characterization and alternative pre-mRNA splicing. *Biochim. Biophys. Acta - Gene Struct. Expr.* **1729,** 81–87 (2005).

296. Szczesny, R. J. *et al.* Down-regulation of human RNA/DNA helicase SUV3 induces apoptosis by a caspase- and AIF-dependent pathway. *Biol. Cell* **99,** 323–32 (2007).

297. Kazak, L. *et al.* Alternative translation initiation augments the human mitochondrial proteome. *Nucleic Acids Res.* **41,** 2354–2369 (2013).

298. Wang, D. D. H., Shu, Z., Lieser, S. A., Chen, P. L. & Lee, W. H. Human mitochondrial SUV3 and polynucleotide phosphorylase form a 330-kDa heteropentamer to cooperatively degradedouble-stranded RNA with a 3′-to-5′ directionality. *J. Biol. Chem.* **284,** 20812–20821 (2009).

299. Chen, H.-W. *et al.* Mammalian Polynucleotide Phosphorylase Is an Intermembrane Space RNase That Maintains Mitochondrial Homeostasis. *Mol. Cell. Biol.* **26,** 8475–8487 (2006).

300. Slomovic, S. & Schuster, G. Stable PNPase RNAi silencing: Its effect on the processing and adenylation of human mitochondrial RNA. *RNA* **14,** 310–323 (2008).

301. Bruni, F., Gramegna, P., Oliveira, J. M. A., Lightowlers, R. N. & Chrzanowska-Lightowlers, Z. M. A. REXO2 Is an Oligoribonuclease Active in Human Mitochondria. *PLoS One* **8,** e64670 (2013).

302. Sharma, M. R. *et al.* Correction for Kaushal et al., Cryo-EM structure of the small subunit of the mammalian mitochondrial ribosome. *Proc Natl Acad Sci U S A* **112,** 303–308 (2015).

303. Agrawal, R. K. & Sharma, M. R. Structural aspects of mitochondrial translational apparatus. *Curr. Opin. Struct. Biol.* **22,** 797–803 (2012).

304. O'Brien, T. W. Evolution of a protein-rich mitochondrial ribosome: Implications for human genetic disease. in *Gene* **286,** 73–79 (2002).

305. Kietrys, A. M., Szopa, A. & Bąkowska-Zywicka, K. Structure and function of intersubunit bridges in procaryotic ribosome. *Biotechnologia* **115,** 48–58 (2009).

306. Christian, B. E. & Spremulli, L. L. Preferential selection of the 5???-terminal start codon on leaderless mRNAs by mammalian mitochondrial ribosomes. *J. Biol. Chem.* **285,** 28379–28386 (2010).

307. Liu, M. & Spremulli, L. Interaction of mammalian mitochondrial ribosomes with the inner membrane. *J. Biol. Chem.* **275,** 29400–29406 (2000).

308. Gruschke, S. & Ott, M. The polypeptide tunnel exit of the mitochondrial ribosome is tailored to meet the specific requirements of the organelle. *BioEssays* **32,** 1050–1057 (2010).

309. De Silva, D., Tu, Y. T., Amunts, A., Fontanesi, F. & Barrientos, A. Mitochondrial ribosome assembly in health and disease. *Cell Cycle* **14,** 2226–2250 (2015).

310. Kotani, T., Akabane, S., Takeyasu, K., Ueda, T. & Takeuchi, N. Human G-proteins, ObgH1 and Mtg1, associate with the large mitochondrial ribosome subunit and are involved in translation and assembly of respiratory complexes. *Nucleic Acids Res.* **41,** 3713–3722 (2013).

311. Linder, P. & Jankowsky, E. From unwinding to clamping ĝ€" the DEAD box RNA

helicase family. *Nature Reviews Molecular Cell Biology* **12,** 505–516 (2011).

312. Wredenberg, A. *et al.* MTERF3 Regulates Mitochondrial Ribosome Biogenesis in Invertebrates and Mammals. *PLoS Genet.* **9,** e1003178 (2013).

313. Popow, J. *et al.* FASTKD2 is an RNA-binding protein required for mitochondrial RNA processing and translation. *RNA* **21,** 1873–1884 (2015).

314. Nolden, M. *et al.* The m-AAA protease defective in hereditary spastic paraplegia controls ribosome assembly in mitochondria. *Cell* **123,** 277–289 (2005).

315. Rorbach, J., Gammage, P. A. & Minczuk, M. C7orf30 is necessary for biogenesis of the large subunit of the mitochondrial ribosome. *Nucleic Acids Res.* **40,** 4097–4109 (2012).

316. Fung, S., Nishimura, T., Sasarman, F. & Shoubridge, E. A. The conserved interaction of C7orf30 with MRPL14 promotes biogenesis of the mitochondrial large ribosomal subunit and mitochondrial translation. *Mol. Biol. Cell* **24,** 184–193 (2013).

317. Christian, B. E. & Spremulli, L. L. Mechanism of protein biosynthesis in mammalian mitochondria. *Biochimica et Biophysica Acta - Gene Regulatory Mechanisms* **1819,** 1035–1054 (2012).

318. Suhm, T. & Ott, M. Mitochondrial translation and cellular stress response. *Cell Tissue Res.* 1–11 (2016). doi:10.1007/s00441-016-2460-4

319. Chrzanowska-Lightowlers, Z. M. A., Pajak, A. & Lightowlers, R. N. Termination of protein synthesis in mammalian mitochondria. *Journal of Biological Chemistry* **286,** 34479–34485 (2011).

320. Suzuki, T., Nagao, A. & Suzuki, T. Human Mitochondrial tRNAs: Biogenesis, Function, Structural Aspects, and Diseases. *Annu. Rev. Genet.* **45,** 299–329 (2011).

321. Amunts, A., Brown, A., Toots, J., Scheres, S. H. W. & Ramakrishnan, V. The structure of the human mitochondrial ribosome. *Science (80-.).* **348,** 95–98 (2015).

322. Greber, B. J. *et al.* The complete structure of the 55S mammalian mitochondrial ribosome. *Science (80-.).* **348,** 303–308 (2015).

323. Tucker, E. J. *et al.* Mutations in MTFMT underlie a human disorder of formylation causing impaired mitochondrial translation. *Cell Metab.* **14,** 428–434 (2011).

324. Cai, Y. C., Bullard, J. M., Thompson, N. L. & Spremulli, L. L. Interaction of mitochondrial elongation factor Tu with aminoacyl-tRNA and elongation factor Ts. *J. Biol. Chem.* **275,** 20308–20314 (2000).

325. Soleimanpour-Lichaei, H. R. *et al.* mtRF1a Is a Human Mitochondrial Translation Release Factor Decoding the Major Termination Codons UAA and UAG. *Mol. Cell* **27,** 745–757 (2007).

326. Temperley, R., Richter, R., Dennerlein, S., Lightowlers, R. N. & Chrzanowska-Lightowlers, Z. M. Hungry codons promote frameshifting in human mitochondrial ribosomes. *Science* **327,** 301 (2010).

327. Akabane, S., Ueda, T., Nierhaus, K. H. & Takeuchi, N. Ribosome Rescue and Translation Termination at Non-Standard Stop Codons by ICT1 in Mammalian

Mitochondria. *PLoS Genet.* **10,** e1004616 (2014).

328. Rorbach, J. *et al.* The human mitochondrial ribosome recycling factor is essential for cell viability. *Nucleic Acids Res.* **36,** 5787–5799 (2008).

329. Tsuboi, M. *et al.* EF-G2mt Is an Exclusive Recycling Factor in Mammalian Mitochondrial Protein Synthesis. *Mol. Cell* **35,** 502–510 (2009).

330. Roberts, G. G. & Hudson, A. P. Transcriptome profiling of Saccharomyces cerevisiae during a transition from fermentative to glycerol-based respiratory growth reveals extensive metabolic and structural remodeling. *Mol. Genet. Genomics* **276,** 170–186 (2006).

331. Couvillion, M. T., Soto, I. C., Shipkovenska, G. & Churchman, L. S. Synchronized mitochondrial and cytosolic translation programs. *Nature* **533,** 499–503 (2016).

332. Weraarpachai, W. *et al.* Mutation in TACO1, encoding a translational activator of COX I, results in cytochrome c oxidase deficiency and late-onset Leigh syndrome. *Nat. Genet.* **41,** 833–837 (2009).

333. Mick, D. U. *et al.* MITRAC links mitochondrial protein translocation to respiratory-chain assembly and translational regulation. *Cell* **151,** 1528–1541 (2012).

334. Szklarczyk, R. *et al.* Iterative orthology prediction uncovers new mitochondrial proteins and identifies C12orf62 as the human ortholog of COX14, a protein involved in the assembly of cytochrome c oxidase. *Genome Biol.* **13,** R12 (2012).

335. Weraarpachai, W. *et al.* Mutations in C12orf62, a factor that couples COX i synthesis with cytochrome c oxidase assembly, cause fatal neonatal lactic acidosis. *Am. J. Hum. Genet.* **90,** 142–151 (2012).

336. Miller, J. L., Cimen, H., Koc, H. & Koc, E. C. Phosphorylated proteins of the mammalian mitochondrial ribosome: Implications in protein synthesis. *J. Proteome Res.* **8,** 4789–4798 (2009).

337. O'Brien, T. W., Denslow, N. D., Anders, J. C. & Courtney, B. C. The translation system of mammalian mitochondria. *BBA - Gene Struct. Expr.* **1050,** 174–178 (1990).

338. Denslow, N. D., Anders, J. C. & O'Brien, T. W. Bovine mitochondrial ribosomes possess a high affinity binding site for guanine nucleotides. *J. Biol. Chem.* **266,** 9586–9590 (1991).

339. Metodiev, M. D. *et al.* NSUN4 Is a Dual Function Mitochondrial Protein Required for Both Methylation of 12S rRNA and Coordination of Mitoribosomal Assembly. *PLoS Genet.* **10,** e1004110 (2014).

340. Boczonadi, V. & Horvath, R. Mitochondria: Impaired mitochondrial translation in human disease. *Int. J. Biochem. Cell Biol.* **48,** 77–84 (2014).

341. Mita, S. *et al.* Recombination via flanking direct repeats is a major cause of large-scale deletions of human mitochondrial DNA. *Nucleic Acids Res.* **18,** 561–567 (1990).

342. Larsson, N.-G. & Clayton, D. A. Molecular Genetic Aspects of Human Mitochondrial Disorders. *Annu. Rev. Genet.* **29,** 151–178 (1995).

343. Rötig, A. Human diseases with impaired mitochondrial protein synthesis. *Biochimica*

et Biophysica Acta - Bioenergetics **1807,** 1198–1205 (2011).

344. Borowski, L. S. & Szczesny, R. J. Measurement of mitochondrial RNA stability by metabolic labeling of transcripts with 4-thiouridine. *Methods Mol. Biol.* **1125,** 277–286 (2014).

345. Peikert, C. D. *et al.* Charting organellar importomes by quantitative mass spectrometry. *Nat. Commun.* **8,** (2017).

346. Cox, J. *et al.* Andromeda: A peptide search engine integrated into the MaxQuant environment. *J. Proteome Res.* **10,** 1794–1805 (2011).

347. Cox, J. & Mann, M. MaxQuant enables high peptide identification rates, individualized p.p.b.-range mass accuracies and proteome-wide protein quantification. *Nat. Biotechnol.* **26,** 1367–1372 (2008).

348. Akbari, M., Visnes, T., Krokan, H. E. & Otterlei, M. Mitochondrial base excision repair of uracil and AP sites takes place by single-nucleotide insertion and long-patch DNA synthesis. *DNA Repair (Amst).* **7,** 605–616 (2008).

349. Banci, L. *et al.* Molecular chaperone function of Mia40 triggers consecutive induced folding steps of the substrate in mitochondrial protein import. *Proc. Natl. Acad. Sci.* **107,** 20190–20195 (2010).

350. Chacinska, A. *et al.* Essential role of Mia40 in import and assembly of mitochondrial intermembrane space proteins. *EMBO J.* **23,** 3735–46 (2004).

351. Bottinger, L. *et al.* In vivo evidence for cooperation of Mia40 and Erv1 in the oxidation of mitochondrial proteins. *Mol. Biol. Cell* **23,** 3957–3969 (2012).

352. Furda, A. M., Bess, A. S., Meyer, J. N. & Van Houten, B. in *Methods in molecular biology (Clifton, N.J.)* **920,** 111–132 (2012).

353. Maso, V. Di *et al.* Subcellular Localization of APE1/Ref-1 in Human Hepatocellular Carcinoma: Possible Prognostic Significance. *Mol. Med.* **13,** 30–39 (2006).

354. Vascotto, C. *et al.* Knock-in reconstitution studies reveal an unexpected role of Cys-65 in regulating APE1/Ref-1 subcellular trafficking and function. *Mol. Biol. Cell* **22,** 3887–3901 (2011).

355. Petruk, S., Fenstermaker, T. K., Black, K. L., Brock, H. W. & Mazo, A. Detection of RNA-DNA association by a proximity ligation-based method. *Sci. Rep.* **6,** (2016).

356. Quinlan, C. L., Gerencser, A. A., Treberg, J. R. & Brand, M. D. The mechanism of superoxide production by the antimycin-inhibited mitochondrial Q-cycle. *J. Biol. Chem.* **286,** 31361–31372 (2011).

357. Tanaka, M. *et al.* RNA oxidation catalyzed by cytochrome c leads to its depurination and cross-linking, which may facilitate cytochrome c release from mitochondria. *Free Radic. Biol. Med.* **53,** 854–862 (2012).

358. Tanaka, M., Han, S., Küpfer, P. A., Leumann, C. J. & Sonntag, W. E. Quantification of oxidized levels of specific RNA species using an aldehyde reactive probe. *Anal. Biochem.* **417,** 142–148 (2011).

359. Knight, E. Mitochondria-Associated Ribonucleic Acid of the Hela Cell. Effect of

Ethidium Bromide on the Synthesis of Ribosomal and 4S Ribonucleic Acid. *Biochemistry* **8,** 5089–5093 (1969).

360. McKee, E. E., Ferguson, M., Bentley, A. T. & Marks, T. A. Inhibition of mammalian mitochondrial protein synthesis by oxazolidinones. *Antimicrob. Agents Chemother.* **50,** 2042–2049 (2006).

361. Acín-Pérez, R. *et al.* Respiratory complex III is required to maintain complex I in mammalian mitochondria. *Mol. Cell* **13,** 805–815 (2004).

362. Li, Y. *et al.* An assembled complex IV maintains the stability and activity of complex I in mammalian mitochondria. *J. Biol. Chem.* **282,** 17557–17562 (2007).

363. Cortés-Hernández, P., Vázquez-Memije, M. E. & García, J. J. ATP6 homoplasmic mutations inhibit and destabilize the human F 1F0-ATP synthase without preventing enzyme assembly and oligomerization. *J. Biol. Chem.* **282,** 1051–1058 (2007).

364. Su, D. *et al.* Interactions of apurinic/apyrimidinic endonuclease with a redox inhibitor: evidence for an alternate conformation of the enzyme. *Biochemistry* **50,** 82–92 (2011).

365. Luo, M., He, H., Kelley, M. R. & Georgiadis, M. M. Redox regulation of DNA repair: implications for human health and cancer therapeutic development. *Antioxid. Redox Signal.* **12,** 1247–69 (2010).

366. Puglisi, F. *et al.* Prognostic significance of Ape1/ref-1 subcellular localization in non-small cell lung carcinomas. *Anticancer Res.* **21,** 4041–4050 (2001).

367. Sheng, Q. *et al.* Prognostic significance of APE1 cytoplasmic localization in human epithelial ovarian cancer. *Med. Oncol.* **29,** 1265–1271 (2012).

368. Woo, J. *et al.* Prognostic value of human apurinic/apyrimidinic endonuclease 1 (APE1) expression in breast cancer. *PLoS One* **9,** e99528 (2014).